

**STUDIES IN SYNTHESIS OF SOME LIGANDS
CONTAINING SULFA DRUGS AND THEIR METAL
COMPLEXES AND ANTIBACTERIAL ACTIVITIES**

A THESIS

**Submitted for the Award of the Ph.D. Degree of
PACIFIC ACADEMY OF HIGHER EDUCATION AND
RESEARCH UNIVERSITY**

By

CHINTANKUMAR PRAVINBHAI PATEL

Under the Supervision of

Dr. JAYESH PRADEEP BHATT

Dr. PIYUSH J. VYAS



**DEPARTMENT OF CHEMISTRY
FACULTY OF SCIENCE
PACIFIC ACADEMY OF HIGHER EDUCATION
AND RESEARCH UNIVERSITY
UDAIPUR**

DEPARTMENT OF CHEMISTRY
PAHER UNIVERSITY, UDAIPUR

Dr. JAYESH PRADEEP BHATT
Assistant Professor

CERTIFICATE

It gives me immense pleasure in certifying that the thesis entitled “**STUDIES IN SYNTHESIS OF SOME LIGANDS CONTAINING SULFA DRUGS AND THEIR METAL COMPLEXES AND ANTIBACTERIAL ACTIVITIES**” submitted by **Mr. CHINTANKUMAR PRAVINBHAI PATEL** is based on the research work carried out under my guidance. He has completed the following requirements as per Ph.D. regulations of the University.

- (i) Course work as per University rules.
- (ii) Residential requirements of the University.
- (iii) Regularly submitted Half Yearly Progress Report.
- (iv) Published/accepted minimum of two research paper in a refereed research journal.

I recommend the submission of thesis.

Date:

(Dr. JAYESH PRADEEP BHATT)
Supervisor

DEPARTMENT OF CHEMISTRY
SHETH M.N. SCIENCE COLLEGE, PATAN

Dr. PIYUSH J. VYAS
Assistant Professor

CERTIFICATE

It gives me immense pleasure in certifying that the thesis entitled “**STUDIES IN SYNTHESIS OF SOME LIGANDS CONTAINING SULFA DRUGS AND THEIR METAL COMPLEXES AND ANTIBACTERIAL ACTIVITIES**” submitted by **Mr. CHINTANKUMAR PRAVINBHAI PATEL** is based on the research work carried out under my guidance. He has completed the following requirements as per Ph.D. regulations of the University.

- (i) Course work as per University rules.
- (ii) Residential requirements of the University.
- (iii) Regularly submitted Half Yearly Progress Report.
- (iv) Published/accepted minimum of two research paper in a refereed research journal.

I recommend the submission of thesis.

Date:

(Dr. PIYUSH J. VYAS)
Co-Supervisor

DECLARATION

I, **Mr. CHINTANKUMAR PRAVINBHAI PATEL**, resident of Bharuch, Gujarat hereby declare that the research work incorporated in the present thesis entitled “**STUDIES IN SYNTHESIS OF SOME LIGANDS CONTAINING SULFA DRUGS AND THEIR METAL COMPLEXES AND ANTIBACTERIAL ACTIVITIES**” is my own work and is original. This work (in part or in full) has not been submitted to any University for the award of a Degree or a Diploma. I have properly acknowledged the material collected from secondary sources, wherever required. I solely own the responsibility for the originality of the entire content.

Date :
Place:

(CHINTANKUMAR PRAVINBHAI PATEL)

COPYRIGHT

I, **Mr. CHINTANKUMAR PRAVINBHAI PATEL**, hereby declare that the Pacific Academy of Higher Education and Research University, Udaipur, Rajasthan shall have the rights to preserve, use and disseminate this thesis entitled **“STUDIES IN SYNTHESIS OF SOME LIGANDS CONTAINING SULFA DRUGS AND THEIR METAL COMPLEXES AND ANTIBACTERIAL ACTIVITIES”** in print or electronic format for academic/research purpose.

Date :
Place:

(CHINTANKUMAR PRAVINBHAI PATEL)

ACKNOWLEDGEMENT

I am grateful to the Supreme Being and the epitome of benevolence, “*The Almighty God*” for giving me all the grace that I need to pursue this work.

Before presenting this work in the conscious circle, I humbly and solemnly acknowledge the selfless help and guidance received from all benign and amicable quarters. In this regard, I honestly admit that there are some magnanimous hands without whose cooperation, help and guidance, this dissertation might not have seen the light of the day.

No action or words would be adequate to express gratitude to my esteemed teacher and elite guide, **Dr. JAYESH P. BHATT**, Department of Chemistry, PAHER University, Udaipur for guiding and sharing with me his experience and knowledge. His incessant encouragement and critical evaluation had been a constant source of inspiration for me. It is my privilege to be a student of such a dedicated and honest personality. I could not have imagined having a better advisor and mentor for my Ph.D. than him. Without his continuous guidance, expert advice and unfailing interest, this work could not have been completed.

I am especially thankful to, **Professor SURESH C. AMETA**, Department of Chemistry, PAHER University, Udaipur for giving me inspiration, critical suggestions and meticulous guidance from the beginning of the work to its completion.

I am thankful from my heart to my Co guide, **Dr. PIYUSH VYAS** for their constant encouragement and valuable advices.

I am highly indebted to my maternal uncle **Mr. HARIVADAN PATEL** and **Mr. RAKESH PATEL** for helpful during my research work.

I bow my head in respect for my parents **Mr. PRAVIN PATEL** and **Mrs. PARUL PATEL**. I thank them for their blessings, constant love, support and encouragement. They are my mentors and well-wishers for every moment of my life.

I am highly indebted to my maternal uncle **Mr. HARIVADAN PATEL** and **Mr. RAKESH PATEL** helping me during tough time.

I gratefully thank my brothers **Mr. JAYMIN PATEL, Mr. GAURANG PATEL, Mr. Neel Patel** and **Mr. Darshan Patel** for being supportive and caring sibling.

I am thankful to my wife **Ms. DRASHTI PATEL** for her patience and constant support during the course of present work.

Thanks are also due to non-teaching staff of the Department of Chemistry for their helping attitude during the course of the present study.

I would like to thank each one of them, who directly or indirectly rendered their help to me in the completion of this work, and my apologies to all those, who have helped me, but are not acknowledged.

The final one, my distinctive thanks to **Dr. Rajesh Kanja, M/s SHORYA THESIS PRINTING & BINDING, UDAIPUR** for their role in shaping this research, creative design work and bringing out this document meticulously, neatly and timely.

(CHINTANKUMAR PRAVINBHAI PATEL)

PREFACE

Transition metals play a pivotal role in the innovation of novel metal based drugs and also in certain cosmetic formulation. Transition metal complexes are cation and anionic or neutral species which contain co-ordination bond between ligand and metal. There is significant role in application of transition metal complexes as drugs to cure many human diseases. The mode of action of metal complexes drugs on living organism is quite different from non-metals. With different oxidation state of transition metals, it can be exploited for designing new drugs. The metal complexes offer a great diversity in their medicinal actions; like anti-cancer, anti-inflammatory, anti-infective, anti-diabetic activities, etc. Transition metal complexes are also important in catalysis. In material/polymer synthesis, photochemistry, etc.

Looking to above properties of transition metal complexes, it was thought to synthesize the ligand having drug segment. With excellent pharmaceutical activity of sulfa drugs, the novel ligands containing various sulfa drugs have been prepared. The sulfa drugs; viz; Sulfathiazole, Sulfapyridine, Sulfadiazine, Sulfaquinoxaline, sulfapyridazine and trimethoprim were selected. Each of these drugs having free amine group. So these can easily be condensed with tetrahydrophthalic anhydride. The ligands were prepared and characterized duly. The research work has been presented in four chapters;

Chapter – I: Literature pertinent to transition metal complexes, their applications, ligand containing amide group (mainly derived by condensation of acid anhydride and amines) are summarised.

Chapter – II: It presents materials and methods adopted in whole work. Details of chemical reagents either analytical methods like elemental content, spectral techniques, magnetic susceptibility, thermogravimetry, and antimicrobial activity are also furnished in this chapter.

Chapter – III: Various ligand synthesis process based on tetrahydrophthalic anhydride and sulfa drugs have been described in this chapter. Following this, the synthetic details of ligands are given with structural characterisation.

Chapter IV: The measurement of metal-ligand ratio, magnetic moment, thermal stability, and antimicrobial activity of metal chelates have been presented in this chapter and discussed in terms of structural activity relationships.

□□□

CONTENTS

CHAPTER - I	INTRODUCTION	01 – 23
	REFERENCES	24 – 35
CHAPTER – II	MATERIALS AND METHODS	36 – 42
CHAPTER - III	SYNTHESIS AND	43 – 75
	CHARACTERIZATION OF	
	LIGANDS	
	REFERENCES	76
CHAPTER - IV	SYNTHESIS	77 - 142
	CHARACTERIZATION AND	
	ANTIMICROBIAL ACTIVITY	
	OF METAL CHELATES	
	REFERENCES	143 – 145
	PUBLICATIONS	146 - 147

DEDICATION

Dedicated to my parents

Mr. Pravinbhai Patel & Mrs. Parulben Patel



CHAPTER – I

INTRODUCTION

CONTENTS

1.1 INTRODUCTION

1.2 METAL COMPLEXES IN PHARMACEUTICALS

1.3 COMMON AROMATIC LIGANDS

1.4 POLYDENTATE LIGANDS OF AMIDE GROUPS

1.1 INTRODUCTION

A Lewis acid-base reaction product of organic ligand and metal ion via co-ordination bond is known as metal complex. Here bases are ligands and metal ions are acids. The metal complexes are known as co-ordination compounds and their physical/chemical properties are almost different from parent ligands & metal ions.

1.1.1 History

Metal complexes are known from beginning of chemistry, the dye Prussian blue is known from 1800s and it is well recognized by C. Blomstrand (1869)¹. He established the theory of metal complexes and later on Jorgensen² improved the theory. He claimed that the ammonium ion binds directly to metal ion in solution. Werner³ established the metal complexation theory. He explained that two possible ions could be located in co-ordination sphere. The ions bound directly to metal ions within co-ordination cluster. The spatial arrangement of ligands and metal ions in coordination sphere was also discussed.

1.1.2 Geometry

The structures of coordination compounds can be established by their coordination numbers (Number of ligands coordinated to central metal ions). They are mostly 2 to 9. The numbers are dependent on size, charge and electronic configuration of metal ions and the ligands. The possible geometries of coordination compounds are given in the Table 1.1.

Table 1.1: Geometries of coordination compounds

Geometry	Coordination number	Examples
Linear	2	$[\text{Ag}(\text{NH}_3)_2]^+$
Trigonal planar	3	$[\text{Cu}(\text{CN})_3]^{2-}$
Tetrahedral square planar	4	$[\text{NiCl}_4]^{2-}$
Square pyramidal	5	$[\text{VO}(\text{CN})_4]^{2-}$
Octahedral	6	$[\text{CoCl}_6]^{3-}$
Pentagonal	7	$[\text{ZrF}_7]^{3-}$
Square antiprismatic	8	$[\text{ReF}_8]^{2-}$
Tricapped trigonal prismatic	9	$[\text{ReH}_9]^{2-}$

The main Structure of the metal chelates are Square Planar, Octahedral and Tetrahedral (Fig. 1.1).

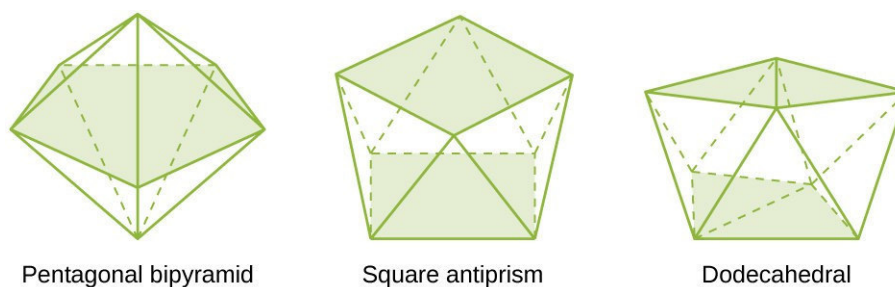


Fig. 1.1: Some Common Sphere of Complexes

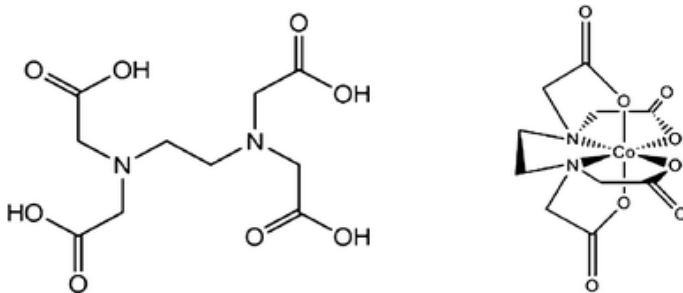
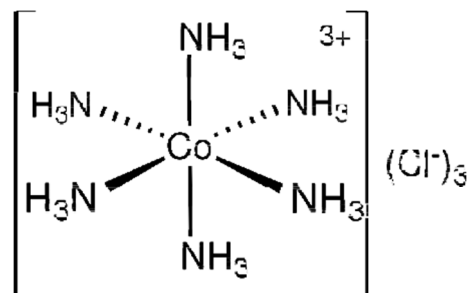
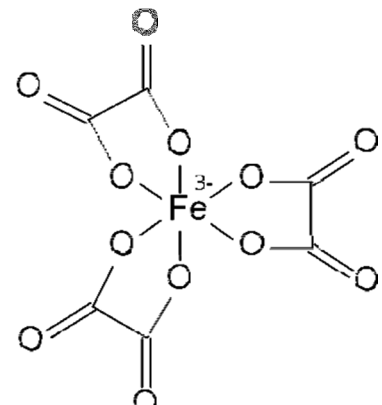
Stereoisomerism is there in certain cases. These are cis- and trans- isomerism.

1.1.3 Classification

The co-ordination complexes are classified as follow:

(a) Classical or Werner complexes

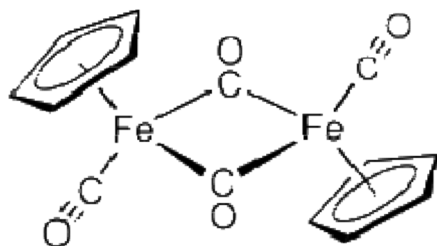
In this structure metal binds by ligand via lone pair of electrons. e.g., H_2O , NH_3 , Cl^- , CN^- . Some examples are:

Example	Structure
Cobalt-EDTA complex	
Hexamminecobalt(III) chloride	
Ferrioxalate	

(b) Organo-metallic compounds

Alkenes / alkynes, cycloalkyls with phosphines, hydride, CO, etc.

Cyclopentadienyliron dicarbonyl dimer is a good example

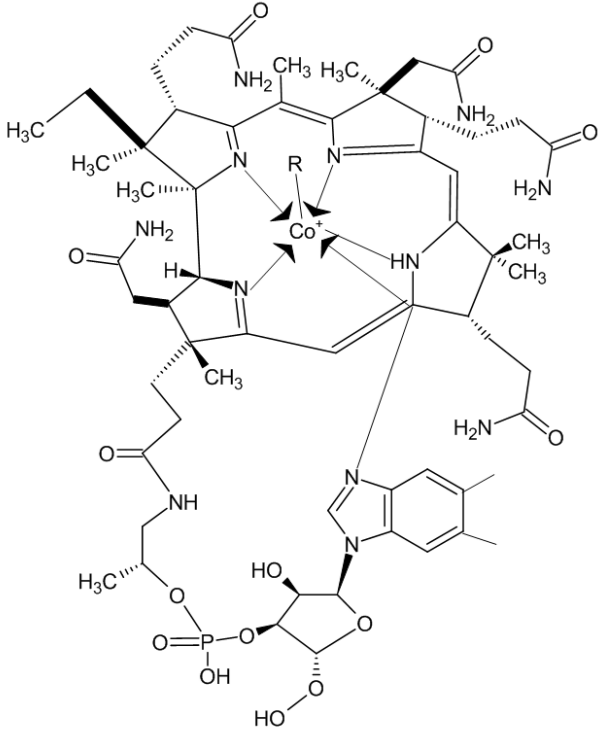
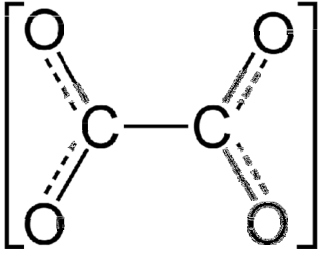


(c) **Bioinorganic complexes**

These complexes are obtained naturally. It includes side chains of amino acids, co-factors, porphyrins, etc.

Some examples are:

Example	Structure
Hemoglobin – Fe complex	
Chlorophyll – Mg complex	

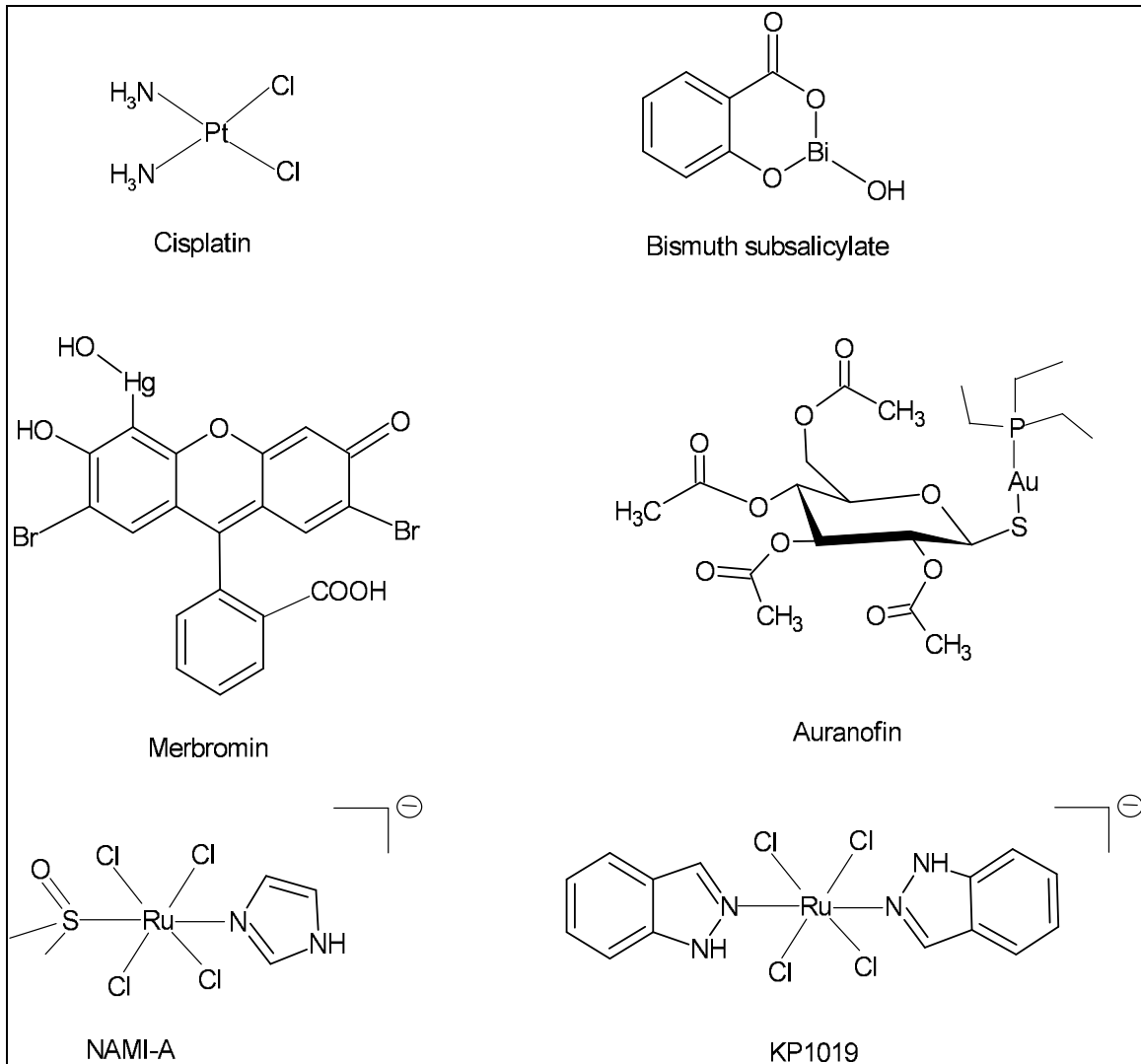
<p>Vitamin B12 – Co complex</p>	 <p>The diagram shows the complex structure of Vitamin B12, specifically the cobalamin ring system coordinated to a central cobalt (Co) ion. The cobalt ion is coordinated to four nitrogen atoms within the corrin ring. Various side chains are attached to the ring, including methyl groups (CH₃), amino groups (NH₂), and a dimethylbenzoyl group. A ribityl chain is attached to the ring, which is further linked to a ribose sugar. The ribose sugar is phosphorylated at the 5' position, forming a phosphate group (P=O, OH) that is coordinated to the cobalt ion. The overall structure is highly complex and multi-ring.</p>
<p>Calcium oxalate – Ca complex</p>	 <p>The diagram shows the chemical structure of the calcium oxalate complex. It consists of two calcium ions (Ca²⁺) coordinated to two oxalate ions (C₂O₄²⁻). The oxalate ions are shown as two carbon atoms (C) bonded to four oxygen atoms (O). The calcium ions are coordinated to the oxygen atoms of the oxalate ions, forming a complex structure. The entire complex is enclosed in square brackets with a charge of 0.</p>

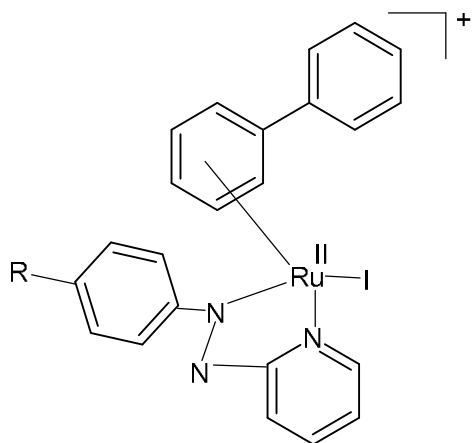
All these complexes are most important for our human life.

1.2 METAL COMPLEXES IN PHARMACEUTICALS

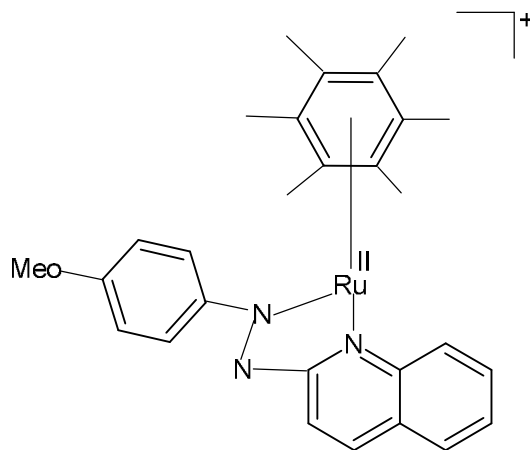
Metal ions play a pivotal role in humans deficiency of some metal created diseases like anemia, growth retardation, heart disease, etc. So, metal complexes in form of drug become an important platform in medicinal chemistry. It is known that transition metal complexes can be used as drug to cure several human diseases⁴⁻⁶. Metal like platinum, gold, lithium, zinc, silver, copper, lanthanum, bismuth, barium, mercury, etc. are useful for drug applications.

Some important metal complexes are used (Anticancer agents). These metal complexes are well known for their use as *in vivo* and *in vitro* anticancer activities⁷⁻¹⁰.

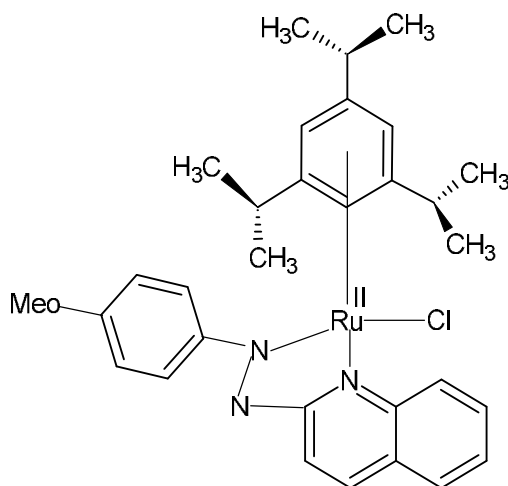




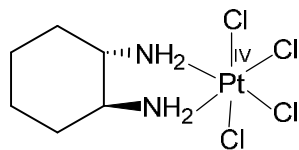
$[Ru(h^6\text{-bip})(p\text{-azpy-R})]^+$
 $R=N(CH_3)_2OH$



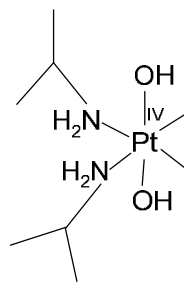
RAS - 1H



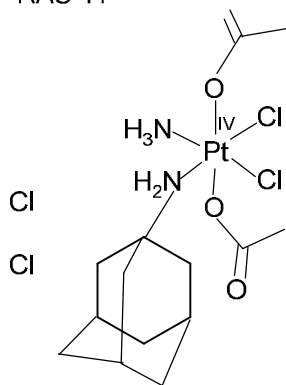
RAS-1T



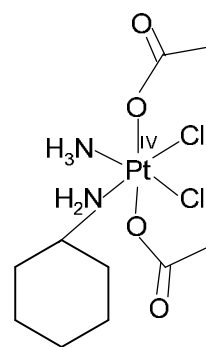
Tetraplatin



Iroplatin



LA-12



Starplatin

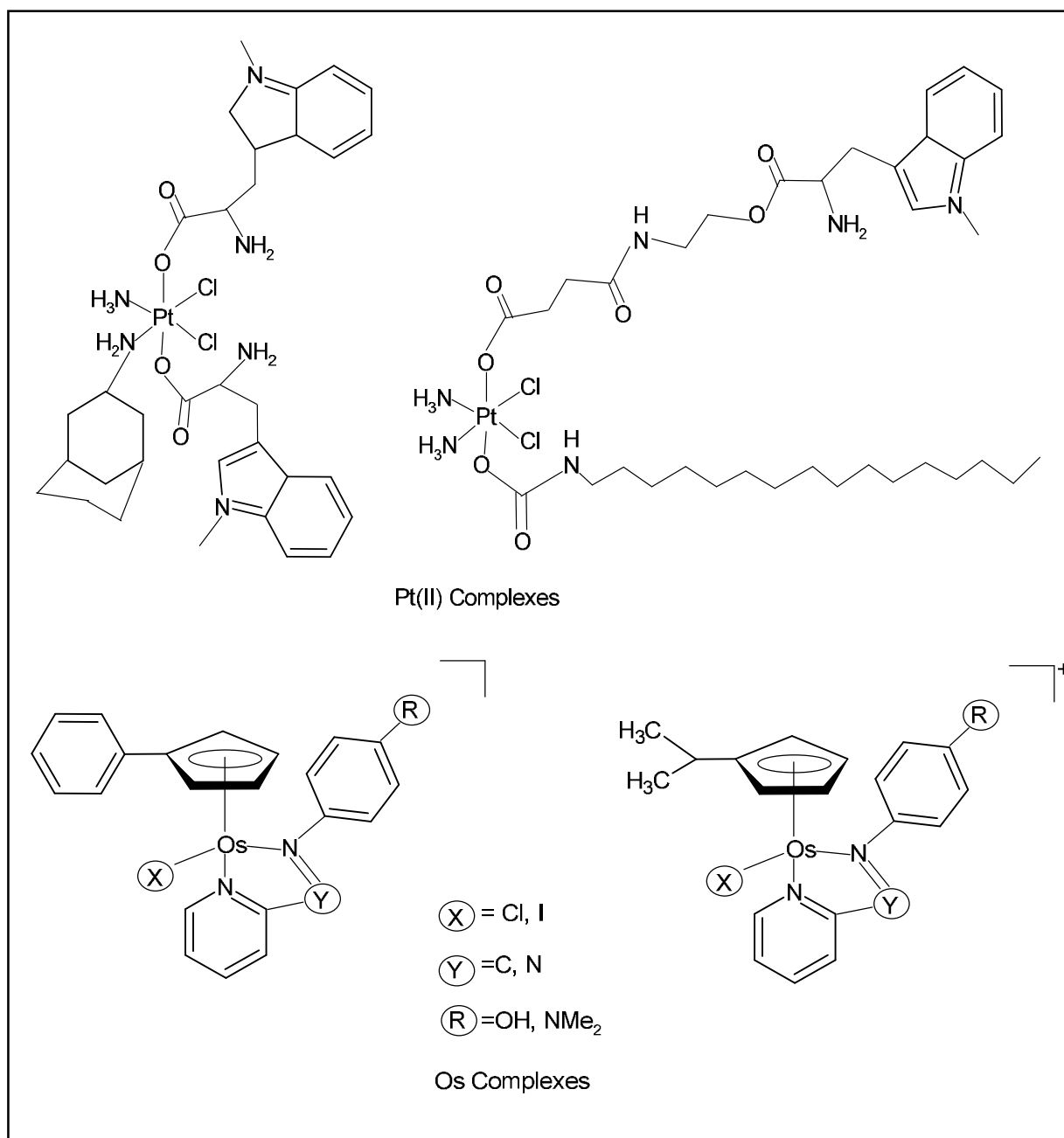


Fig. 1.2: Some Co, Ru, Pt and Os metal complexes exhibiting redox mediated anticancer activity

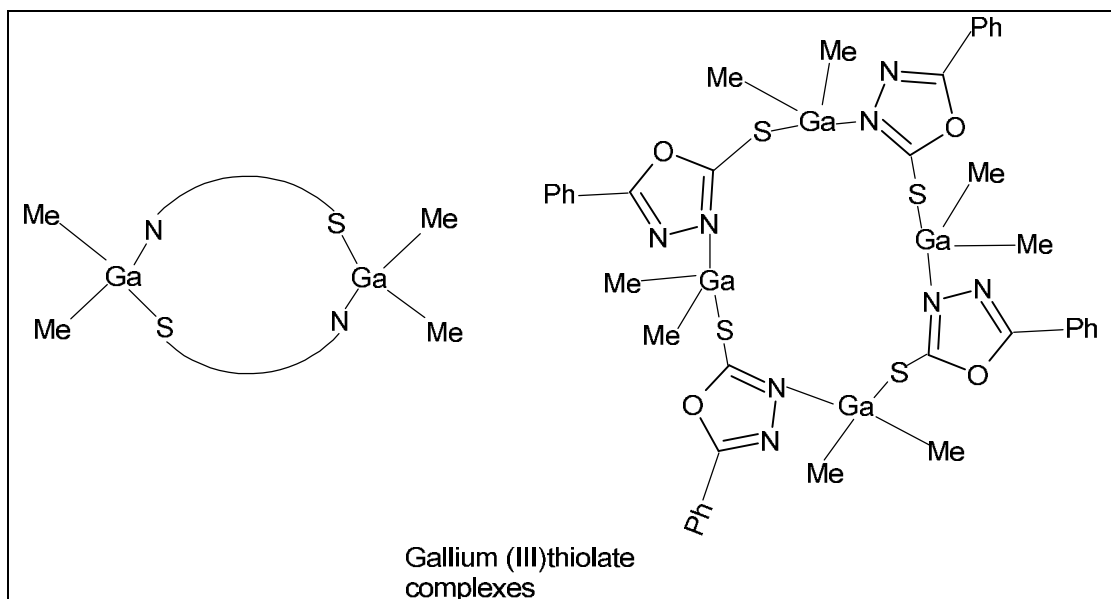


Fig. 1.3: Heterocyclic thiolate polynuclear gallium (III) derivatives with anticancer activity.

Many metal complexes¹¹⁻²⁴ solved the problem created in insulin injection for diabetic patients.

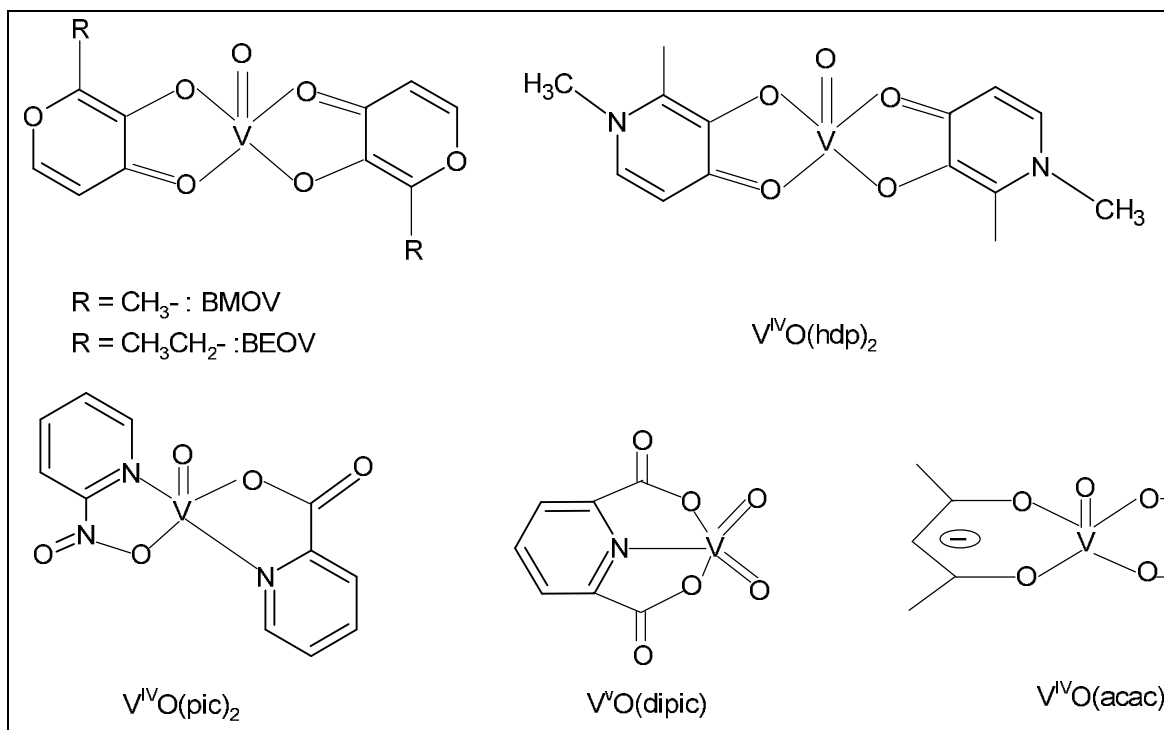


Fig. 1.4: Structures of some insulin mimetic vanadium complexes.

The amyloid β -targeted metal complexes bear excellent anti Alzheimer's diseases²⁵.

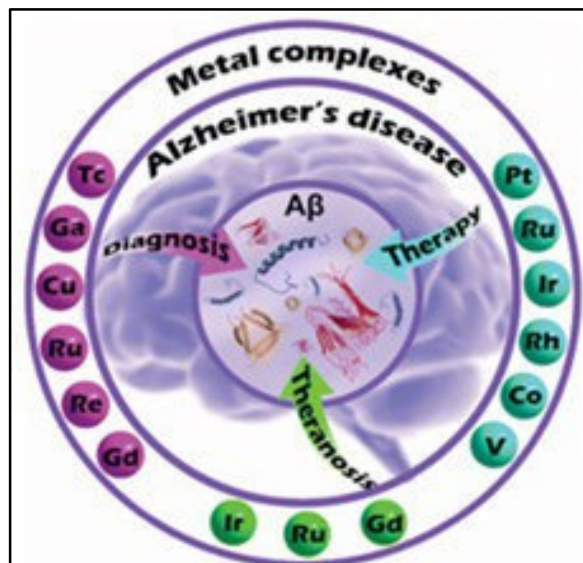


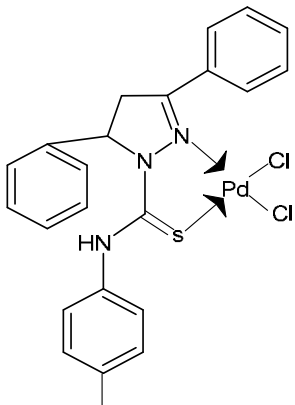
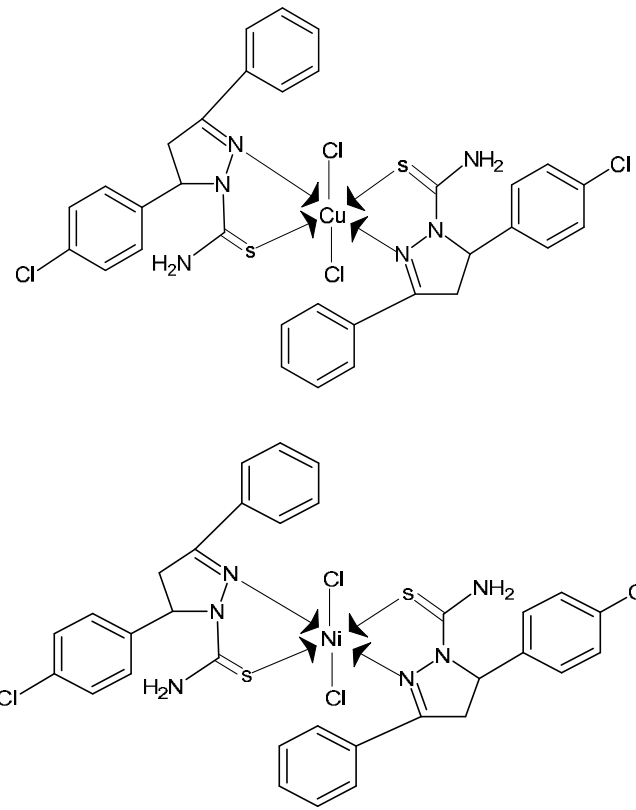
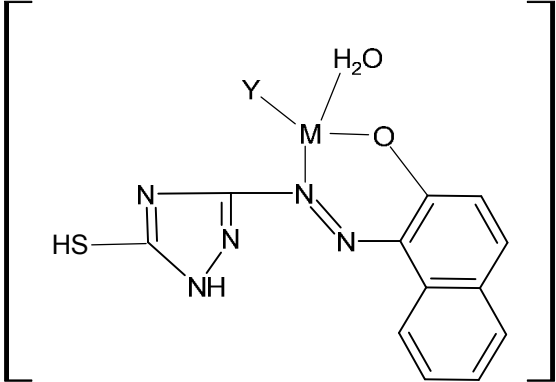
Fig. 1.5: Metal complexes for potential applications in Alzheimer's disease

Number of metal complexes of zinc, silver, mercury, etc. are used commonly as:

Antimicrobial:

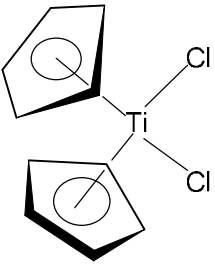
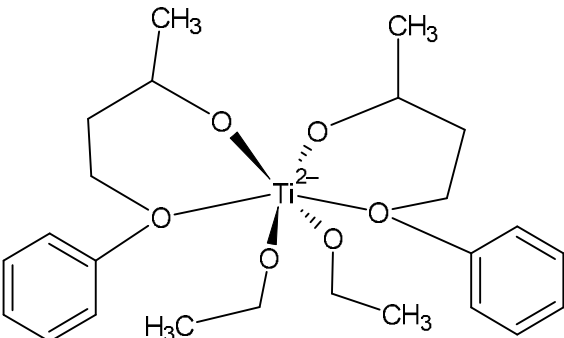
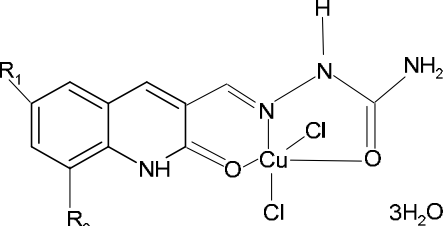
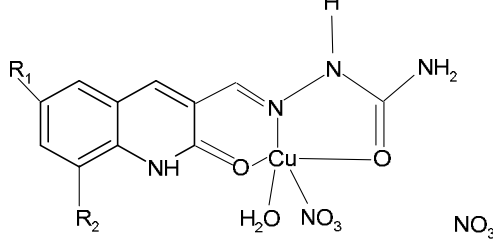
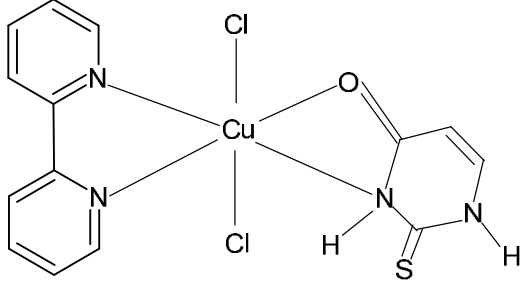
The complexes with their antimicrobial activity²⁶⁻³².

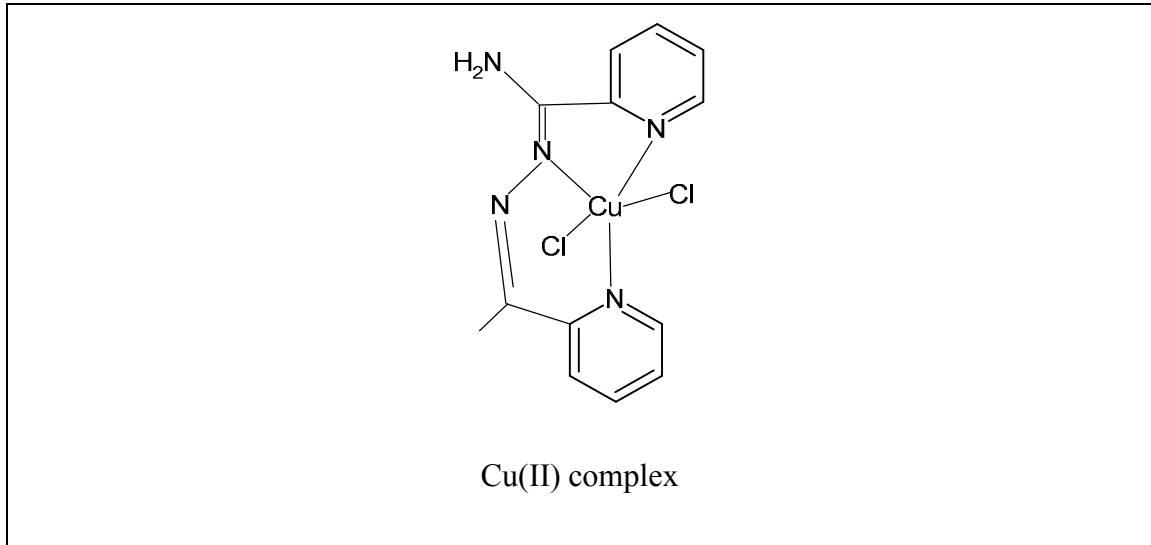
Structure	Activity
<p>Y.x H₂O Y= 2Cl, SO₄, or 2(CH₃COO)</p>	<p><i>Escherichia coli</i> and <i>Staphylococcus aureus</i></p>

	<p><i>Entamoebahistolytica</i></p>
	<p><i>Candida strains</i></p>
 <p style="text-align: right;">.X H₂O</p>	<p><i>Escherichia coli,</i> <i>Staphylococcus aureus,</i> <i>Aspergillus flavus</i> and <i>Candida albicans</i></p>

Anticancer:

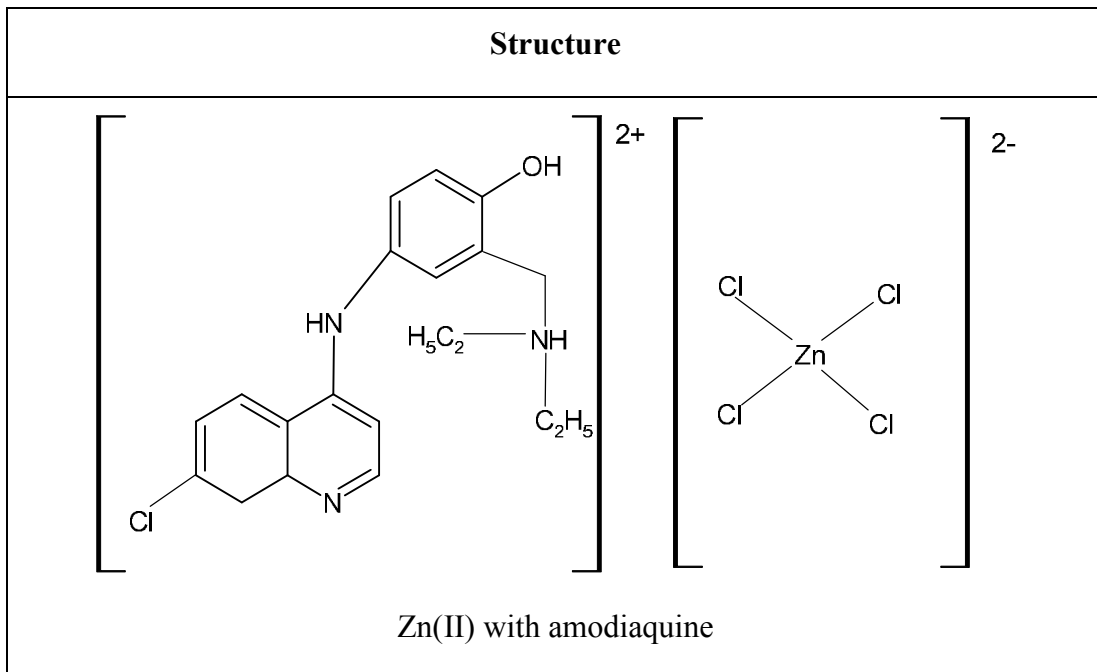
These complexes of Ti and Cu display anticancer activity³³⁻³⁶.

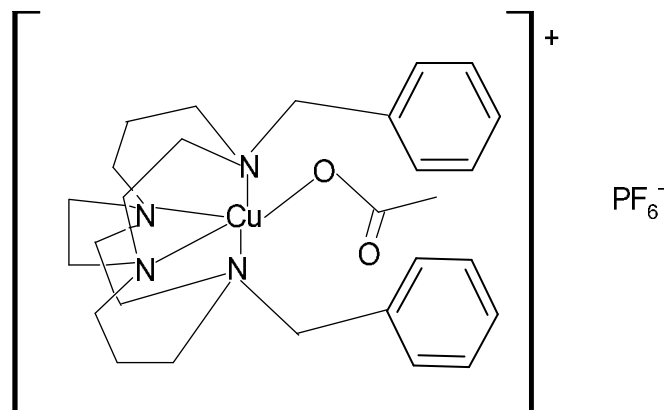
Structure	
	
Titanocene dichloride	Budotitane
	
Cu (II) complexes	
	
Cu(II) complex	



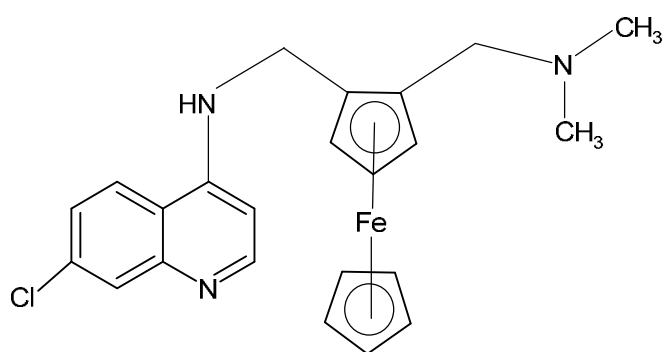
Antimalarial:

Some metal chelates such of gold, ruthenium, cobalt, rhodium, copper, cobalt, zinc, osmium and palladium show effective antimalarial activity³⁷⁻⁴⁵.

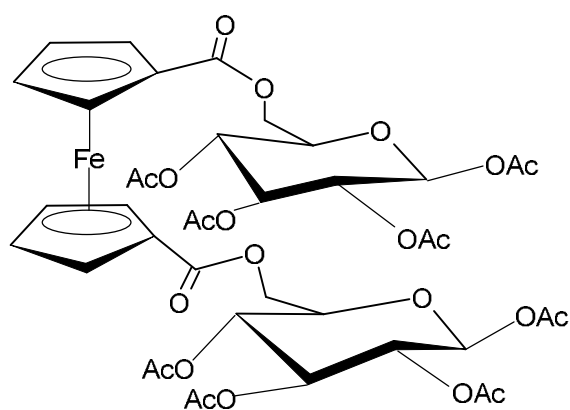




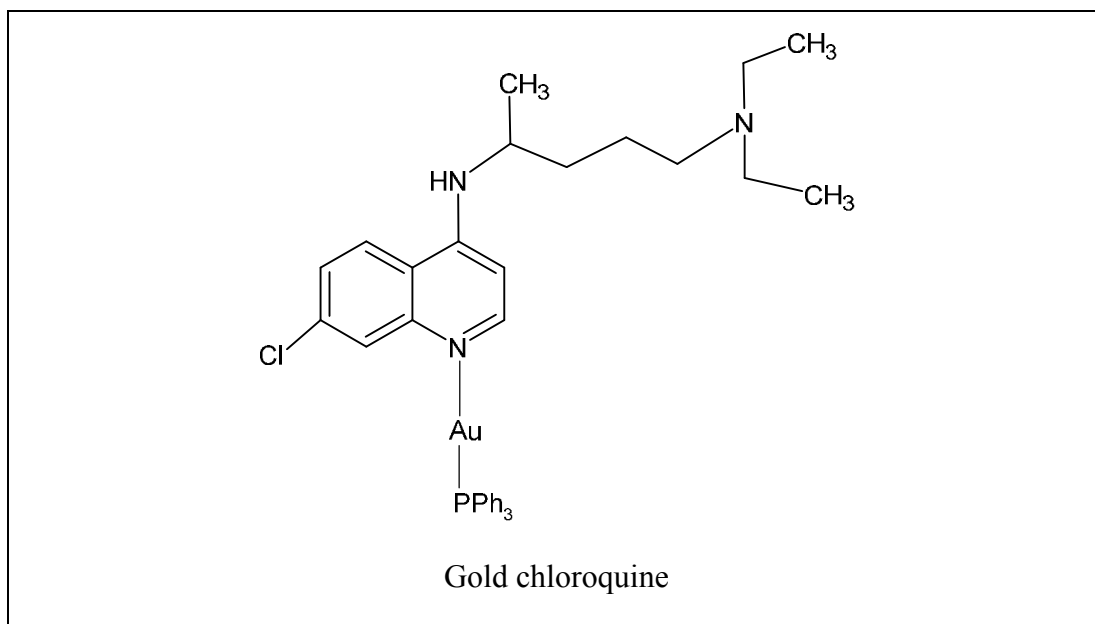
Cu(II) Complex



Ferroquine(7-chloro-[2-N,N-dimethyl-aminomethyl]
ferrocenylmethylamino]quinolone

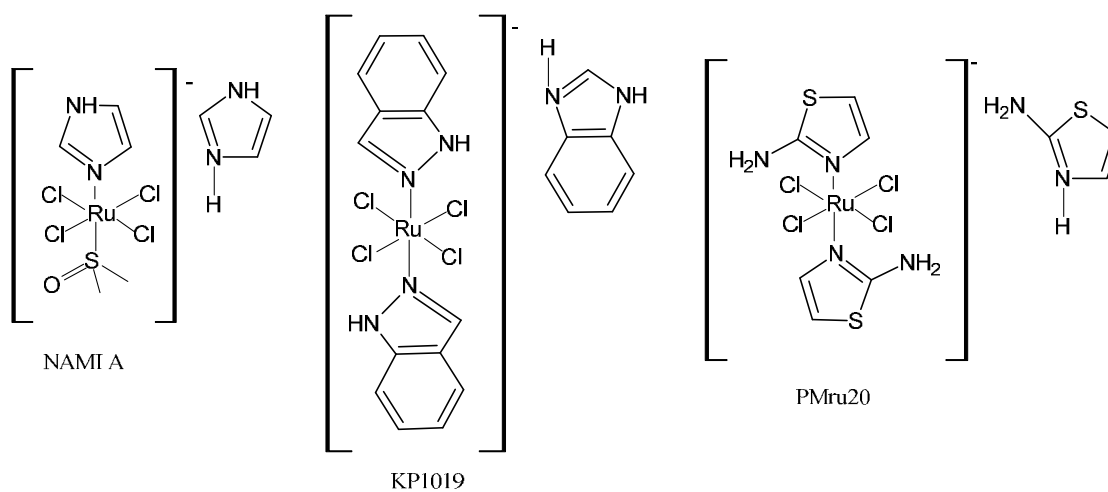


Ferrocenyl carbohydrate conjugate



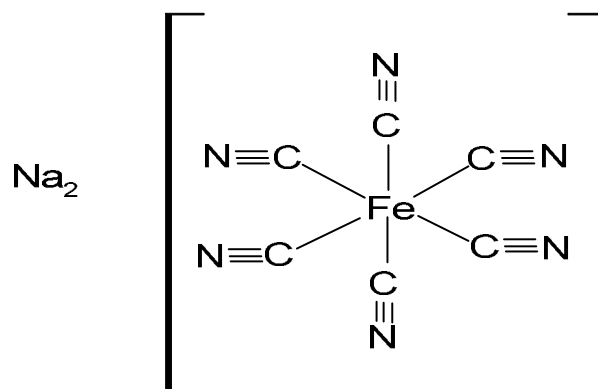
Anti-Alzheimer:

These metal complexes exhibited ability in blocking β -amyloid aggregation and scavenging its toxicity. Some complexes of ruthenium (III) exhibited significant role as anti-Alzheimer agents such as NAMI A, KP1019 and PMRU20⁴⁶.



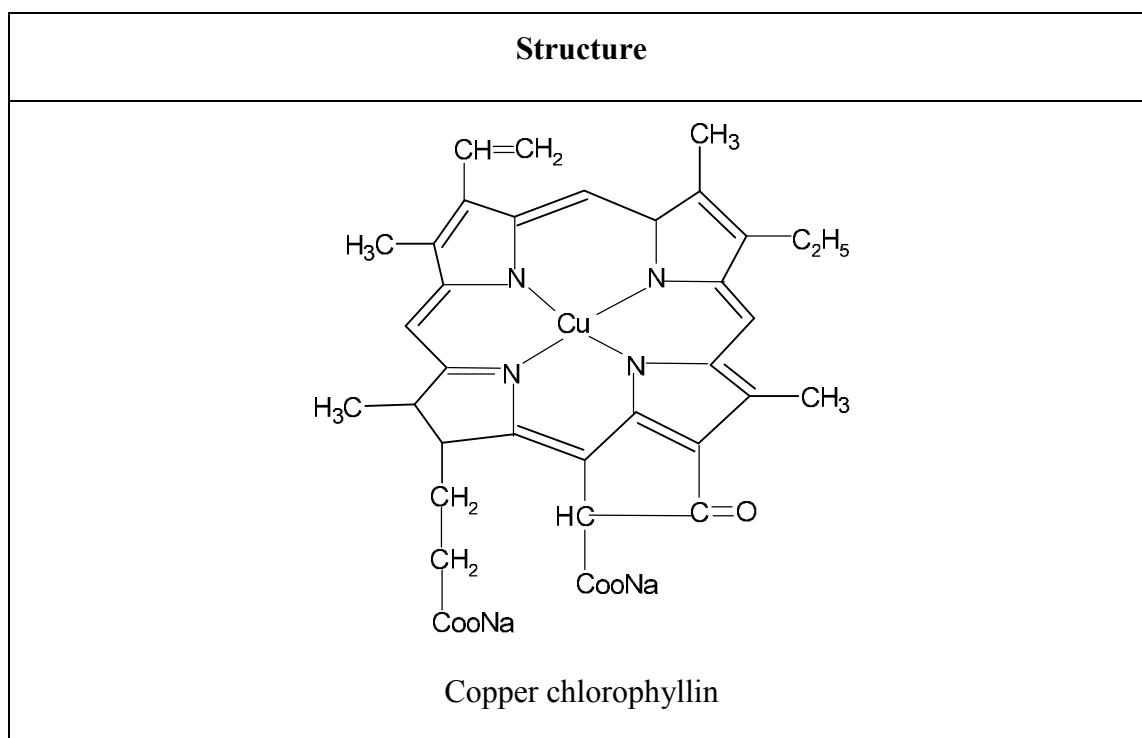
Antihypertensive:

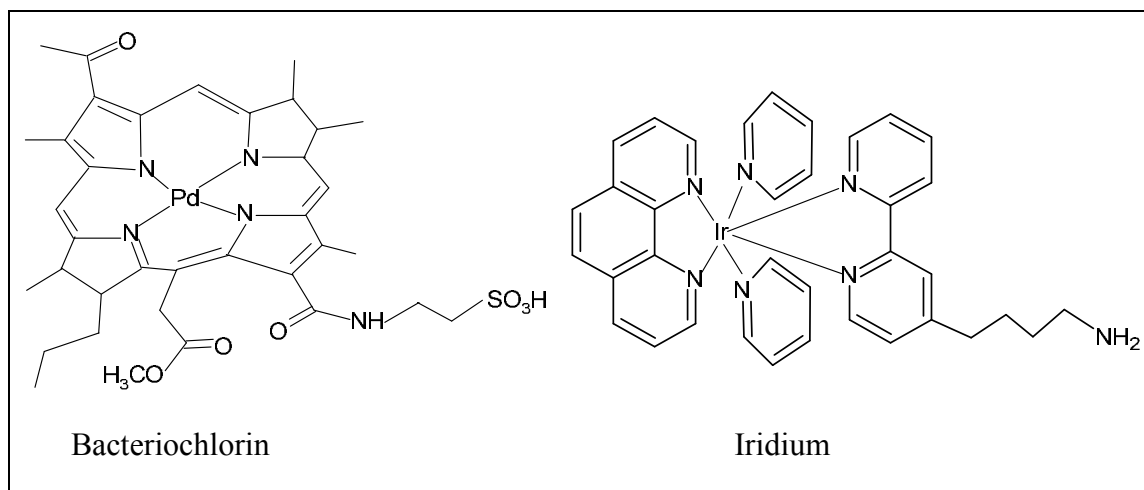
Sodium nitroprusside was below used for lowering blood pressure.⁴⁷⁻⁵²



Sodium nitroprusside

Some metal complexes also find utility in cosmetics, photodynamic therapy more particularly Covid-19 virus.⁵²⁻⁵⁶

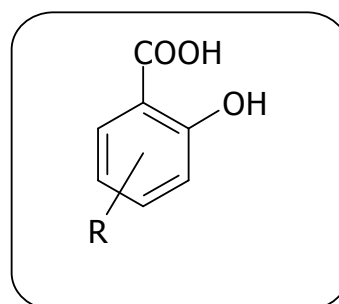




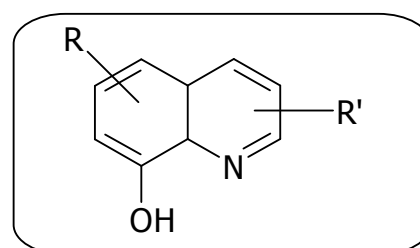
1.3 COMMON AROMATIC LIGANDS

Some of aromatic ligands used mostly are bidentate and these are;

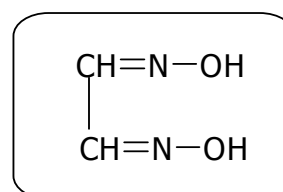
- Salicylic acid



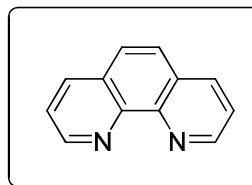
- 8-Hydroxy quinoline



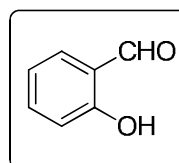
- Dimethylglyoxime



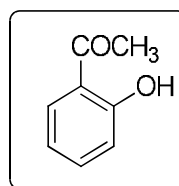
➤ 1,10-Phenanthrene



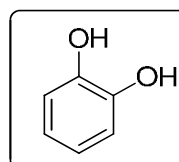
➤ Salicylaldehyde



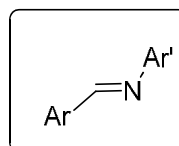
➤ o-Hydroxy acetophenone



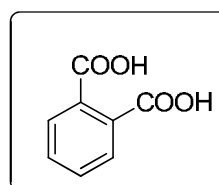
➤ Catechol



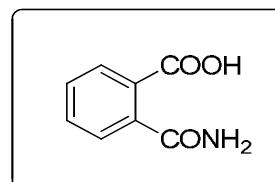
➤ Schiff base



➤ Phthalic acid



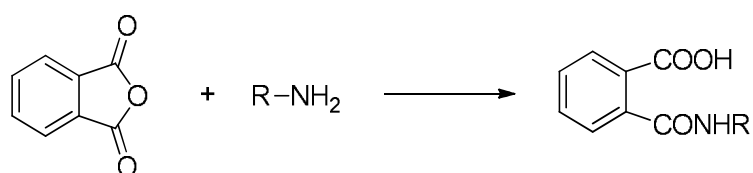
➤ Phthalamic acid



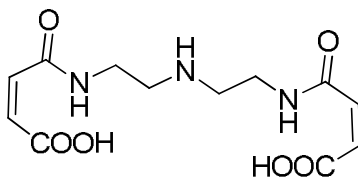
1.4 POLYDENTATE LIGANDS OF AMIDE GROUPS

Over the past few decades, revealed that peptides (Amides) have stability, versatility, optical properties and ease of their availability and in modification⁵⁷. Their transition metal complexes have prominent application as catalyst in organic synthesis. As metal complexes of such ligands are more stable under physiological conditions, and they also received attraction in the field of physics, biology and medicines⁵⁸⁻⁹⁶.

The amide groups are based on acid-amine reactions. The easy reaction between anhydride and amine afforded amide.



Such amide can display metal complexing capacity. Vishwanathan and Krishnan⁹⁷ studied the metal complexation of such amides prepared from maleic anhydride and diamine.

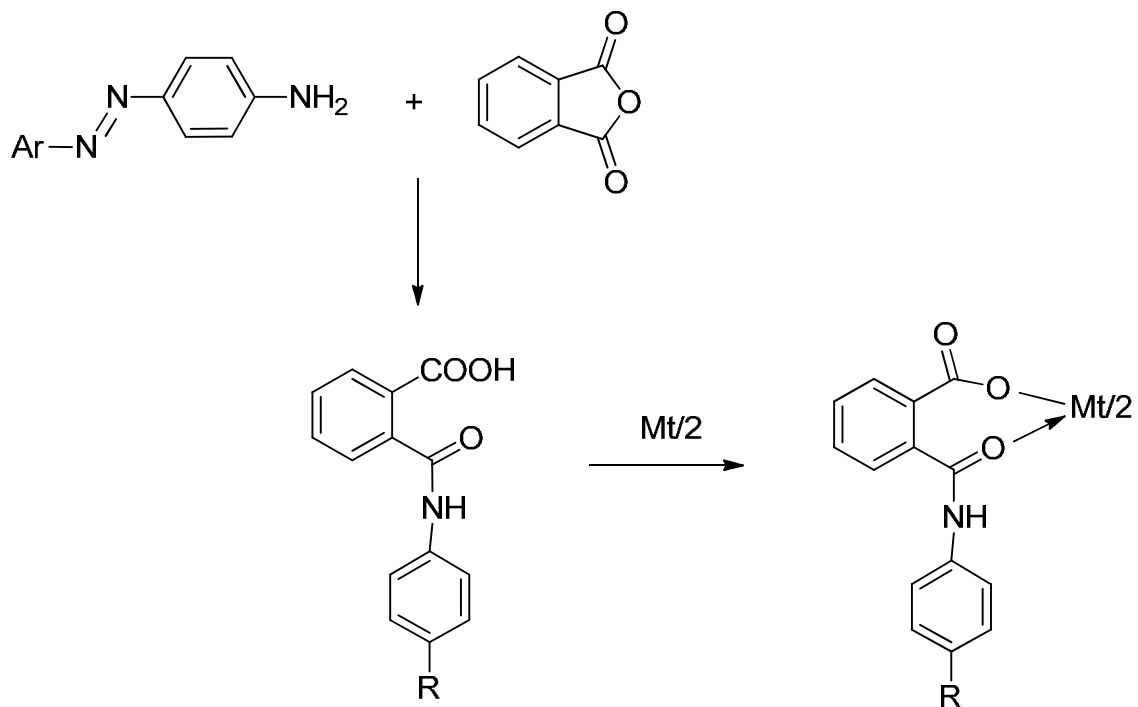


Polydentate lignd

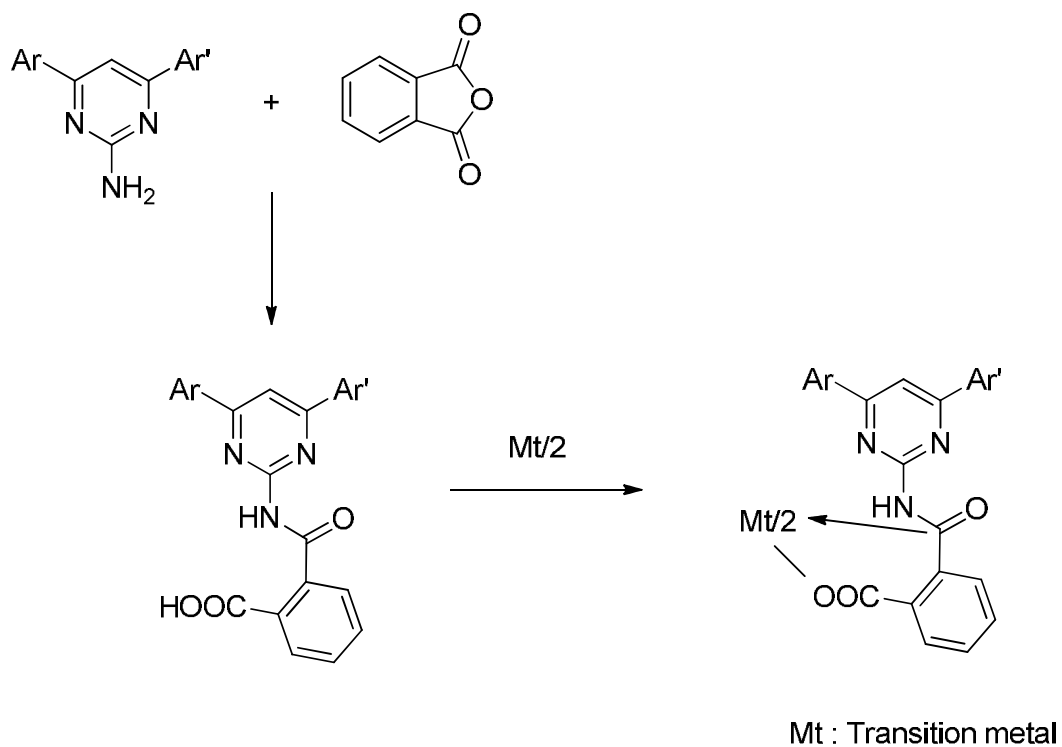
The structure as Mn²⁺, Co²⁺, Ni²⁺, Cu²⁺, Zn²⁺, Cu²⁺, Zn²⁺, Cd²⁺, and VO⁴⁺ complexes have been studied.

Patel and Patel⁹⁸ prepared ligand from the reaction between an azo dye/aminopyrimidine and phthalic anhydride. They also prepare complexes of this ligand with metal ions.

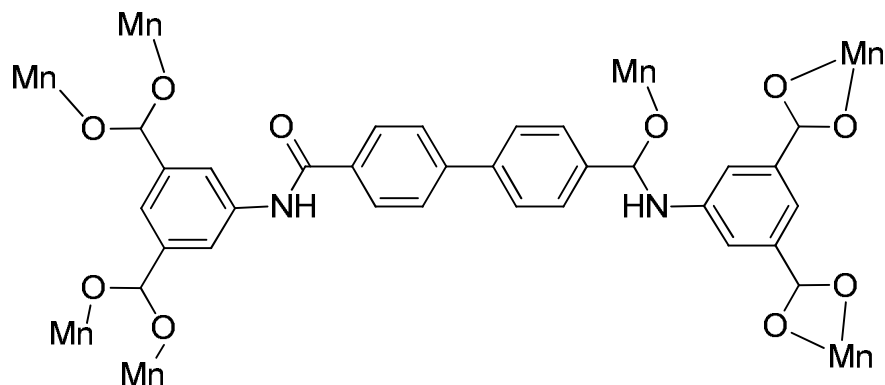
Basic azo dyes + Phthalic anhydride



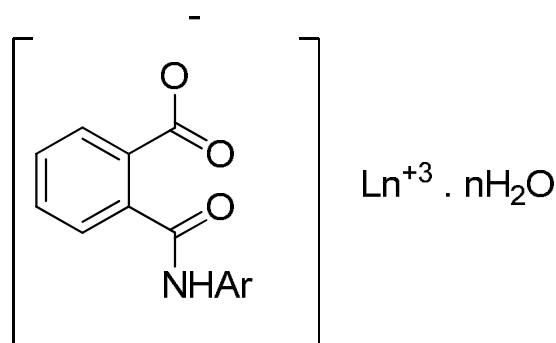
Amino Pyrimidine + Phthalic anhydride



Zhu et al.⁹⁹ Synthesized the ligand from amino isophthalic acid and biphenyl acid. The Mn²⁺ complex of this ligand was prepared and characterized by X-ray diffraction, IR spectroscopy and thermogravimetry.

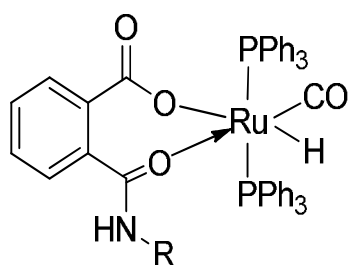


Chernyshova et al.¹⁰⁰ Synthesized and used it for preparation of complexes of europium, terbium and gadolinium derivatives. They also studied their luminescent behavior. It was also indicated that Eu³⁺ and Tb³⁺ complexes bear luminescence.



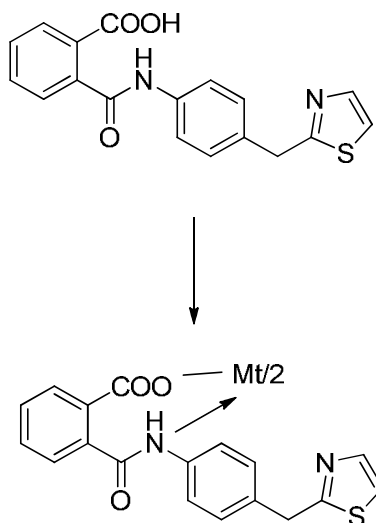
Where, Ln³⁺= Eu³⁺, Gd³⁺ and Tb³⁺

Deyakar and Lingaiah¹⁰¹ reported ruthenium complexes of phthalamic acid and observed their physicochemical properties. Ashok et al.¹⁰² also reported Ru³⁺ complexes at phthalamic acid and reported their catalytic activity.



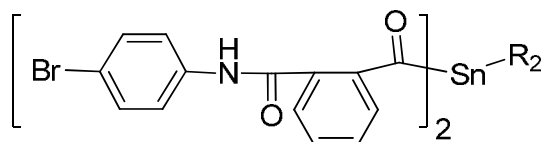
R = Phenyl, 2-Benzimidazolyl, 1-Naphthyl

Edozie et al.¹⁰³ used sulfathiazole containing phthalamic acid as ligand. They prepared Fe^{2+} and Mn^{2+} complexes and observed charge transfer intensity and antibacterial activity. It was found that complexes show very good antibacterial activity.



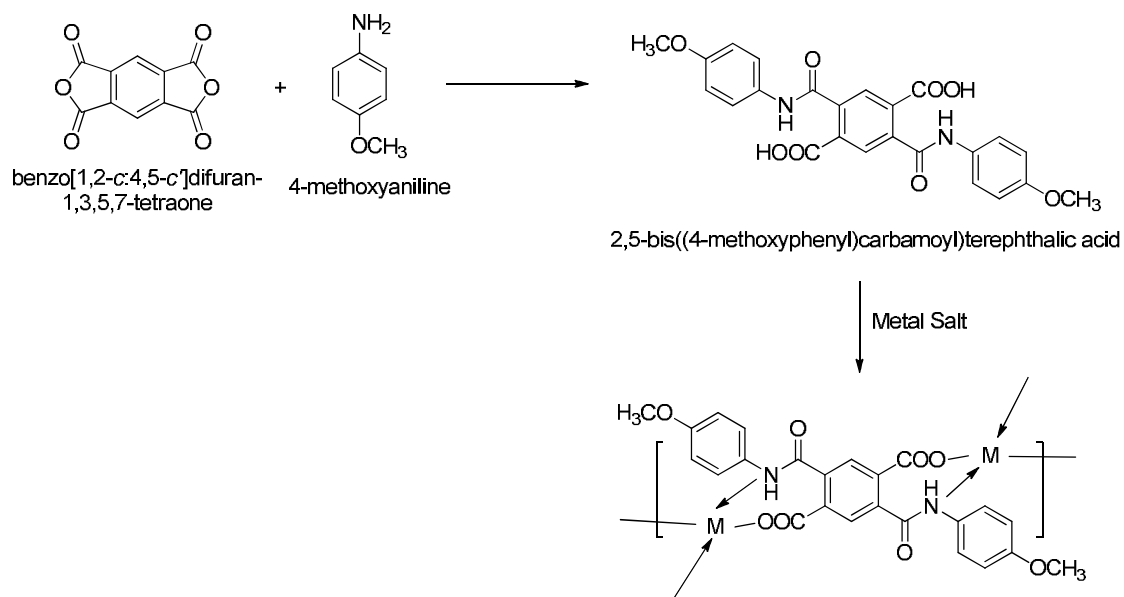
Where, $\text{Mt}/2 = \text{Fe}^{+2} \text{ \& \ } \text{Mn}^{+2}$

Shahid et al.¹⁰⁴ synthesized organo tin complexes of phthalamic acid and characterized these.



$\text{R} = \text{Me}$

Patel et al.¹⁰⁵ reported the coordination polymer based on bistype phthalamic acid. They synthesized ligand containing terephthalic acid with orthoarylaminocarbonyl derivatives.



Various ligands have been utilized from time to time to form complexes of metal ions. These were found biologically active. There is great scope in making some new ligands to prepare metal ion complexes and investigate their antimicrobial activity.



REFERENCES

- [1.] G. N. Lewis, The Atom and the Molecules. *J. Ann. Chem. Soc.*, **38**(4), 762-785 (1916).
- [2.] A. Kraft, on the discovery and History of Purssuine Blue. *Bull. Hist. Chem.*, **33**(2), 61-67 (2008).
- [3.] G. B. Kauhman, C. W. Blomstrand, Swedish Chemist Mineralogist., *Annals. of Sci.*, **32**, 13-37 (1975).
- [4.] C. Orvig, and M. J. Abrams, Medicinal Inorganic Chemistry: Introduction. *Chem. Rev.*, **99**(9), 2201–2204 (1999).
- [5.] M. Yaman, G. Kaya, and H. Yekeler, Distribution of trace metal concentrations in paired cancerous and non-cancerous human stomach tissues. *World. J. Gastroenterol.*, **13**(4), 612–618 (2007).
- [6.] A. A. Warra, Transition metal complexes and their application in drugs and cosmetics – A Review *J. Chem. Pharm. Res.*, **3**(4), 951-958 (2011).
- [7.] C. F. Shaw, Gold-based therapeutic agents. *Chem. Rev.*, **99**(9), 2589-2600 (1999).
- [8.] C. S. Allardyce, and P. J. Dyson, Metal-based drugs that break the rules. *Daltan. Trans.*, **45**(8): 3201-3209 (2016).
- [9.] R.W. Sun, D. L. Ma, E. L. Wong, and C. M. Che, Some uses of transition metal complexes as anti-cancer and anti-HIV agents. *Dalton Trans.*, **43**, 4884– 4892 (2007).
- [10.] P. Zhang, and P. J. Sadler, Redox-Active Metal Complexes for Anticancer Therapy. *Eur. J. Inorg. Chem.*, **12**, 1541–1548 (2017).
- [11.] S. Yoshimoto, K. Sakamoto, I. Wakabayashi, and H. Masui, Effect of chromium administration on glucose tolerance in stroke prone spontaneously hypertensive rats with streptozotocin –induced diabetes. *Metabolism*, **41**(6), 636-642 (1992).

- [12.] S. Subasinghe, A. L. Greenbaum, and P. McLean, The insulin-mimetic action of Mn^{2+} : involvement of cyclic nucleotides and insulin in the regulation of hepatic hexokinase and glucokinase. *Biochem. Med.*, **34**(1): 83-92 (1985).
- [13.] A. T. Ozcelikay, D. J. Becker, L. N. Ongemba, A. M. Pottier, and J. C. Henquin, et al. Improvement of glucose and lipid metabolism in diabetic rats treated with molybdate. *Am. J. Physiol.*, **270**(2 Pt 1): E344-352 (1996).
- [14.] S. Sitasawad, M. Deshpande, M. Katdare, S. Tirth, and P. Parab, Beneficial effect of supplementation with copper sulfate on STZ-diabetic mice (IDDM). *Diab. Res. Clin. Pract.*, **52**(2): 77-84 (2001).
- [15.] P. L. Walter, A. Kampkötter, A. Eckers, A. Barthel, and D. Schmoll, et al. Modulation of FoxO signaling in human hepatoma cells by exposure to copper or zinc ions., *Arch. Biochem. Bio.*, **454**(2), 107-113 (2006).
- [16.] J. Ybarra, A. Behrooz, A. Gabriel, M. H. Koseoglu, and F. Ismail-Beigi Glycemia-lowering effect of cobalt chloride in the diabetic rat: increased GLUT1 mRNA expression. *Mol. Cell. Endo.*, **133**, 151-160 (1997).
- [17.] J. M. May, and C. S. Contoreggi, The mechanism of the insulin-like effects of ionic zinc. *J. Biol. Chem.*, **257**(8), 4362-4368 (1982).
- [18.] H. Sakurai, K. Tsuchiya, M. Nukatsuka, M. Sofue, and J. Kawada, Insulin- like effect of vanadyl ion on streptozotocin-induced diabetic rats. *J. Endo.*, **126**(3), 451-459 (1990).
- [19.] J. Meyerovitch, Z. Farfel, J. Sack, and Y. Shechter, Oral Administration of Vanadate Normalizes Blood Glucose Levels in Streptozotocin-treated Rats. *J. Biolchem.*, **262**(14), 6658-6662 (1987).
- [20.] Y. Shechter, and S. J. Karlsh, Insulin-like stimulation of glucose oxidation in rat adipocytes by vanadyl (IV) ions. *Nature*, **284**(5756), 556-558 (1980).
- [21.] C. E. Heyliger, A. G. Tahiliani, and J. H. McNeill, Effect of vanadate on elevated blood glucose and depressed cardiac performance of diabetic rats. *Science*, **227**(4693), 1474-1477 (1985).

- [22.] B. A. Reul, S. S. Amin, J. P. Buchet, L. N. Ongemba, D. C. Crans , S. M. Brichard, Effects of vanadium complexes with organic ligands on glucose metabolism: a comparison study in diabetic rats. *Br. J. Pharm.*, **126**(2), 467- 477 (1999).
- [23.] Y. Ellahioui, S. Prashar, and S. Gómez-Ruiz, Anticancer Applications and Recent Investigations of Metallodrugs Based on Gallium, Tin and Titanium. *Inorganics*, **5**, doi.10.3390/inorganics5010004 (2017).
- [24.] H Liu, Y. Qu, and X. Wang, Amyloid β -targeted metal complexes for potential applications in Alzheimer's disease. *Future Med. Chem.*, **10**(6), 679–701 (2018).
- [25.] M. R. Díaz, and P. E. Vivas-Mejia, Nanoparticles as drug delivery systems in cancer medicine: emphasis on RNAi-containing nanoliposomes. *Pharmaceuticals (Basel)*, **6**(11), 1361–1380 (2013).
- [26.] H. S. Mohammed, and V. D. Tripathi, Medical applications of coordination complexes, *J. of Phy. Conference series*, **1664**, doi.10.1088/1742-6596/1664/1/012070 (2020).
- [27.] H. S Mohammed, and V. D. Tripathi, Synthesis, characterization, DFT calculation and antimicrobial activity of Co(II) and Cu(II) complexes with azo dye. *J. of Phy. Conference series*, **1294**, doi:10.1088/1742- 6596/1294/5/052051 (2019).
- [28.] V. Uivarosi, Metal complexes of quinolone antibiotics and their applications, *Molecules*, **18**, 11153-11197 (2013).
- [29.] Z. H Chohan, H. A Shad, and H. Ben, Some new biologically active metal based sulfonamide. *Eur. J. of Med. Chem.*, **45**, 2893-2901 (2010).
- [30.] G. Psomas, A. Tarushi, Y. Sanakis, and N. Katsaros, Synthesis, structure and biological activity of Copper (II) complexes with oxolinic acid. *J. of Inorg. Biochem.*, **100**, 1764-1773 (2006).

- [31.] Y. O. Ayipo, J. A. Obaleye, and U. M. Badeggi, Novel metal complexes of mixed Piperazine-acetaminophen and Piperazine-acetylsalicylic acid: synthesis, characterization and antimicrobial activities. *J. of Turk. Chem. Society Section-A, Chemistry*, **4**(1), 313-326 (2016).
- [32.] M. S. Hossain, C. M. Zakaria, et al. Metal complexes as potential antimicrobial agent: A Review. *Am J. of Hetero. Chem.*, **4**, 1-21 (2018).
- [33.] K. M. Buettner, and A. M. Valentine., Bioorganic chemistry of titanium, *Chemical Reviews*, **112**(3), 1863-1881 (2012).
- [34.] F. Caruso, and M. Rossi, Antitumor titanium compounds, *Mini reviews in Medicinal Chemistry*, **4**, 49-60 (2004).
- [35.] G. Silva, F. Dantas, and A. Araujo de Almeida-Apolonio, A promising copper (II) complex as antifungal and antibiofilm drug against yeast infection, *Molecules*, **23**, doi.10.3390/molecules23081856 (2018).
- [36.] Gokhale, N. H., Padhye S. S., Copper complexes of carboxamidrazone derivatives as anticancer agents. *Inorg. Chem. Acta.*, **319**, doi.10.1016/S0020-1693(01)00446-7 (2001).
- [37.] R. O. Arise, S. N. Elizabeth, S. T. Farohunbi, M. O. Nafiu, and A. C. Tella, Mechano-chemical Synthesis, In vivo Anti-malarial and Safety Evaluation of Amodiaquine-zinc Complex. *Acta Facultatis Medicae Naissensis*, **34**, 221-233 (2017).
- [38.] S. Rafique, M. Idrees, A. Nasim, H. Akbar, and A. Athar, Transition metal complexes as potential therapeutic agents. *Biotechnology and Molecular Biology Reviews*, **5**, 38-45 (2010).
- [39.] T. J. Hubin, P. N. Amoyaw, K. D. Roewe, N. C. Simpson, R. D. Maples, et al. Synthesis and antimalarial activity of metal complexes of cross-bridged tetraazamacrocyclic ligands. *Bioorg. Med. Chem.*, **22**, 3239–3244 (2014).
- [40.] C. Roux, and C. Biot, Ferrocene-based antimalarials. *Future Med. Chem.*, **4**, 783–797 (2012).

- [41.] W. Daher, C. Biot, T. Fandeur, H. Jouin, and L. Pelinski, Assessment of *Plasmodium falciparum* resistance to ferroquine (SSR97193) in field isolates and in W2 strain under pressure. *Malar J.*, **5**, doi.10.1186/1475-2875-5-11 (2006).
- [42.] M. Barends, A. Jaidee, N. Khaohirun, P. Singhasivanon, and F. Nosten, In vitro activity of ferroquine (SSR 97193) against *Plasmodium falciparum* isolates from the Thai-Burmese border., *Malar. J.*, **6**, doi.10.1186/1475-2875-6-81. (2007).
- [43.] F. Dubar, J. Khalife, J. Brocard, D. Dive, and C. Biot, Ferroquine, an Ingenious Antimalarial Drug –Thoughts on the Mechanism of Action. *Molecules*, **13**, 2900–2907 (2008).
- [44.] C. Herrmann, P. F. Salas, J. F. Cawthray, C. de Kock, B. O. Patrick, P. J. Smith, M. J. Adam, and C. Orvig, 1,1'-Disubstituted Ferrocenyl Carbohydrate Chloroquine Conjugates as Potential Antimalarials. *Organometallics*, **31**, 5736–5747 (2012).
- [45.] M. Patra, G. Gasser, and N. Metzler-Nolte, Small organometallic compounds as antibacterial agents. *Dalton Trans.*, **41**, 6350–6358 (2012).
- [46.] L. Messori, M. Camarri, T. Ferraro, C. Gabbiani, and D. Franceschini, Promising in Vitro anti-Alzheimer Properties for a Ruthenium(III) Complex. *ACS Med. Chem. Lett.*, **4**, 329-332 (2013).
- [47.] D. G. Hottinger, D. S. Beebe, T. Kozhimannil, R. C. Prielipp, and K. G. Belani, Sodium nitroprusside in 2014: A clinical concepts review. *Journal of anaesthesiology, Clinical Pharmacology*, **30**(4), 462-471 (2014).
- [48.] A. Speckyj, M. Kosmopoulos, K. Shekar, C. Carlson, R. Kalra, J. Rees, T. P. Aufderheide, J. A. Bartos, and D. Yannopoulos, Sodium Nitroprusside–Enhanced Cardiopulmonary Resuscitation Improves Blood Flow by Pulmonary Vasodilation Leading to Higher Oxygen Requirements. *JACC: Basic to Translational Science*, **5**, 183-192 (2020).

- [49.] E. G. Villarreal, S. Flores, C. Kriz, N. Iranpour, R. A. Bronicki, and R. S. Loomba, Sodium nitroprusside versus nicardipine for hypertension management after surgery: A systematic review and meta-analysis. *J. Card. Surg.*, **35**(5), 1021-1028 (2020).
- [50.] T. Tumolo, and U. M. Lanfer-Marquez, Copper chlorophyllin: A food colorant with bioactive properties. *Food Research International*, **46**, 451–459 (2012).
- [51.] B. Kebowski, J. Depciuch, and J. Parlinska-Wojtan, Baran, Applications of Noble Metal-Based Nanoparticles in Medicine. *Int. J Mol. Sci.*, **19**(12), doi. 10.3390/ijms19124031 (2018).
- [52.] K. Duan, B. Liu, C. Li, H. Zhang, T. Yu, J. Qu, M. Zhou, L. Chen, S. Meng, Y. Hu, and C. Peng, Effectiveness of convalescent plasma therapy in severe COVID-19 patients. *PNAS*, **117**, 9490–9496 (2020).
- [53.] A. Wiehe, J. M. O'Brien, and M. O. Senge, Trends and targets in antiviral phototherapy. *Photochemical & Photobiological Sciences*, **18**, 2565-2612 (2019).
- [54.] J. Zhao, W. Meng, P. Miao, Z. Yu, and G Li, (2008) Photodynamic Effect of Hypericin on the Conformation and Catalytic Activity of Haemoglobin. *Int. J. Mol. Sci.*, **9**, 145–153 (2008).
- [55.] L. Costa, M. A. Faustino, M. G. Neves, A. Cunha, and A. Almeida, Photodynamic inactivation of mammalian viruses and bacteriophages. *Viruses*, **4**, 1034-1074 (2012).
- [56.] J. Wang, A. M. Potocny, J. Rosenthal, and E. S. Day, Gold Nanoshell-Linear Tetrapyrrole Conjugates for Near Infrared-Activated Dual Photodynamic and Photothermal Therapies. *ACS Omega*, **5**, 926–940 (2020).
- [57.] A. M Borys, An Illustrated Guide to Schlenk Line Techniques. *Organometallics*, **42**, 182-196 (2023).

- [58.] Y. Y. Titova, Dynamics EPR Studies of the Formation of Catalytically Active Centres in Multicomponent Hydrogenation Systems. *Catalysts*, **13**, doi.org/10.3390/catal13040653 (2023).
- [59.] G. Li, D. Li, M. Alshalalfeh, J. Cheramy, H. Zhang, Y. Xu, Stereochemical Properties of Two Schiff-Base Transition Metal Complexes and Their Ligand by Using Multiple Chiroptical Spectroscopic Tools and DFT Calculations. *Molecules*, **28**, doi.10.3390/molecules28062571 (2023).
- [60.] D. Aguiar, C. Schroder-Holzacker, J. Pecak, B. Stoger, and K. Kirchner, Synthesis and Characterization of TADDOL-Based Chiral Group Six PNP Pincer Tricarbonyl Complexes. *Mona. Chem.*, **150**, 103-109 (2019).
- [61.] S. Sharma, M. Chauhan, A. Jamsheera, S. Tabassum, and F. Arjmand, Chiral Transition Metal Complexes: Synthetic Approach and Biological Applications. *Inorg. Chem. Acta.*, **458**, 8-27 (2016).
- [62.] P. Manimaran, S. Balasubramaniyan, M. Azam, D. Rajadurai, S. I. Al-Resayes, G. Mathubala, A. Manikandan, S. Muthupandi, Z. Tabassum, and I. Khan, Synthesis, Spectral Characterization and Biological Activities of CO(II) and NI(II), Mixed Ligand Complexes. *Molecules*, **26**, 823-831 (2021).
- [63.] J. Karges, R. W. Stokes, and S. M. Cohen, Metal Complexes for Therapeutic Applications. *Trend. Chem.*, **3**, 523-534 (2022).
- [64.] K. Endo, Y. Liu, H. Ube, K. Nagata, and M. Shionoya, Asymmetric Construction of Tetrahedral Chiral Zinc with High Configurational Stability and Catalytic. *Nat. Commun.*, **11**, doi.org/10.1038/s41467-020-20074-7 (2020).
- [65.] S. X. Ye, and C. Tan, Chemical Science by Chiral Cations. *Chem. Sci.* **12**, 533-539 (2021).
- [66.] Y. Hong, T. Cui, S. Ivlev, X. Xie, and E. Meggers, Chiral-at-Iron Catalyst for Highly Enantioselective and Diastereoselective Hetero-Diels-Alder Reaction. *Chem. Eur. J.*, **27**, 8557-8563 (2021).

- [67.] F. Leon, A. Comas-Vives, E. Alvarez, and A. Pizzano, A Combined Experimental and Computational Study to Decipher Complexity in the Asymmetric Hydrogenation of Imines with Ru Catalyst Bearing Atropisomerizable Ligands. *Catal. Sci. Technol.*, **11**, 2497-2511 (2021).
- [68.] P. S. Steinlandt, L. Zhang, and E. Meggers, Metal Stereogenicity in Asymmetric Transition Metal Catalysis. *Chem. Rev.*, **123**, 4764-4794 (2023).
- [69.] P. S. Steinlandt, X. Xie, S. Ivlev, and E. Meggers, Stereogenicity-at-Iron with a Chiral Tripodal Pentadentate Ligand. *ACS Catal.*, **11**, 7467-7476 (2021).
- [70.] M. Wang, and W. Li, Feng Ligand: Privileged Chiral Ligand in Asymmetric Catalysis. *Chin. J. Chem.*, **39**, 969-984 (2021).
- [71.] H. Wang, J. Wen, and X. Zhang, Chiral Tridentate Ligands in Transition Metal-Catalyzed Asymmetric Hydrogenation. *Chem. Rev.*, **121**, 7530–7567 (2021).
- [72.] M. Dieguez, (Ed.), *Chiral Ligands: Evolution Of Ligands Libraries For Asymmetric Catalysis (New Directions in organic & Biological Chemistry)*; CRC Press: Boca Raton, FL, USA, (2021).
- [73.] Y Huang, and T. Hayashi, Chiral Diene Ligands in Asymmetric Catalysis. *Chem. Rev.*, **122**, 14346-14404 (2022).
- [74.] B. Su, and J. F. Hartwig, Development of Chiral Ligands for the Transition-Metal-Catalyzed Enantioselective Silylation and Borylation of C-H Bonds. *Angew. Chem. Int. ED.* doi.10.1002/anie.202113343. (2022).
- [75.] C. Wang, N. Zhang, C. Hou, X. Han, C. Liu, Y. Xing, F. Bai, and L. Sun, Transition Metal Complexes Constructed by Pyridine– Amino Acid: Fluorescence Sensing and Catalytic Properties. *Transit. Met. Chem.*, **45**, 423-433 (2020).
- [76.] D. A. Rusanov, J. Zou, and M. V. Babak, Biological Properties of Transition Metal Complexes with Metformin and Its Analogues. *Pharmaceuticals*, **15**, doi.10.3390/ph15040453 (2022).

- [77.] D Dolui, S. Das, J. Bharti, S. Kumar, P. Kumar, and A. Dutta, Bio-Inspired Cobalt Catalyst Enables Natural-Sunlight-Driven Hydrogen Production from Aerobic Neutral Aqueous Solution. *Cell. Rep. Phys., Sci.*, **1**, doi.org/10.1016/j.xcrp.2019.100007 (2020).
- [78.] M. J. Schweiger, and W. Beck, Metal Complexes of Biologically Important Ligands, Part CLXXVIII. [1] Addition of the Pentacarbonylrhenium Cation [(OC)₅Re]⁺ to the Xanthine Alkaloids Caffeine, Theophylline, and Theobromine. *Z. Anorg. Allg. Chem.*, **643**, 1335-1337 (2017).
- [79.] Available online: https://www.mdpi.com/journal/molecules/special_issues/metal_biological_ligands (accessed on 20 November 2023).
- [80.] V. M. Chernyshev, and V. P. Ananikov, Nickel and Palladium Catalysis: Stronger Demand than Ever. *ACS Catal.*, **12**, 1180-1200 (2022).
- [81.] V.P. Ananikov, The dawn of cross-coupling. *Nat. Catal.* **4**, 732–733 (2021).
- [82.] R. Nie, Y. Tao, Y. Nie, T. Lu, J. Wang, Y. Zhang, X. Lu, and C. C. Xu, Recent Advances in Catalytic Transfer Hydrogenation with Formic Acid over Heterogeneous Transition Metal Catalysts. *ACS Catal.*, **11**, 1071-1095 (2021).
- [83.] Z. Zhuang, and J. Yu, Pd(II) -Catalyzed Enantioselective γ -C(Sp³)-H Functionalizations of Free Cyclopropylmethylamines. *J. Am. Chem. Soc.*, **142**, 12015-12019 (2020).
- [84.] L. J. Xiao, K. Hong, F. Luo, L. Hu, W. R. Ewing, K. S. Yeung, and J. Q. Yu, Pd(II)-Catalyzed Enantioselective C(Sp³)-H Arylation of Cyclobutyl Ketones Using a Chiral Transient Directing Group. *Angew. Chem. Int. Ed.*, **59**, 9594 – 9600 (2020).
- [85.] H. Li, D. Yang, H. Jing, J. C. Antilla, and Y. Kuninobu, Palladium-Catalyzed Enantioselective C(Sp³)H Arylation of 2-Propyl Azaaryls Enabled by an Amino Acid Ligand. *Org. Lett.*, **24**, 1286-1291 (2022).
- [86.] W. Liu, W. Yang, J. Zhu, Y. Guo, N. Wang, J. Ke, P. Yu, C. He, W. Liu, and W. Yang, et al. Dual Ligand Enabled Ir(III)-Catalyzed Enantioselective C-H

- Amidation for the Synthesis of Chiral Sulfoxides. *ACS Catal.*, **10**, 7207–7215 (2020).
- [87.] I. P. Beletskaya, and V. P. Ananikov, Transition-Metal-Catalyzed C–S, C–Se, and C–Te Bond Formations via Cross-Coupling and Atom-Economic Addition Reactions. Achievements and Challenges. *Chem. Rev.*, **122**, 16110– 16293 (2022).
- [88.] V. Kederien, I. Jaglinskaite, P. Voznikaite, J. Rousseau, A. Sackus, and A. Tatibouet, Mild Copper-Catalyzed, L-Proline-Promoted Cross-Coupling of Methyl 3-Amino-1-Benzothiophene-2-Carboxylate. *Molecules*. **26**, doi.org/10.3390/molecules26226822 (2021).
- [89.] Z. Zhou, Q. Xie, J. Li, Y. Yuan, Y. Liu, Y. Liu, D. Lu, and Y. Xie, Glucopyranoside-Functionalized NHCs-Pd (II)- PEPPSI Complexes: Anomeric Isomerism Controlled and Catalytic Activity in Aqueous Suzuki Reaction. *Catal. Lett.*, **152**, 838–847 (2022).
- [90.] N Mishra, S. K. Singh, A. S. Singh, A. K. Agrahari, and V. K. Tiwari, Glycosyl Triazole Ligand for Temperature-Dependent Competitive Reactions of Cu-Catalyzed Sonogashira Coupling and Glaser Coupling. *J. Org. Chem.*, **86**, 17884–17895 (2021).
- [91.] A. M. Wills, Y. Zheng, J. Martinez-Acosta, L. C. Barbosa, and G. Clarkson, Asymmetric Transfer Hydrogenation of Aryl Heteroaryl Ketones Using Noyori-Ikariya Catalysts. *Chem. Cat. Chem.*, **13**, 4384–4391 (2020).
- [92.] V. Ratovelomanana, P. Phansavath, (Eds.) *Asymmetric Hydrogenation and Transfer Hydrogenation*; Wiley-VCH: Weinheim, Germany, 2021.
- [93.] F. Chen, M. Y. Jin, D. Z. Wang, C. Xu, J. Wang, and X. Xing, Simultaneous Access to Two Enantio-enriched Alcohols by a Single Ru-Catalyst: Asymmetric Hydrogen Transfer from Racemic Alcohols to Matching Ketones. *ACS Catal.*, **12**, 14429–14435 (2022).

- [94.] M. R. Espinosa, M.Z. Ertem, M. Barakat, Q. J. Bruch, A. P. Deziel, M. R. Elsby, F. Hasanayn, N. Hazari, A. J. M. Miller, and M. V. Pecoraro, et al. Correlating Thermodynamic and Kinetic Hydricities of Rhenium Hydrides. *J. Chem. Soc.*, **144**, 17939–17954 (2022).
- [95.] C. M. Bernier, and J. S. Merola, Design of Iridium N-Heterocyclic Carbene Amino Acid Catalysts for Asymmetric Transfer Hydrogenation of Aryl Ketones. *Catalysts*. **11**, doi.org/10.3390/catal11060671 (2021).
- [96.] L Wang, J. Lin, Q. Sun, C. Xia, and W. Sun, Amino Acid Derived Chiral Aminobenzimidazole Manganese Catalysts for Asymmetric Transfer Hydrogenation of Ketones. *ACS Catal.*, **11**, 8033–8041 (2021).
- [97.] Vishwanathan M and Krishnan G, Synthesis and characterization of manganese(II), cobalt(II), nickel(II), copper(II), zinc(II) and cadmium(II) complexes of N,N' -triethylenediamine-bis-(3-carboxypropenamido). *Asi. J. Chem.*, **16**(1): 169-173, (2004)
- [98.] R. R. Patel and V. G. Patel, Synthesis, Characterization, Chelating properties and antimicrobial activity of pyrimidine and phthalic anhydride combined molecule *Ras. J. Chem.*, **3**(1), 188-193, (2010)
- [99.] X. H. Zhu, D. Y. Jiang, X. C. Cheng, D. H. Li and W. G. Dn, A Mn(II) complex with an amide-containing ligand: synthesis, structural characterization, and magnetic properties. *Z. Naturforsch.*, **74**(5), 409-414 (2019).
- [100.] A. V. Chernyshova, A. A. Nikolaev, F. A. Kolokolov, V. V. Dotsenko, M. A. Aksena and I. V. Akseneva, Synthesis and luminescent properties of Eu³⁺, Gd³⁺, and Tb³⁺ complex compounds with some N- substituted phthalamic acids. *Russ. J. Gene. Chem.*, **91**(6), 1063-1069 (2021).
- [101.] G. Dayakar and P. Lingaiah, Synthesis and spectral studied of ruthenium (III) complexes with amide group ligands. *Asian J. Chem., Ind. J. Chem.*, **35**(7), 614-616 (1996).

- [102.] M. Ashok, A. V. S. S. Prasad and V. Ravinder, Synthesis, spectral studies and catalytic activity of ruthenium (II) complexes with organic amide ligands. *J. Braz. Chem. Soc.*, **18**(8): 1492-1499 (2007).
- [103.] O. I. Edozie, I. K. Kalu, and S. O. Paul, Synthesis, characterization and antibacterial studies of Fe(II) and Mn(II) complexes of 2-[(4-[(1,3-thiazol-2-ylamino)sulfonyl]phenyl)amino]carbonyl]benzoic acid. *Int. J. of Innovative Science, Eng & Tech (IJSET)*, **2**(10), 384-389 (2015).
- [104.] K. Shahid, S. Ali and S. shahzadi, Organotin(IV) complex of aniline derivatives, Part-II -Synthesis and spectroscopic characterization of organotin(IV) derivatives of 2-[(4-bromoanilino) carboxyl] benzoic acid. *Turk J. Chem.*, **27**, 209-215 (2003).
- [105.] Y. S. Patel, K. D. Patel, and H. S. Patel, Spectral antimicrobial studies on novel ligand and its co-ordination polymers. *J. Saudi Chem. Soc.*, **20**, 300-305 (2016).

□□□

CHAPTER – II

MATERIALS AND METHODS

CONTENTS

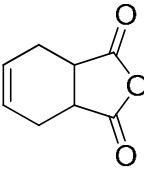
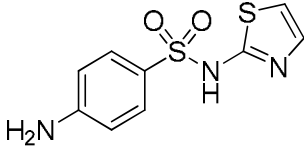
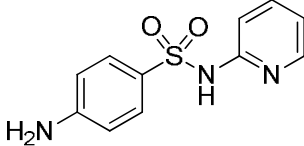
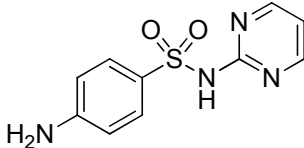
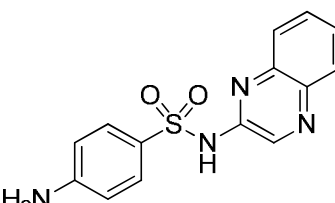
2.1 MATERIALS USED

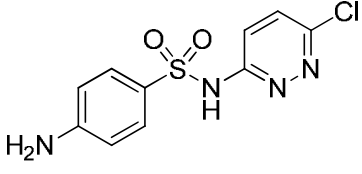
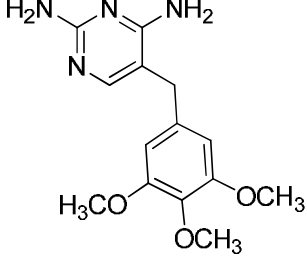
2.2 TECHNIQUES USED

2.1 MATERIALS USED

All the reagents employed in process investigation were received as analar grade locally. The details of chemicals are in Table 2.1.

Table 2.1: Data about reagents and their supplier

Name and structure	Supplier name
 Tetrahydrophthalic anhydride	Otto Chemie Pvt. Ltd.
 Sulfathiazole	Enomark Healthcare
 Sulfapyridine	Triveni Chemicals
 Sulfadiazine	Macsen Laboratories
 Sulfaquinolone	Vea Impex Pvt. Ltd.

 <p>Sulfachloropyradazine</p>	A R Life Sciences
 <p>Trimethoprim</p>	Kavya Pharma
<p>CuCl_2 Copper (II) chloride</p>	Real Metal Chem Pvt. Ltd.
<p>$\text{Cu}(\text{CH}_3\text{COO})_2$ Copper acetate</p>	Lakshita Chemicals
<p>$\text{Co}(\text{C}_2\text{H}_3\text{O}_2)_2$ Cobalt (II) acetate</p>	P K Chlorochem
<p>$\text{Ni}(\text{CH}_3\text{COO})_2$ Nickel (II) acetate</p>	Mahavir Metal Chem
<p>$\text{Zn}(\text{CH}_3\text{COO})_2$ Zinc acetate</p>	Krishna Chemicals
<p>$\text{Mn}(\text{CH}_3\text{COO})_2$ Manganese (II) acetate</p>	Kanha Life science

2.2 TECHNIQUES USED

Different techniques were used in present investigation.

2.2.1 Melting point analysis

The melting points of all the compounds were measured on Digital melting point apparatus (Lab India) and were uncorrected.

2.2.2 Elemental analysis

The elemental content in all the prepared oriental organic compounds were determination Thermo- Scientific Flash Smart elemental analyzer.

2.2.3 Infrared spectroscopy

The IR spectra of all the compounds were performed on FT-IR Spectrometer - 6800 – JASCO Europe instrument. The analysis performed using anhydrous KBr in the 4000-400 cm^{-1} range. The transparent pallet was used for analysis.

2.2.4 NMR spectroscopy:

Proton NMR and ^{13}C NMR of ligands was performed on Bruker Avance III HD 300 MHz wide-bore NMR Spectrometer. Tetra methyl silane (TMS) was used as standard and deuterated Dimethyl formamide (DMF) was used as a solvent.

Bruker Avance III HD 300 MHz wide-bore NMR Spectrometer.

2.2.5 LC-Mass spectroscopy:

Liquid chromatography-mass spectroscopy (LC-MS) is the analytical technique used for identification of unknown compounds as well as to elucidate the of different compounds. The LC-Mass spectrometer (Bruker Avance III HD 300 MHz wide-bore NMR) consists of ionization source, mass analyzer, detectors for data interpretation and analysis and report results.

2.2.6 Magnetism:

The magnetism of metal complexes is an important property which can be anticipated based on molecular structure. This property based measured in terms of molar magnetic susceptibility (χ_m) by considering their molecular weight of test complex magnetism are two types: (i) Diamagnetism exhibited due to changes of orbital and (ii) Paramagnetism exhibited due to orbital electronic spin and angular momentum. It exists only in organic molecules having impurities of electron with parallel spins diamagnetism, a created from the interaction of paired electrons and the magnetic field. Magnetic area compounds having electron creates two Paramagnetism which relate inversely with temperature. In organic compounds two paramagnetism occurs if they are transition metal ions unpaired electrons.

2.2.7 Reflectance / Electronic spectra:

Most of the transition metal complexes have unique UV-visible reflectance spectra, which is useful to study their geometry and electronic structure. This technique is important due to solid state structural chemistry not studied compared to aqueous solution. This diffused electronic spectroscopy is better for study of solid state properties of materials. In present studies the produced metal chelates are amorphous powder, their electronic spectra have been scanned for getting molecular geometry

2.2.8 Thermogravimetric analysis

Thermogravimetric analysis is an analytical tool to analysis of thermal stability of materials. In this method, changes in the weight of compounds are measured with increasing temperature ($^{\circ}\text{C}$). Percentage (%) moisture content and volatile content of a sample can be measured by Thermogravimetric analysis techniques. Evaluation of the thermogravimetric analysis.

The first stage of decomposition of these complexes was observed around 10% in 250-500 $^{\circ}\text{C}$ temperature range and, it may be due to associated water molecules. The second stage of decomposition of all chelates is rapid and about 50% mass loss. This may be due to metal oxide formation during degradation.

2.2.9 Antimicrobial analysis

2.2.9.1 Antibacterial activity:

There are various methods used for the analysis of antibacterial activities,

2.2.9.1.1 Agar well diffuse method: This is most favorable method to monitoring antimicrobial activity of test samples.

2.2.9.1.2 Agar plug diffusion method,

2.2.9.1.3 Cross streak method, and

2.2.9.1.4 Poisoned food method.

In this testing, the antimicrobial materials is transferred to test cultured inoculated thin layer (coated) glass plate. After diffusion on such chromatogram agar plate removed and there incubated from plate the growth inhibition zone of microorganism is measured.

The antimicrobial activity is calculated by,

$$= \frac{\text{Number of bacteria on test sample one day}}{\text{Number of bacteria on without test sample in one day}}$$

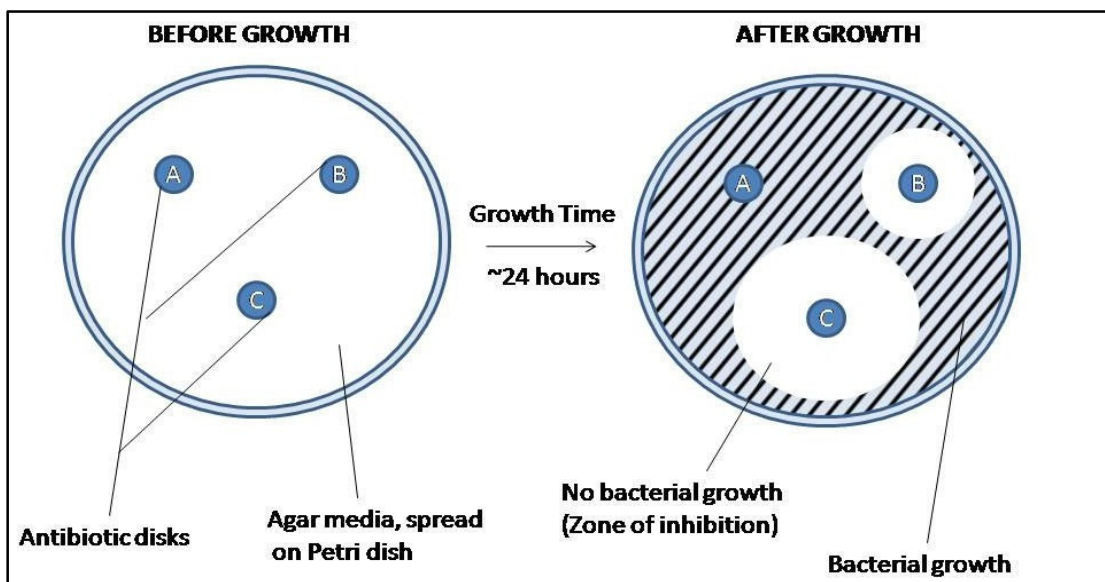


Fig. 2.1: Agar disk diffusion experimental test

(i) Antifungal activity:

The antifungal test methods are divided into main three groups.

- Diffusion method,
- Dilution method,
- Bio-autographic methods and

Many organizations/Labs adopt modified methods for specific samples. In addition to this, there are various test methods used for testing of fungal infections.

- Susceptibility testing (where sample of fungus isolated in culture)
- Antigen testing (where sample are blood, urine, CSF, body fluids)
- Antibody testing [where sample are blood, urine, CSF, body fluids], and
- Molecular tests for DNA, RNA.

Three methods have been standardized for antifungal susceptibility testing of any test sample of compounds.

- Broth dilution method,
 - Disk diffusion method,
 - Azole agar screening for Aspergillus, other common used methods include gradient diffusion and the use of rapid automated instruments.

Antifungal susceptibility testing it has the become standard method for testing and has a same role of the antibacterial susceptibility testing in microbiology laboratories.

In clinical laboratory Antifungal susceptibility testing (AFST) is pivotal test which give MIC value to assists patient therapy.



Fig. 2.2: Antifungal susceptibility test (AFST)

□□□

CHAPTER – III

SYNTHESIS AND CHARACTERIZATION OF LIGANDS

CONTENTS

3.1 INTRODUCTION

3.2 EXPERIMENTAL

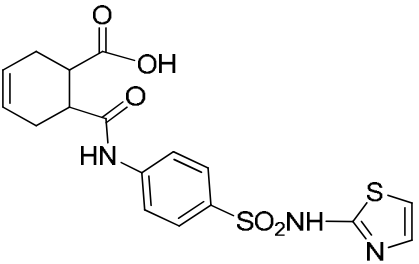
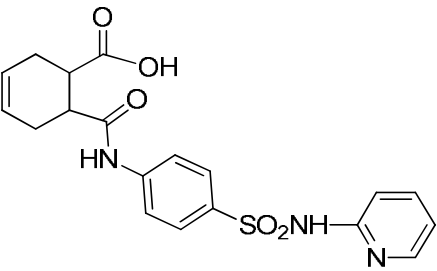
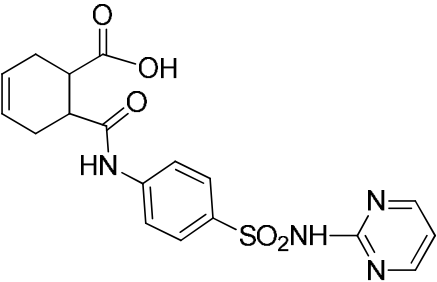
3.3 CHARACTERIZATION OF LIGANDS

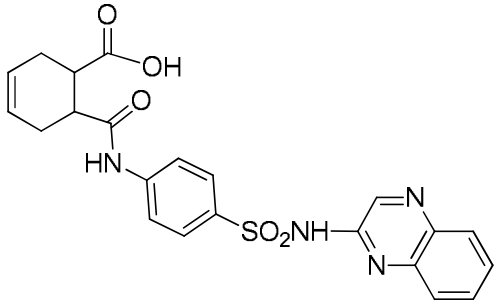
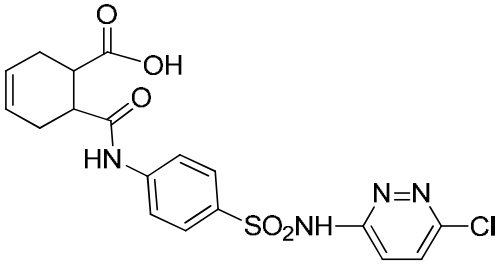
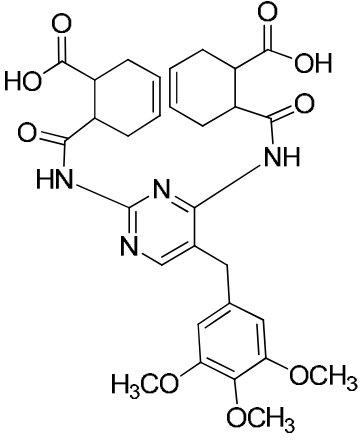
3.1 INTRODUCTION

Synthesized and characterized fine ligands based on sulfa drugs. These are designated as TPAS-1 to TPAS-5. One bis-ligand was also synthesized from trimethoprim and it was designated as TPTB.

Reaction of various sulfa drugs (as an amine source) were carried out with tetrahydrophthalic anhydride to obtain ligand. The details of these ligands are given in Table 3.1.

Table 3.1: List of ligands

Structure	Name	Molecular weight	Melting point (°C)	Yield (%)
	TPAS-1	407.46	181-182	86
	TPAS-2	401.44	188-189	87
	TPAS-3	402.42	198-199	82

	TPAS-4	452.48	195-196	85
	TPAS-5	436.87	178-179	86
	TPTB	594.61	166-167	87

3.2 EXPERIMENTAL

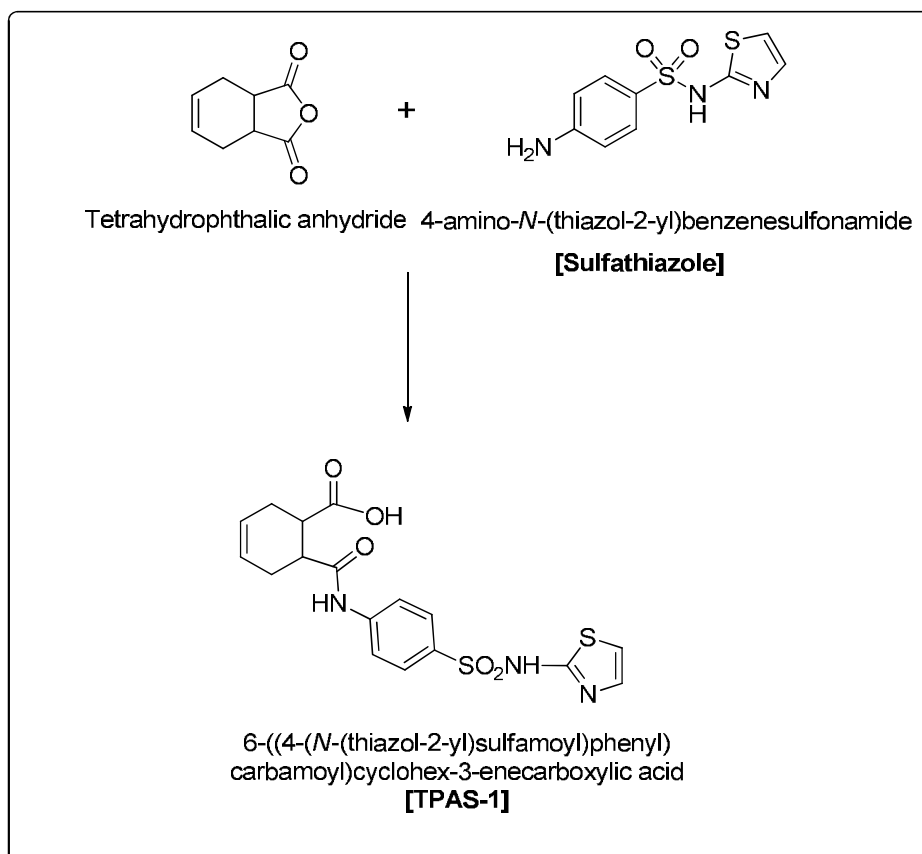
3.2.1 Synthesis of Tetrahydrophthalamic acid derivatives as ligands [TPAS-1 to TPAS-5].

Tetrahydrophthalamic acid derivatives of such drugs as ligands (TPAS-1 to TPAS-5) were prepared by using/reacting tetrahydrophthalic anhydride and various amine derivatives as Sulpha drugs. The method of preparation was based on earlier literature¹⁻⁴.

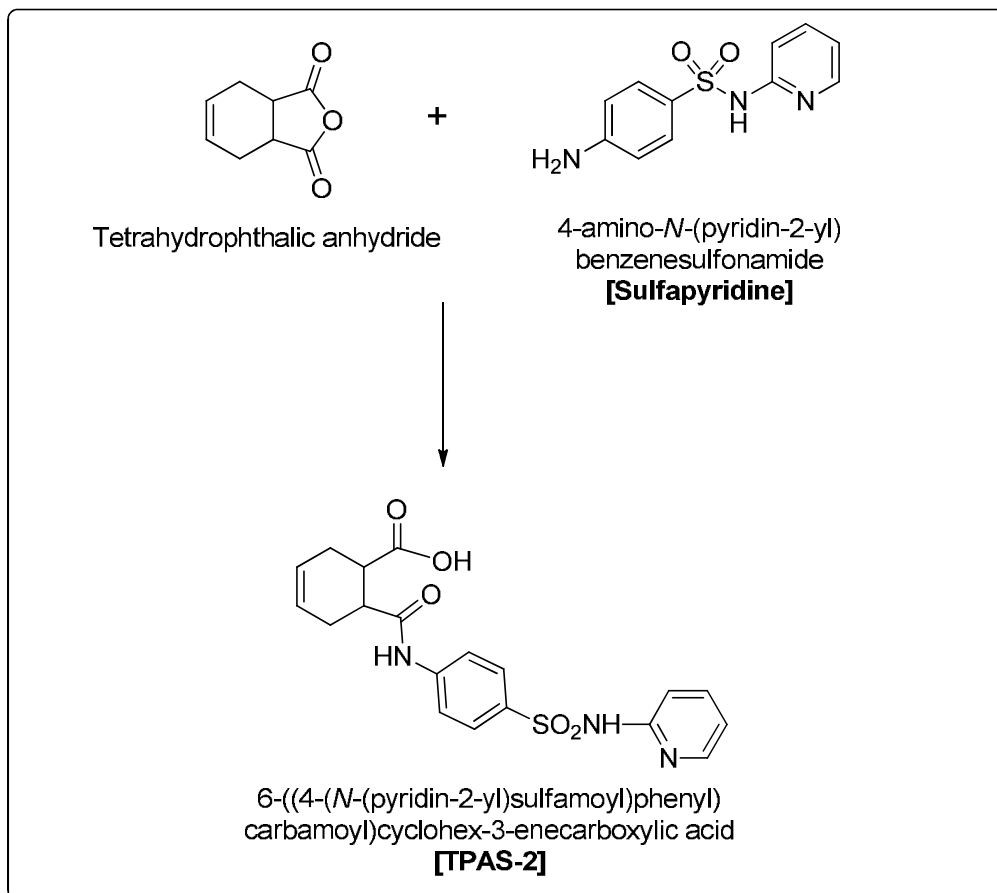
100 mmol of Tetrahydrophthalic anhydride and few drops of pyridine were mixed in 100 ml of 2-propanone solvent in a conical flask then 100 mmol of a sulfa drug dissolved in 100 ml 2-propanol was added portion wise and stirred. The assembly was stirred frequently by placing in an ice bath by maintaining temperature 0-5 °C. The reaction mixture was placed in on the table with stirring at room temperature. The resultant solid product obtained was filtered off, washed with 2-propanone, Then petroleum ether and air – dried (Ligands TPAS-1 to TPAS-5).

The reaction scheme are:

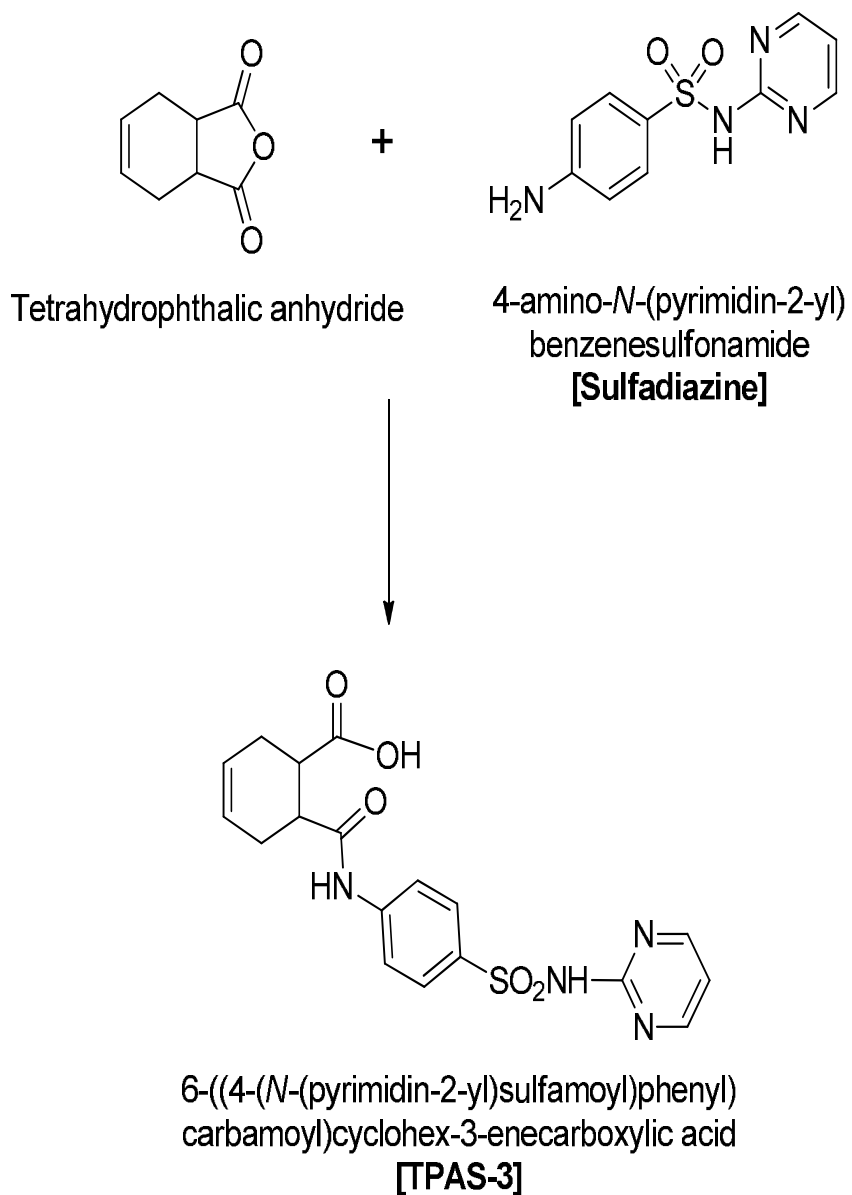
Ligand TPAS-1:



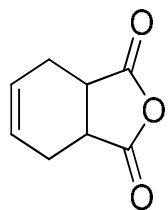
Ligand TPAS-2:



Ligand TPAS-3:

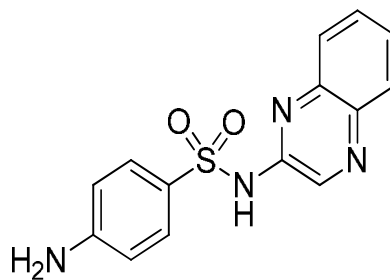


Ligand TPAS-4:

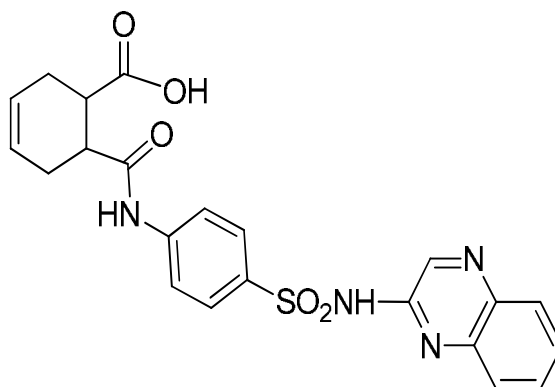


Tetrahydrophthalic anhydride

+

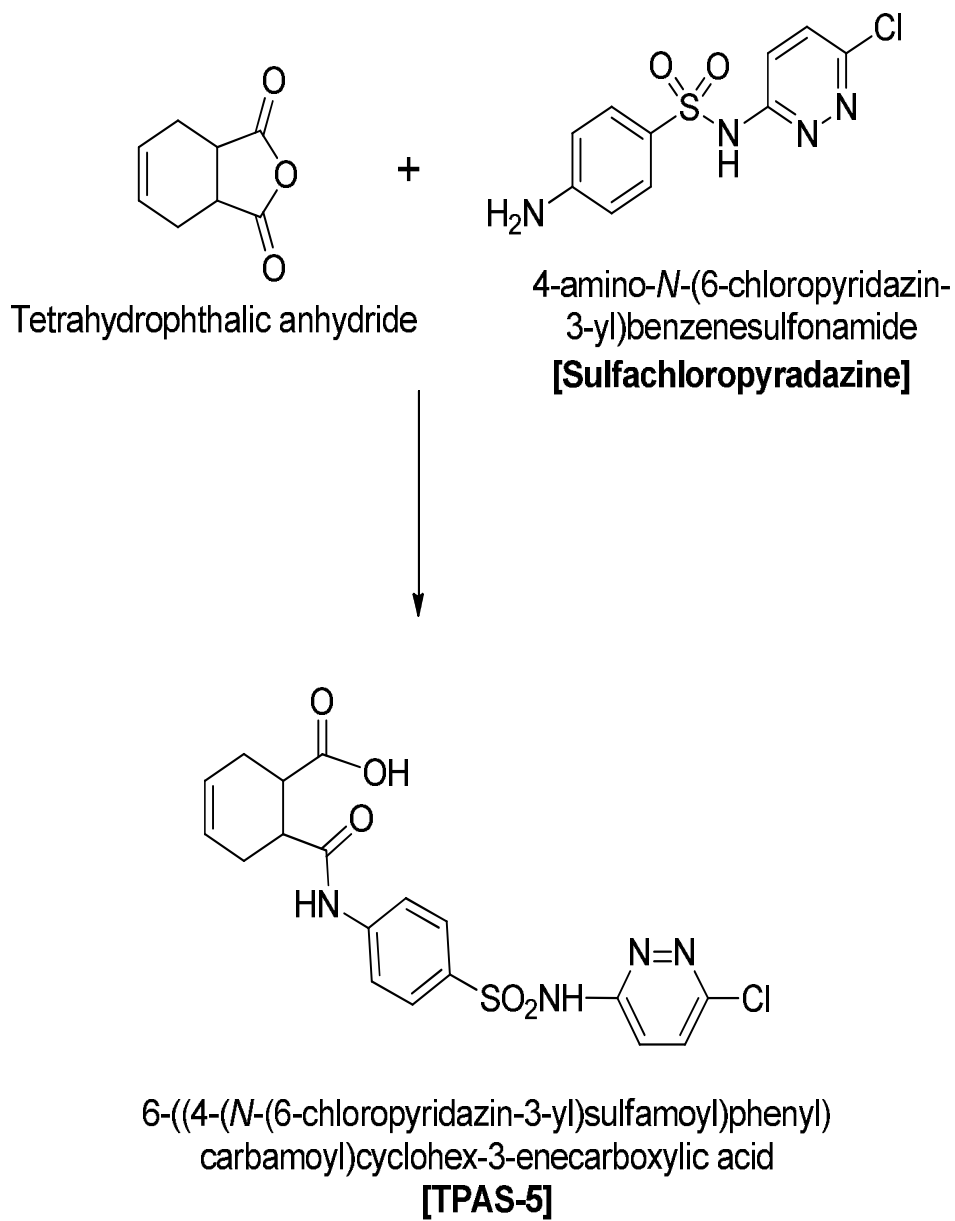


4-amino-*N*-(quinoxalin-2-yl)
benzenesulfonamide
[Sulfaquinoxaline]



6-((4-(*N*-(quinoxalin-2-yl)sulfamoyl)phenyl)
carbamoyl)cyclohex-3-enecarboxylic acid
[TPAS-4]

Ligand TPAS-5:

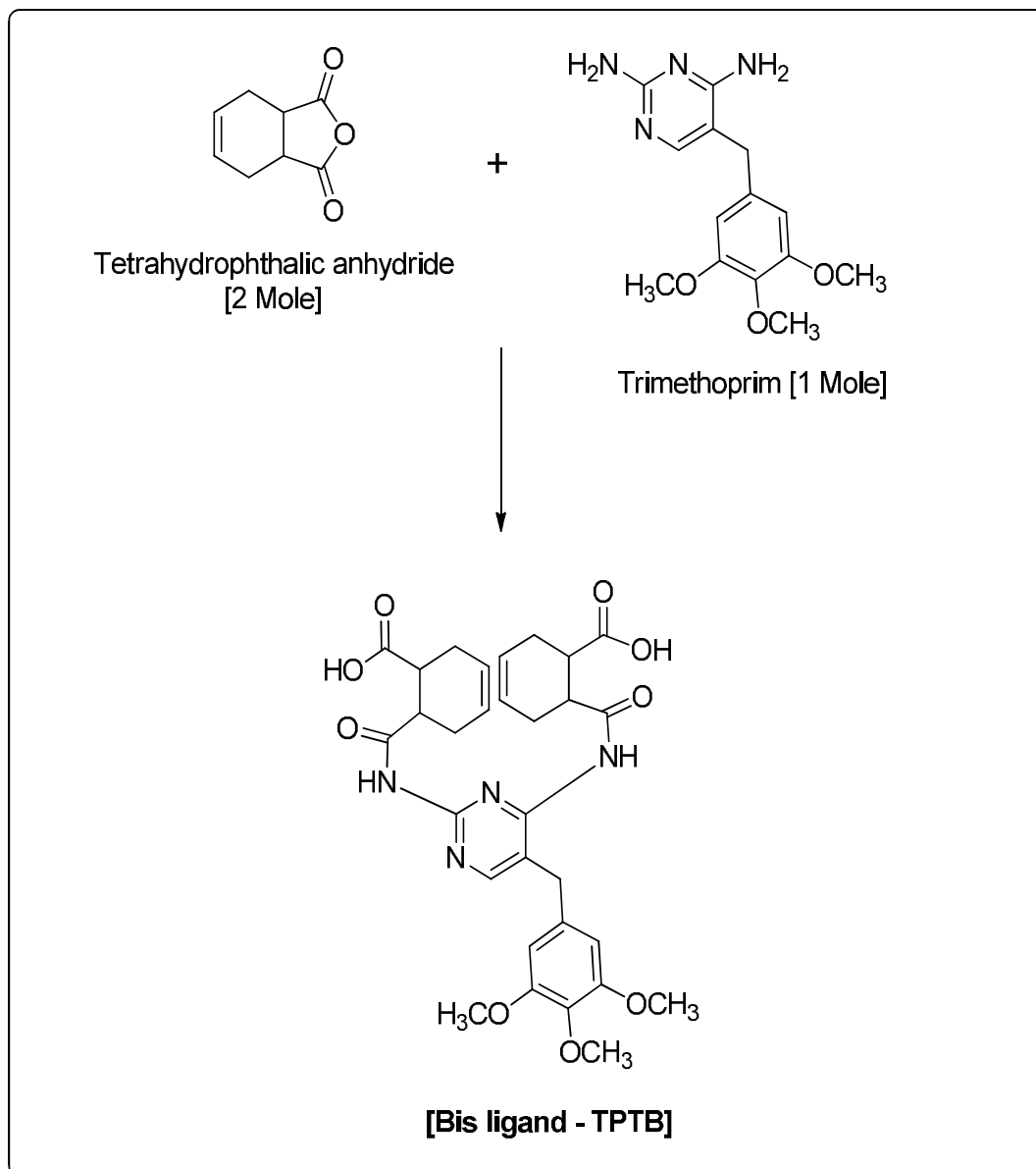


3.2.2 Synthesis of tetrahydrophthalamic trimethoprim bis-ligand (TPTB).

Tetrahydrophthalamic trimethoprim bis-ligand (TPTB) was prepared by condensing 2 mole of tetrahydrophthalic anhydride with trimethoprim. The reported method & were used¹⁻⁴.

Tetrahydrophthalic anhydride (0.2 mole) and 0.1 mL of pyridine in 100 mL acetone were taken in round bottom flask, and stirred. Then a solution of Trimethoprim (0.1 mole) in 100 mL acetone was added in parts within 30-60 min. The whole assembly was placed in ice-cooled bath and maintaing the temperature between 0-5°C during the addition of sulfa drug. The reaction mixture was kept aside with stirring for two hours at room temperature. After completion of the reaction, the precipitates were filtered off, washed with acetone and air-dried to give dry product (Ligand TPTB).

Ligand TPTB:



3.3 CHARACTERIZATION OF LIGANDS

3.3.1 General analysis:

The general analysis of ligands TPAS-1 to TPAS-5 and Bis-ligand (TPTB) observed.

- Melting points (°C) of all the compounds were measured by DSC method. All the melting points checked are uncorrected.
- The yields of all compounds were also measured. All solvents used were distilled and dried. The purity of the compounds was checked by TLC. Column chromatography was also performed using silica gel having 60-120 mesh, if required.

All the ligands were analyzed for their elemental contents. The C, H, N and S elements of all the samples were measured by Elemental analyzer Thermofinigan flash1101 EA. The results are reported in Tables 3.2 and 3.3. The values are in consistence with the proposed structures.

Table 3.2: Characterization of Ligands TPAS-1 to TPAS-5 and bis ligand TPTB

Ligand	Molecular Formula	Mol. Wt.	Yield (%)
TPAS-1	C ₁₇ H ₁₇ N ₃ O ₅ S ₂	407.46	87%
TPAS-2	C ₁₉ H ₁₉ N ₃ O ₅ S	401.44	85%
TPAS-3	C ₁₈ H ₁₈ N ₄ O ₅ S	402.42	86%
TPAS-4	C ₂₂ H ₂₀ N ₄ O ₅ S	452.48	85%
TPAS-5	C ₁₈ H ₁₇ N ₄ O ₅ SCl	436.87	86%
TPTB (Bis Ligand)	C ₃₀ H ₃₄ N ₄ O ₉	594.61	84%

Table 3.3: Elemental analysis of ligands

Ligand No.	Elemental analysis							
	C (%)		H (%)		N (%)		S(%)	
	Cal.	Found	Cal.	Found	Cal.	Found	Cal.	Found
TPAS-1	50.06	50.00	4.17	4.20	10.30	10.30	15.70	15.70
TPAS-2	56.79	56.80	4.73	4.70	10.46	10.50	7.97	8.00
TPAS-3	53.67	53.70	4.47	4.50	13.91	14.00	7.95	8.00
TPAS-4	68.07	68.00	4.42	4.40	12.37	12.40	7.07	7.10
TPAS-5	49.44	49.50	3.89	3.90	12.82	12.80	7.32	7.30
TPTB (Bis Ligand)	60.54	60.50	5.72	5.70	9.42	9.40	-	-

The anticipated IR spectral frequencies of all the ligands are given in Table 3.3. The infrared spectra of selected ligands are presented in Figures 3.1 to 3.3. The infrared spectra of all the ligands indicate that-

- I. All the IR spectra are identical in almost all aspects. The important bands are observed at their respective positions.
- II. The bands at 3450, 1680 and 1580 cm^{-1} are due to $-\text{CONH}-$ (secondary amide) group.
- III. A strong band at 1700 cm^{-1} is due to carbonyl group of $-\text{COOH}$ group.
- IV. The bands at 3030, 1600 and 820 cm^{-1} are mainly from 1, 4-disubstituted aromatic ring.
- V. The bands at 1160, 1350, 1610 and 3320 cm^{-1} are due to $-\text{SO}_2\text{NH}-$ (sulphonamide) group.

Table 3.4: IR spectral features for ligands TPAS-1 to TPAS-5 and TPTB (Bisligand)

Groups	IR frequencies (cm⁻¹)
Amide group -NHCO-	3450, 1680, 1580
Aromatic.	820, 1600, 3030
-C=O of -COOH.	~ 1700
-SO ₂ NH-	1160, 1350, 1610, 3320

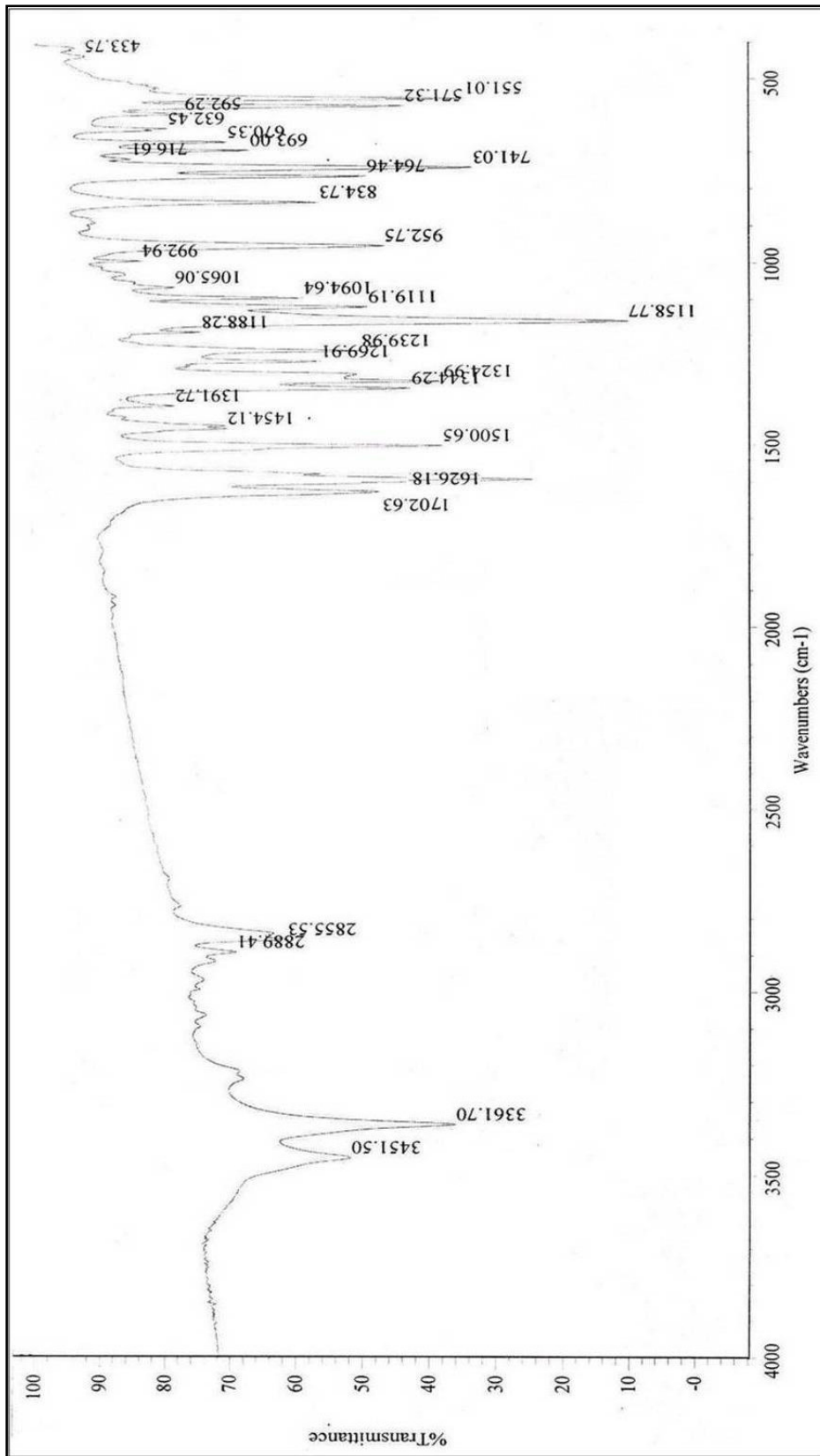


Fig. 3.1: IR spectrum of ligand TPAS-1

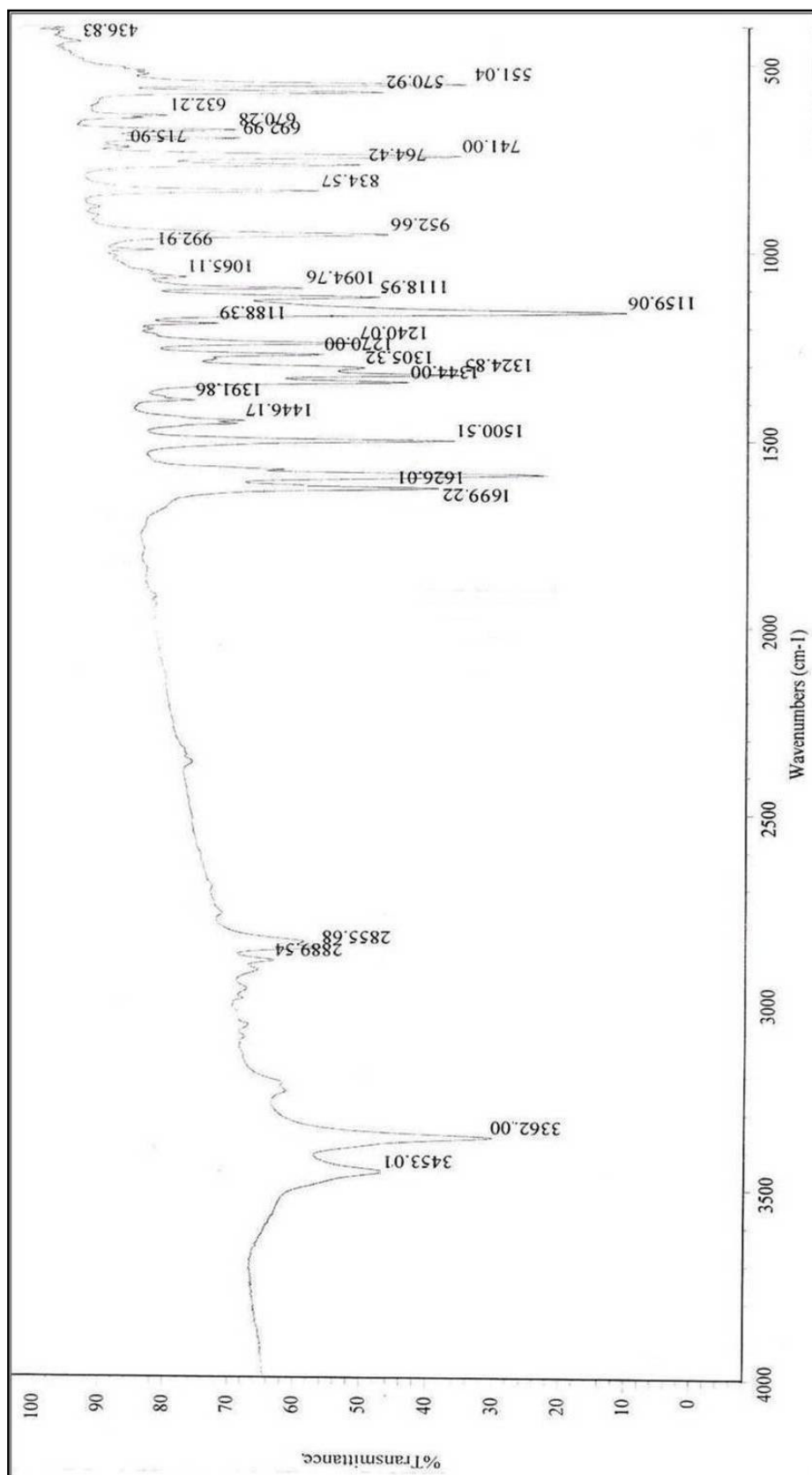


Fig. 3.2: IR spectrum of ligand TPAS-3

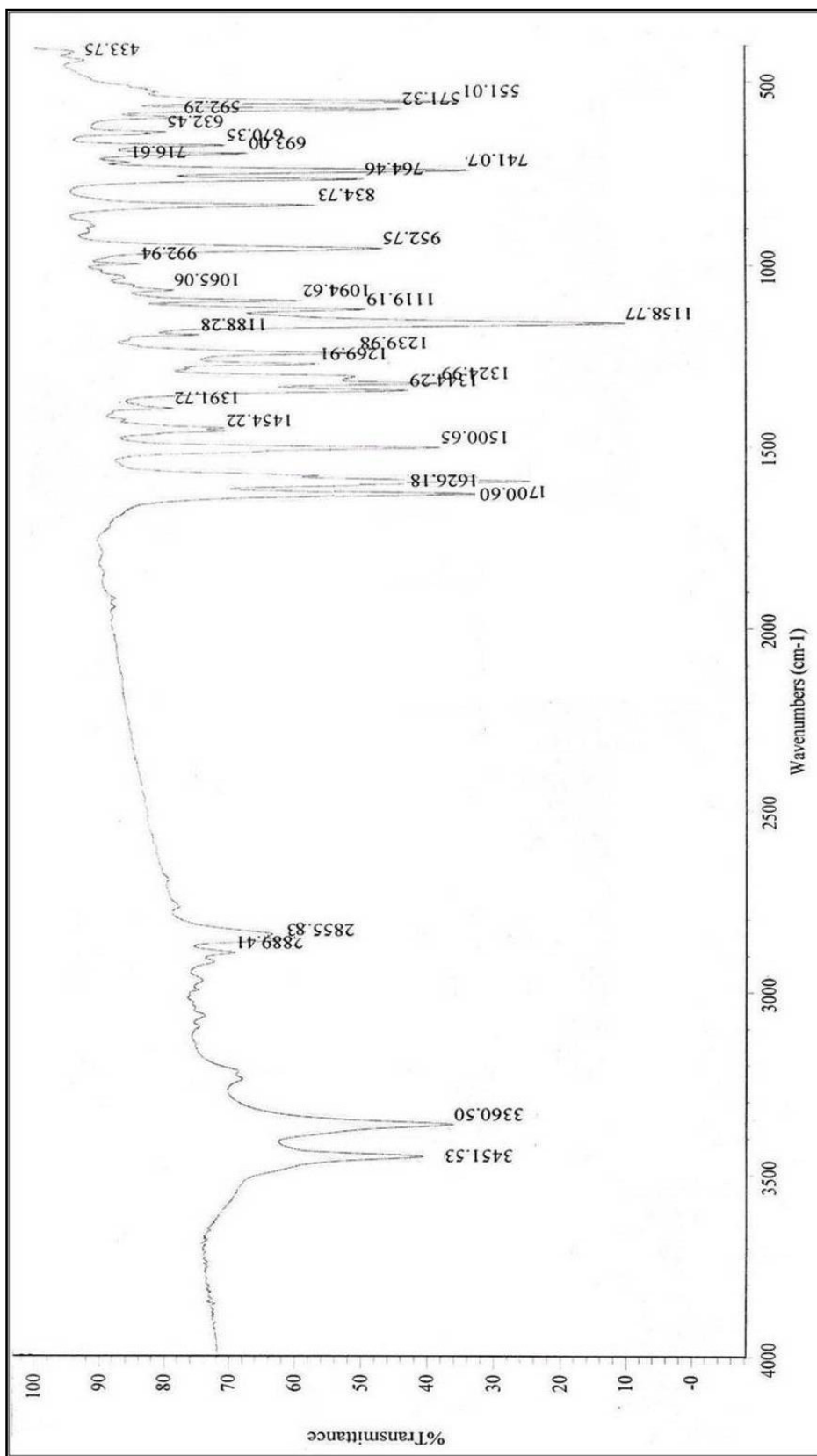


Fig. 3.3: IR spectrum of ligand TPAS-5

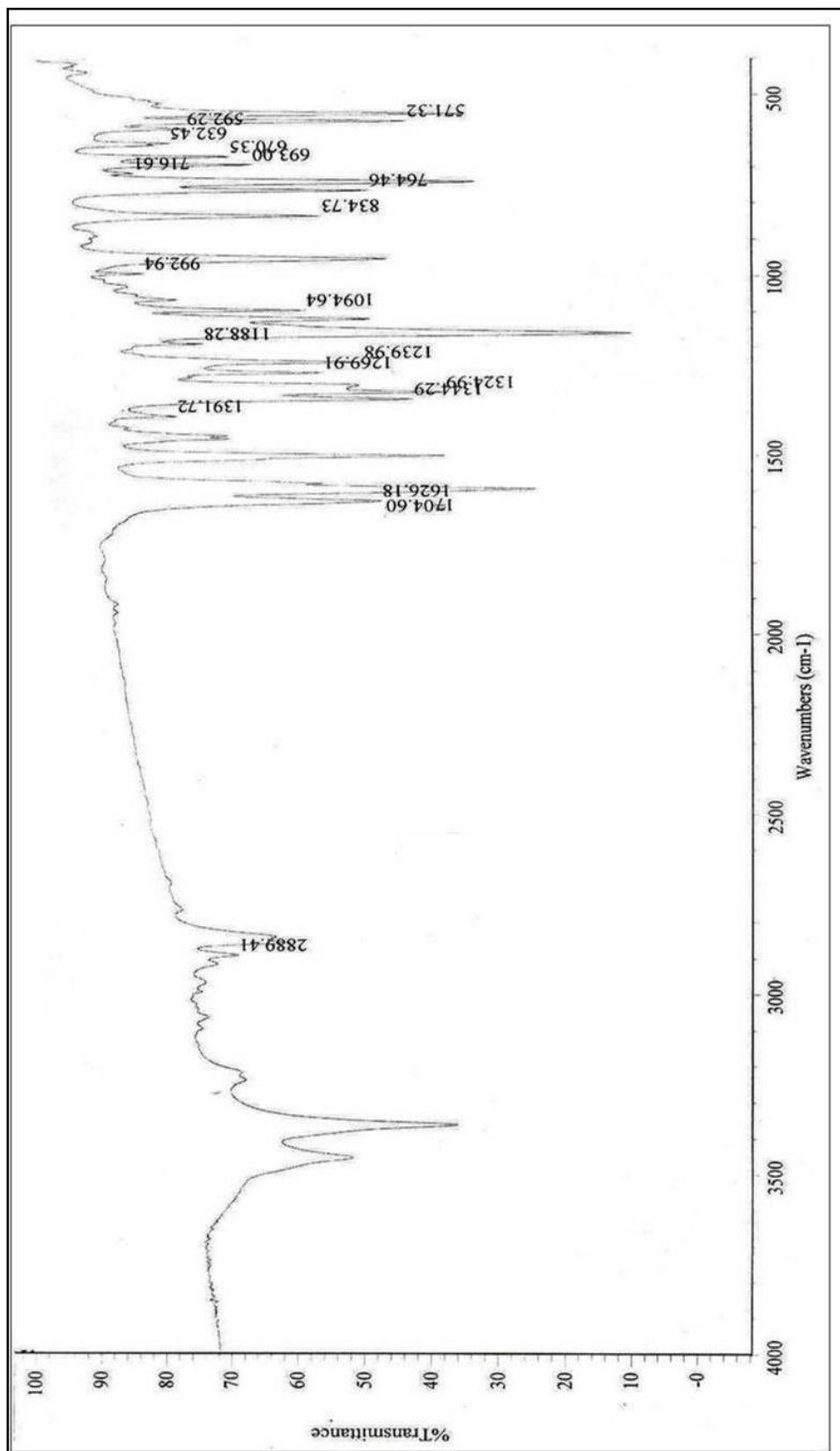


Fig. 3.4: IR spectrum of bis-ligand TPTB

3.3.3 Proton nuclear magnetic resonance spectroscopy

It was observed that that all NMR spectra are almost identical in nature. The NMR spectra of TPAS-1 to TPAS-5 and Bis-ligand TPTB are given in Figs: 3.5 to 3.7. All the spectra comprise the multiplet at 6.3 to 8.1 δ ppm due to from aromatic protons including NH of CONH group. The singlet at around 12 δ ppm might be responsible for H of COOH group.

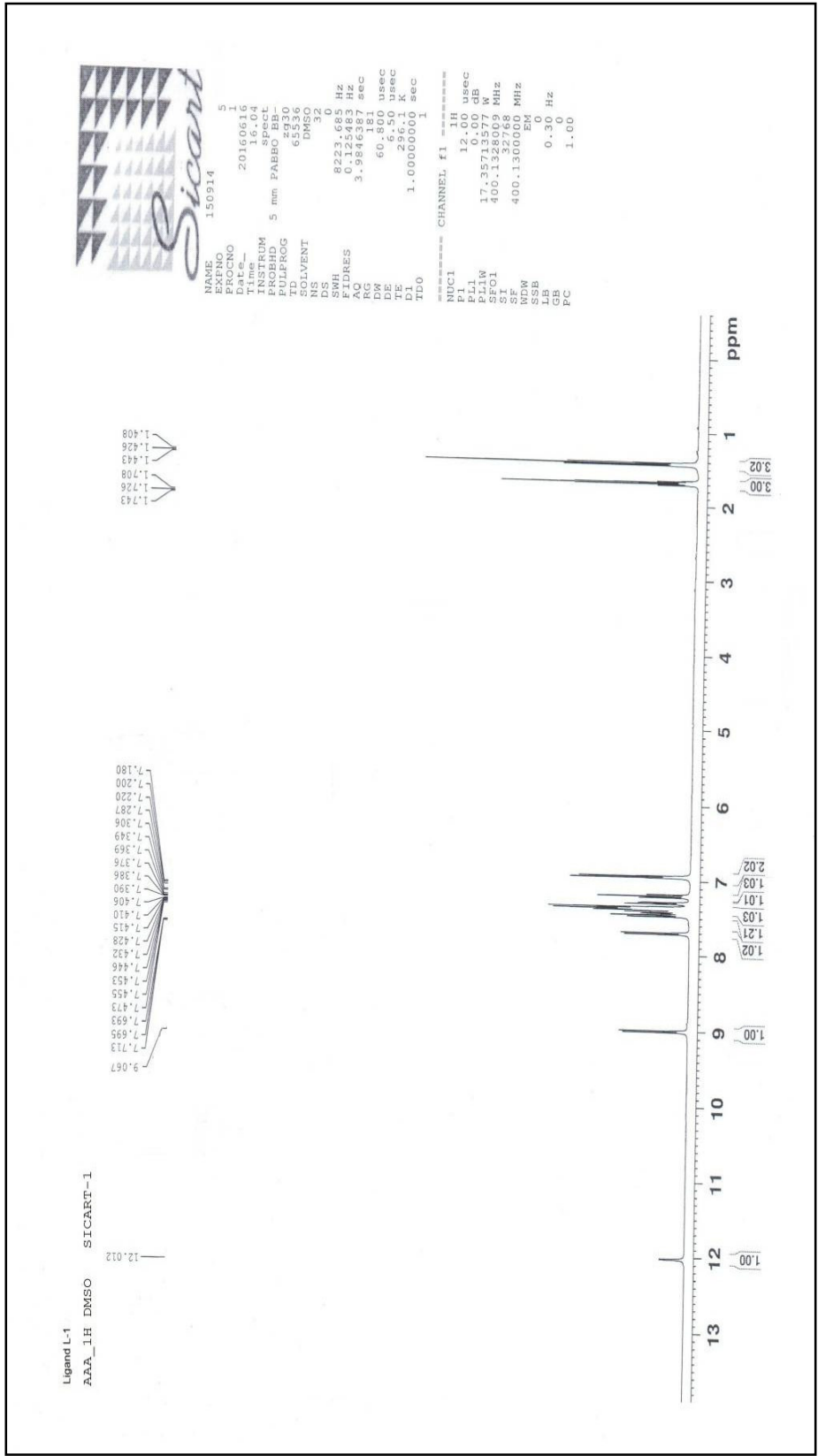


Fig 3.5: NMR spectrum of ligand TPAS-1

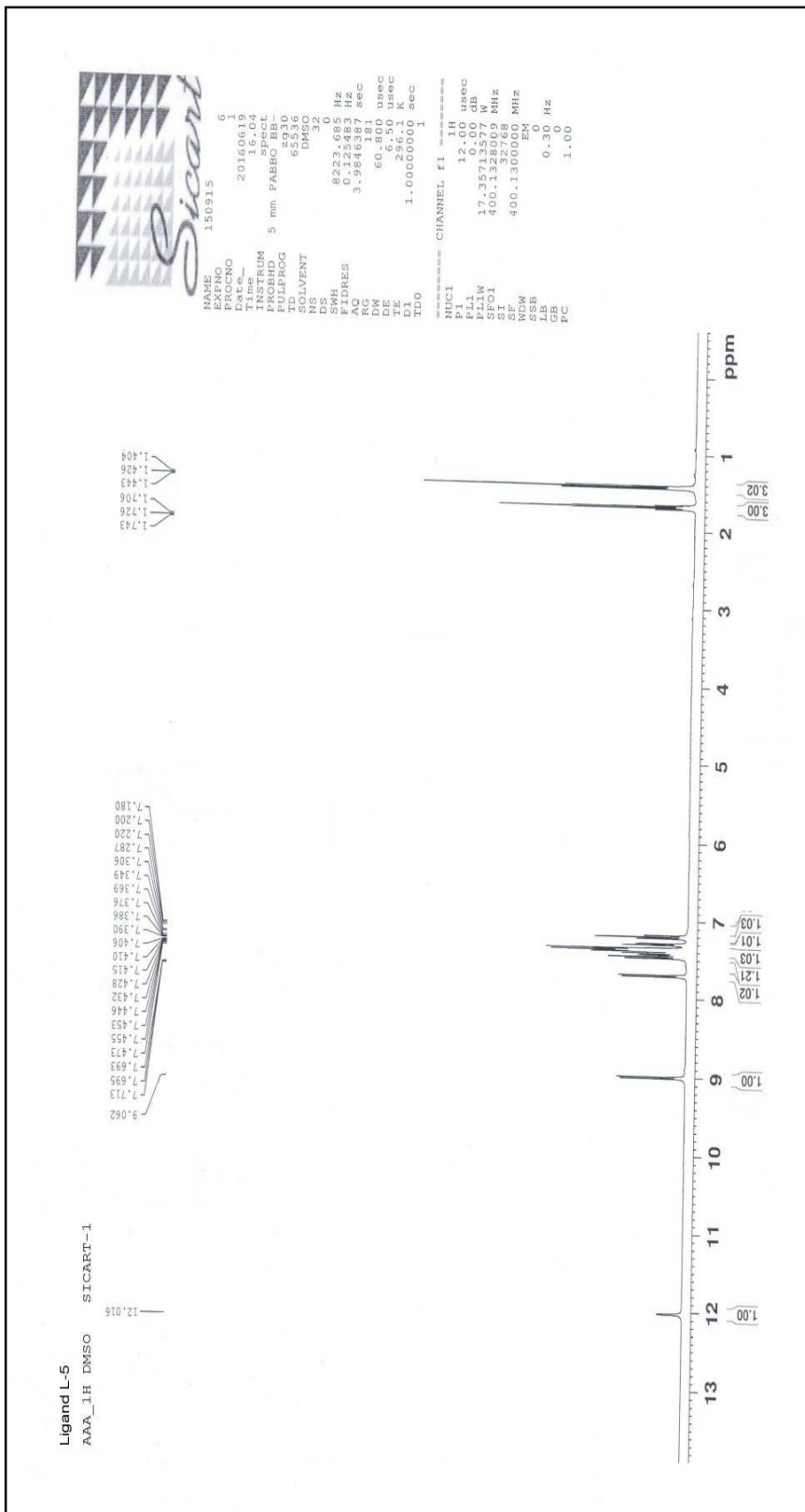
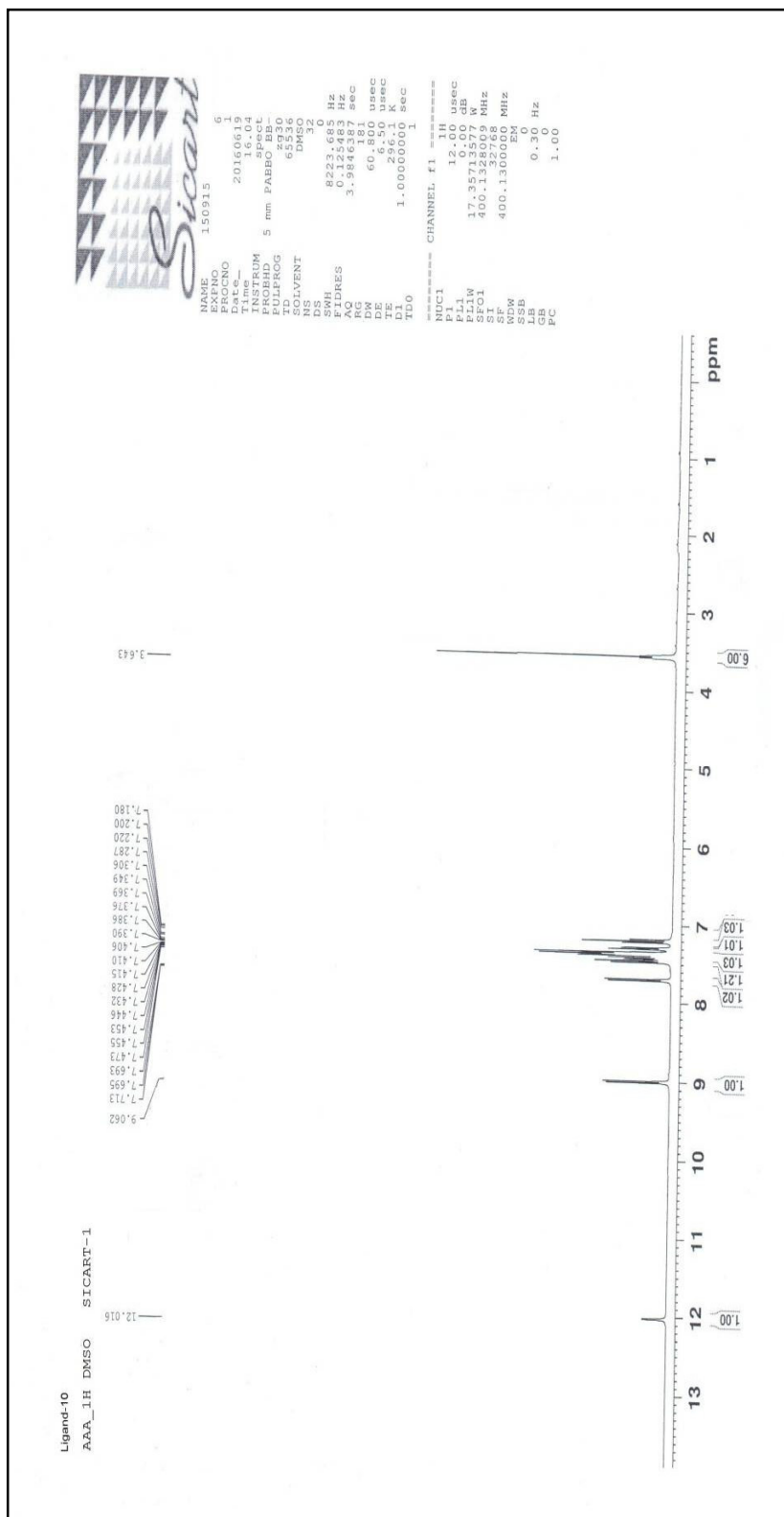


Fig. 3.6: NMR spectrum of ligand TPAS-3



3.3.4 Estimation of Number of carboxylic acid (-COOH) groups in ligands TPAS-1 to TPAS-5 and Bis ligand (TPTB).

The structure of ligand was tested by estimation of number of carboxylic groups (-COOH) per mole of ligands. The nonaqueous conductometric titration was used for -COOH group estimation by method reported in the literature⁵. The titrant used for this non-aqueous titration was tetra-n-butyl ammonium hydroxide (TBAH) in pyridine.

Non-aqueous conductometric titration

The ligand sample was dried at 70°C and finely powdered. This dried sample was used for non-aqueous conductometric titration. Exactly weighed amount of ligand sample was dissolved in 40 mL of anhydrous pyridine.

The solution was allowed to stand overnight for complete solubility. This ligand solution was transferred into conductance cell and it was then stirred magnetically. The base tetra-n-butyl ammonium hydroxide (TBAH) (0.1 N), in pyridine was added to the conductance cell at regular intervals of 0.01 mL of titrant beyond the stage of equivalence. The conductance measurement after addition of each volume of titrant base was carried out by allowing 2-3 mins lapse. During the titration, the temperature of solution was maintained constant about 25°C when the point of equivalence was exceeded, there was a continuous increase in conductance on addition of every additional aliquot of tetra-n-butyl ammonium hydroxide (TBAH) indicating the stage of complete neutralization of all the -COOH groups in the given amount of ligand sample. The volume of base added is converted into millimoles of tetra-n-butyl ammonium hydroxide required for 100 g of ligand. A plot of conductance against millimoles of tetra-n-butyl ammonium hydroxide per 100 g of ligand sample was plotted in (Fig. 3.8 and 3.9). Inspection of such plot revealed one break. From the plot, the millimoles per 100 g of ligand sample corresponding to the break were noted. From this value, the number of -COOH groups were estimated from this value

- Thus millimoles of TBAH required for complete neutralization of -COOH groups present in the sample was found by following formula using break of the titration curve. Finally one no. of COOH group calculated by:

No. of -COOH	Millimoles of TBAH	Molecular weight of
Groups per mole of =	per 100 gm of sample	ligand
Ligand		$\times 10^{-5}$

$$A = B \times M \times 10^{-5}$$

e.g. For TPAS-2	A	=	247 X 401.44 X 10 ⁻⁵
		=	0.99

Thus value of -COOH group for all the ligands are preferred in Table 3.4.

Results and Discussion:

The Titration Plot of each ligands contain one break so the value of -COOH groups is in the range of 0.99 to 1.02. The values confirming the structures.

Table 3.5: Non-aqueous Conductometric titration of Ligands TPAS-1 to TPAS-5 and Bis ligand (TPTB)

Estimation of –COOH groups.

Solvent: - Anhydrous pyridine.

Reagent: - 0.1 N tetra-n-butyl ammonium hydroxide (TBAH) in pyridine.

Ligands	Molecular Weight	Millimoles of TBAH at break per 100 gm of sample.	Estimated No. of –COOH group.
TPAS-1	407.46	245	1.00
TPAS-2	401.44	247	0.99
TPAS-3	402.42	244	0.98
TPAS-4	452.48	225	1.02
TPAS-5	436.87	229	1.00
TPTB	594.61	168	2.00

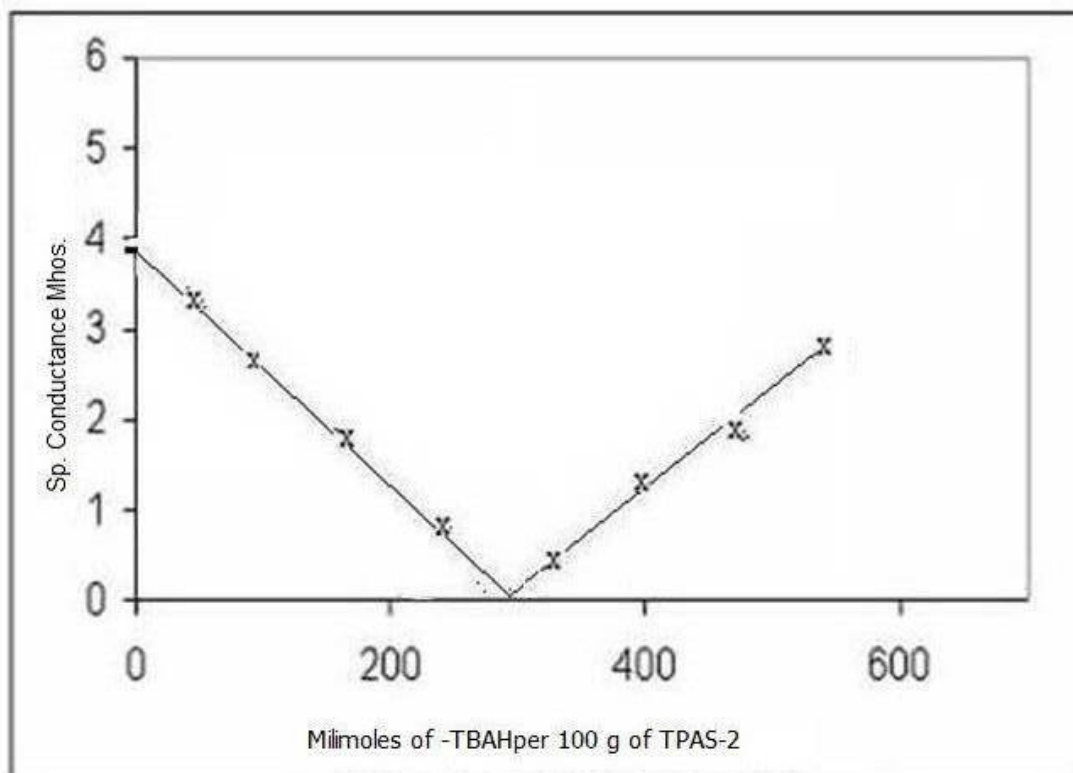


Fig. 3.8: Non-aqueous conductometric titration curve of ligand TPAS-2

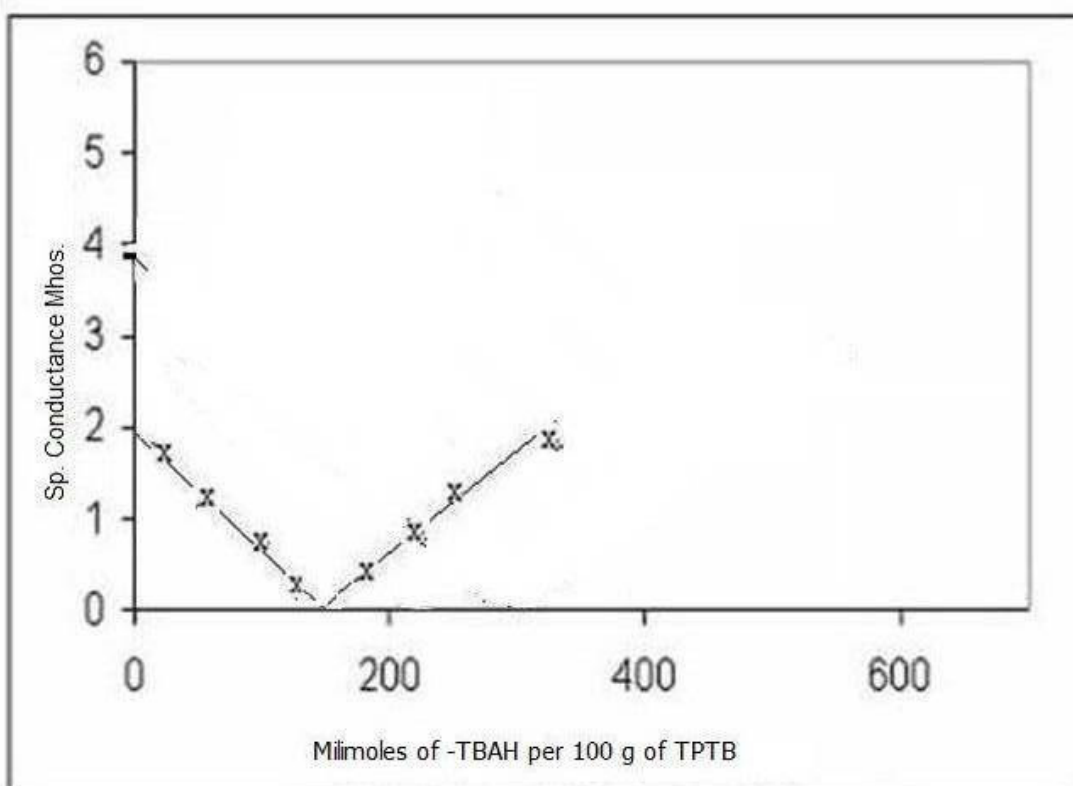


Fig. 3.9: Non-aqueous conductometric titration curve of ligand TPTB

3.3.5 Thermogravimetric study

The TG analysis of all the produced ligand sample was done by “Perkin Elmer Pyris 1 TGA” in an air. The test samples of 5.0 mg was placed in suspended platinum boat. The boat was covered by glass tube and placed in instrument furnace. The heating at the rate of 10°k/min was started with air flow. The automatic plot of wt. of ion vs temperature up to 700°C was obtained. The data were noted and selected TG thermograms are presented in Fig 3.10 to 3.12.

Inspection of the TG plot of all the samples reveals that (i) Each sample degrade in two steps (ii) The initial wt. of ions observed below 200°C - 230 °C for all samples in the range at 15 to 22%. This value id due to decarboxylation of ligand. The ion of -Co₂ is consisted with the value of sample weight. The next step of degrading beyond 230°C was rapid which is depending upon the nature of the ligand.

The calculated value of Co₂ of each ligand and 1st step degradation are shown in Table 3.6.

Table 3.6: Degradation data of ligands

Ligand	Wt. loss in 1st stage of degradation. (%)	Calculated value of decarboxylation (%)
TPAS-1	12.10	12.04
TPAS-2	12.50	12.62
TPAS-3	12.00	11.84
TPAS-4	12.40	12.44
TPAS-5	12.00	12.05
TPTB	11.70	11.68

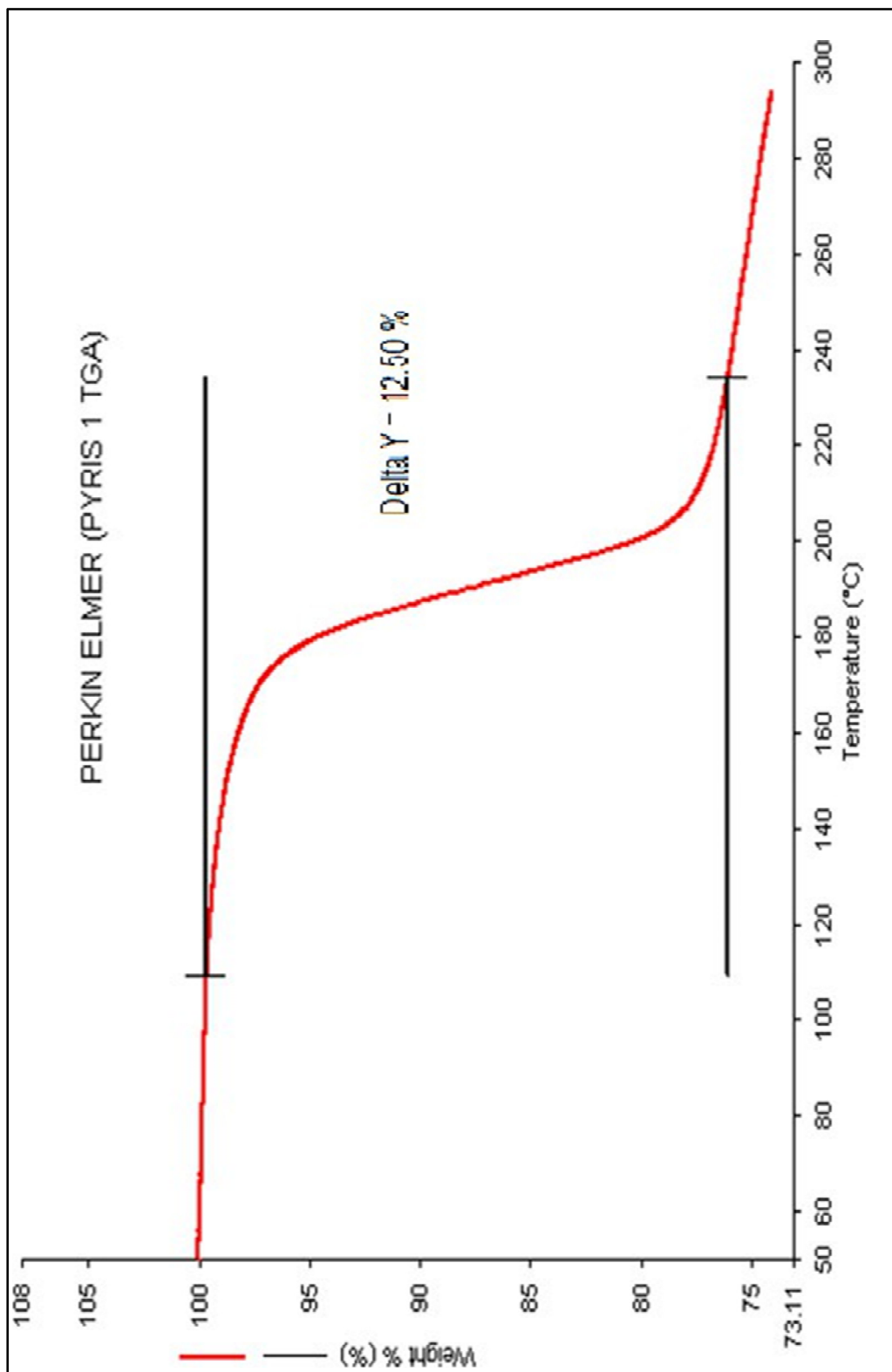


Fig 3.10: TGA thermogram of ligand TPAS-2

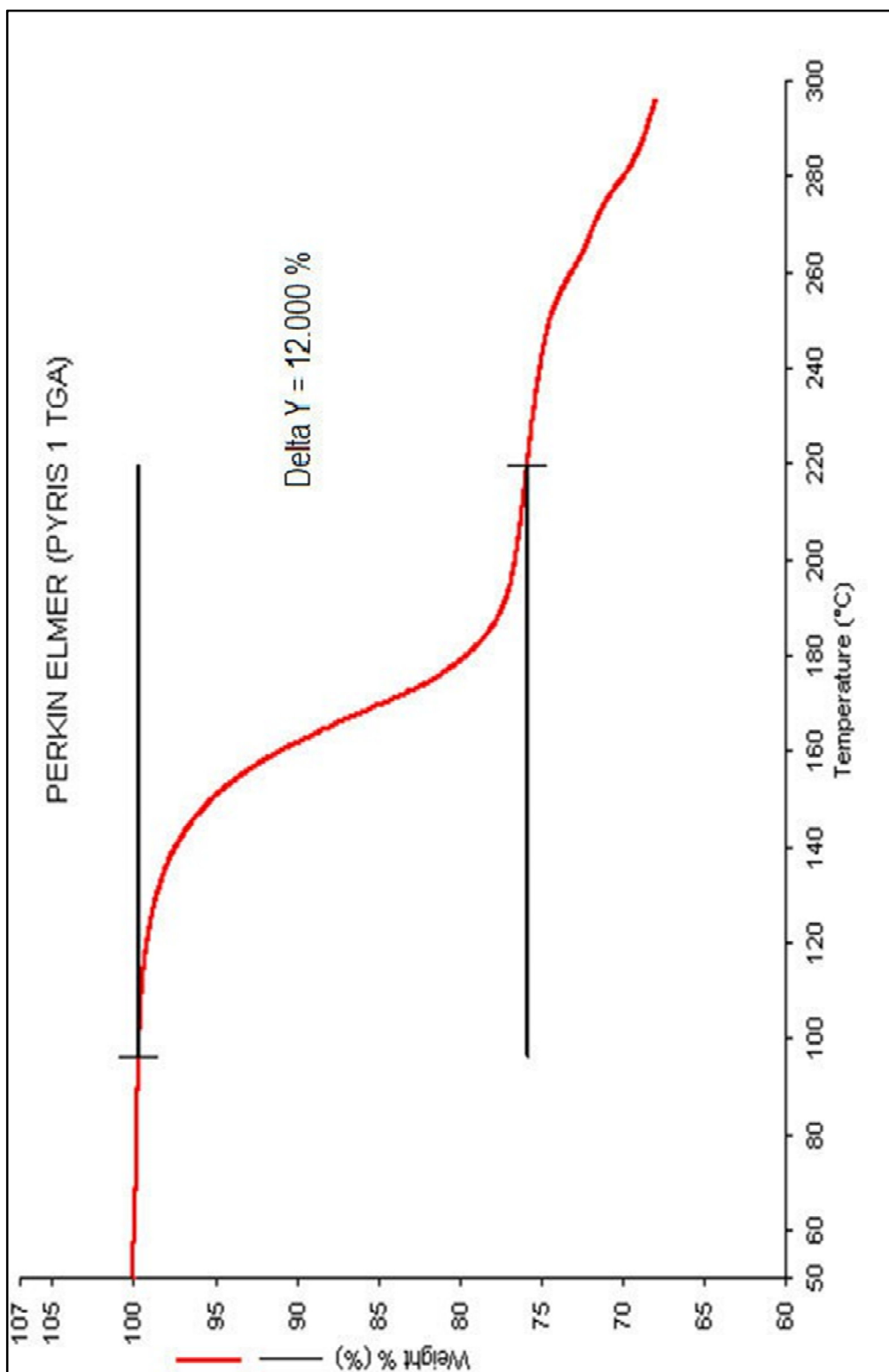


Fig. 3.11: TGA thermogram of ligand TPAS-3

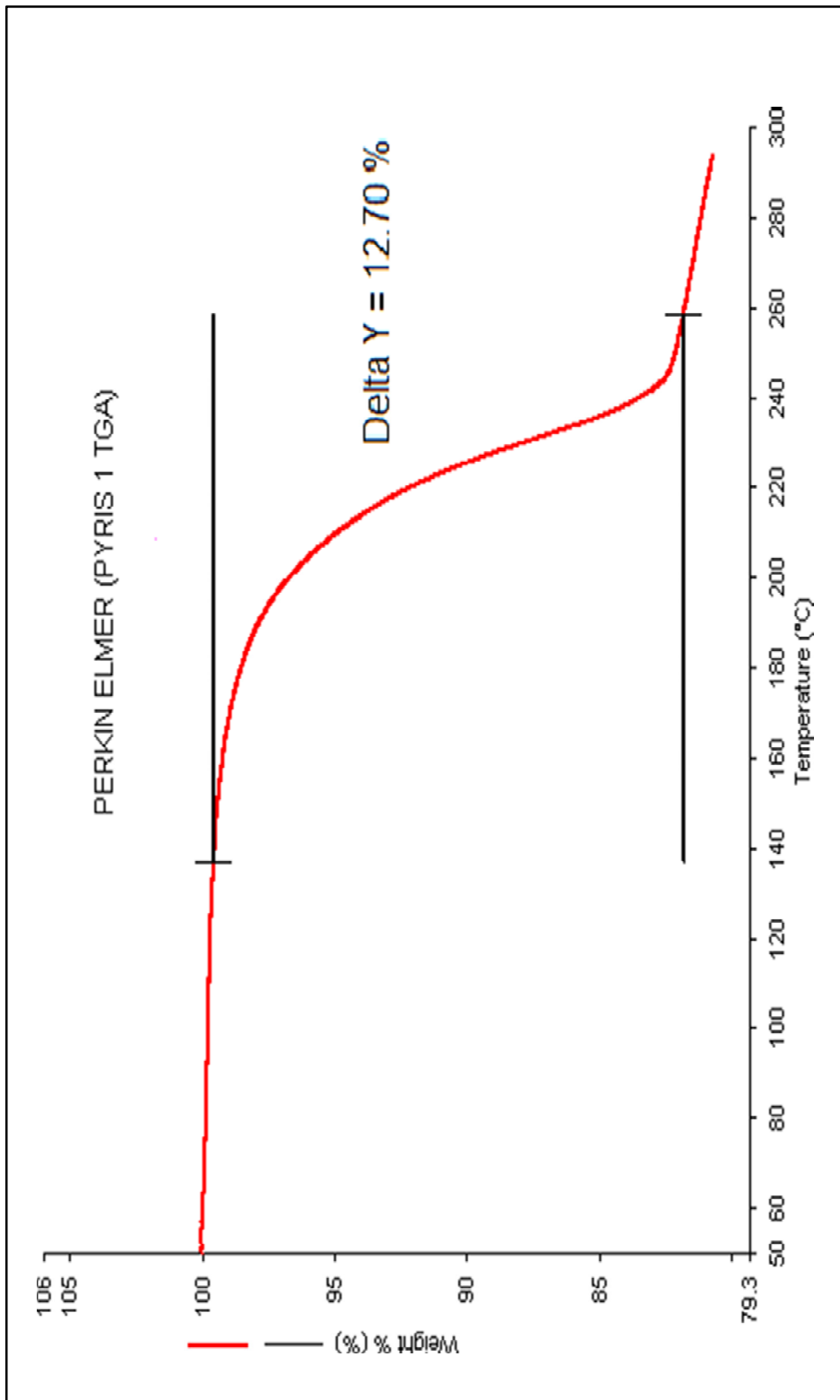


Fig. 3.12: TGA thermogram of Ligand TPTB

3.3.6 Differential scanning calorimeter [DSC]

Differential Scanning Calorimetry is generally applied for determine glass transition temperature and curing temperature, and melting point and exothermic or endothermic reaction of polymer or polymer systems. The ligands TPAS-1 to TPAS-5 and TPTB are big molecules. Their melting points could not be measured properly by capillary method. Hence, their melting points were determined by DSC. The melting point of each ligand was measured on PerkinElmer (Diamond DSC). The value of melting point was observed from DSC thermogram. Typical thermograms are shown in Figs -3.13 to Figure-3.15.

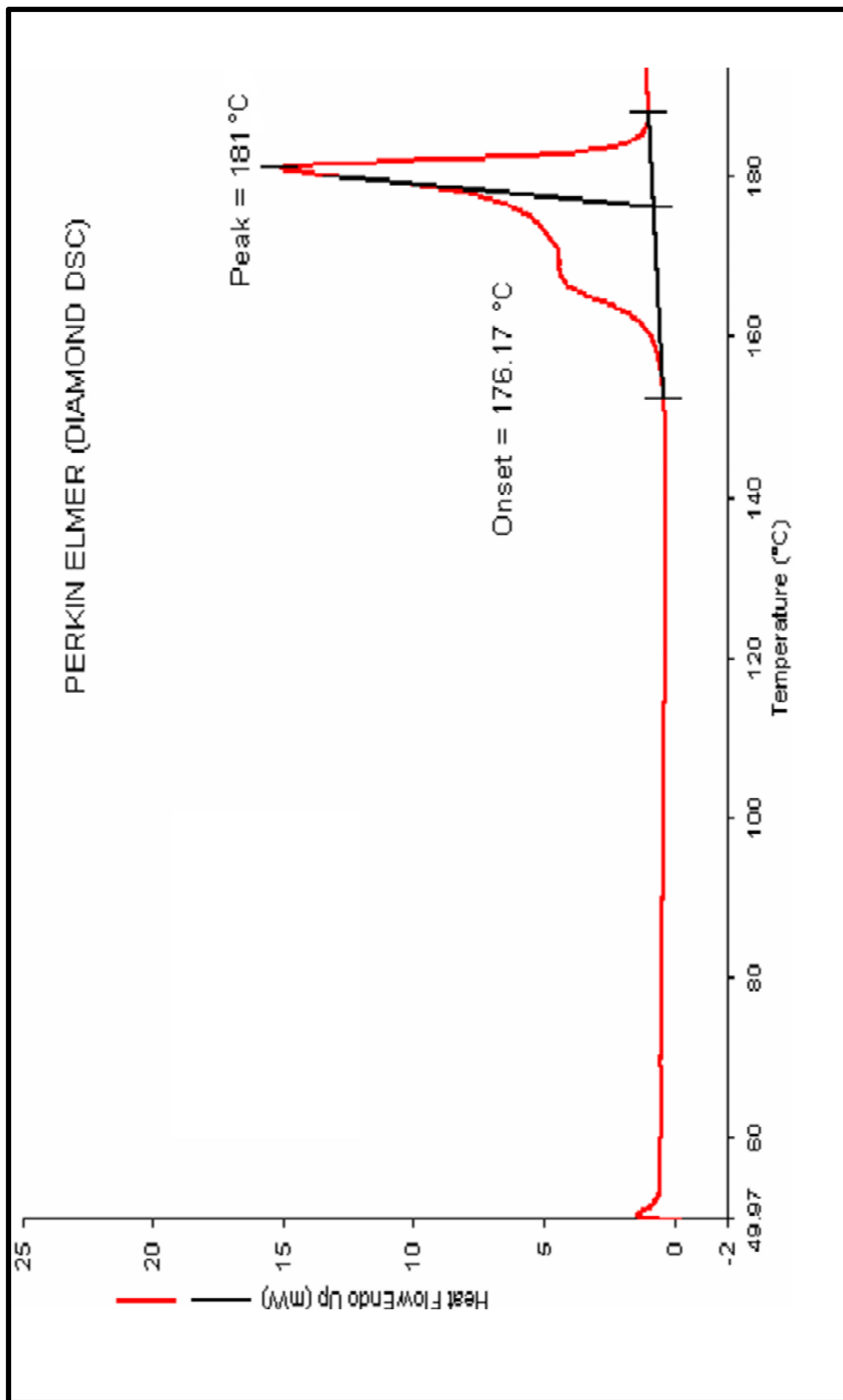


Fig. 3.13: DSC thermogram of ligand (TPAS-

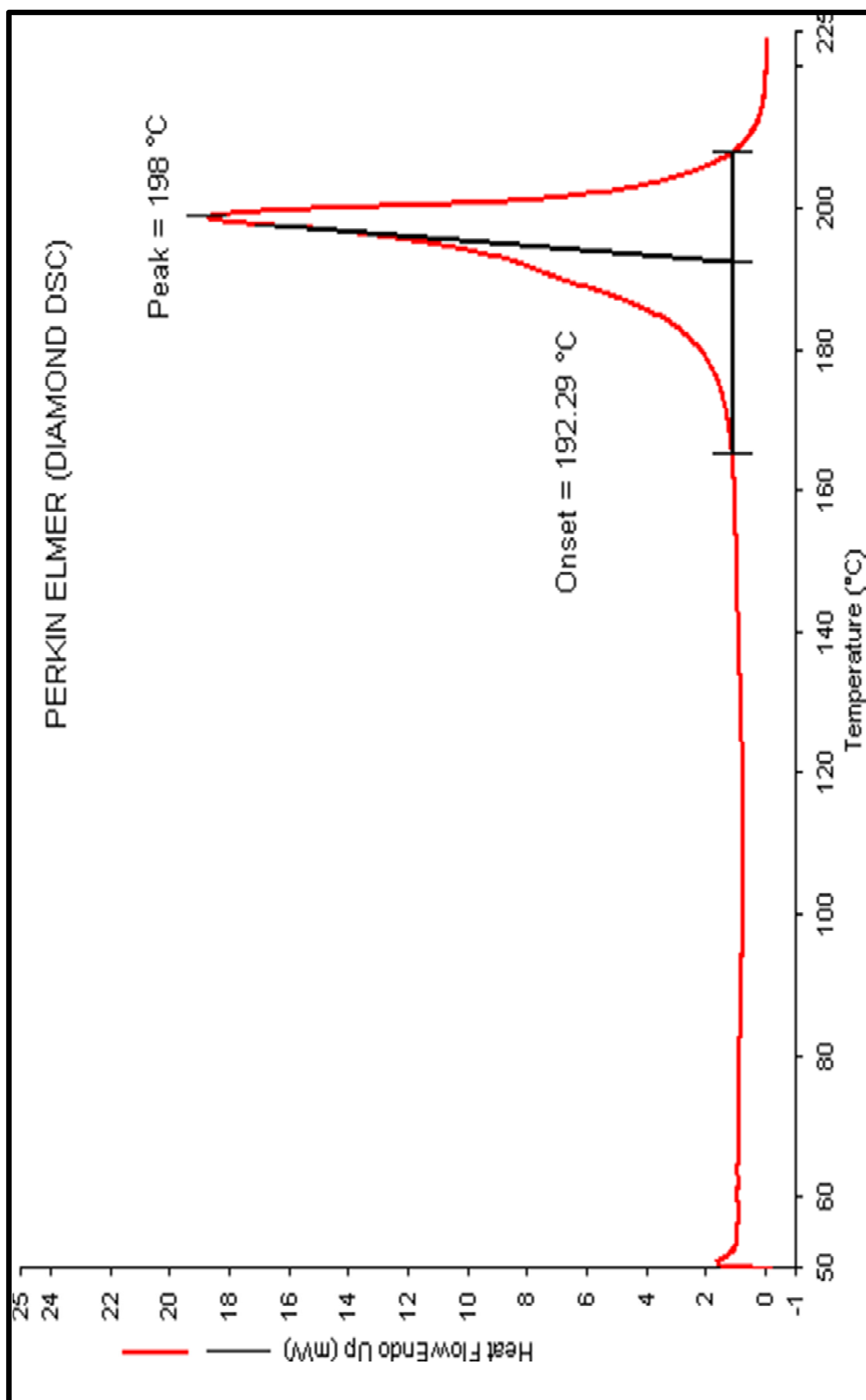


Fig. 3.14: DSC thermogram of ligand (TPAS-

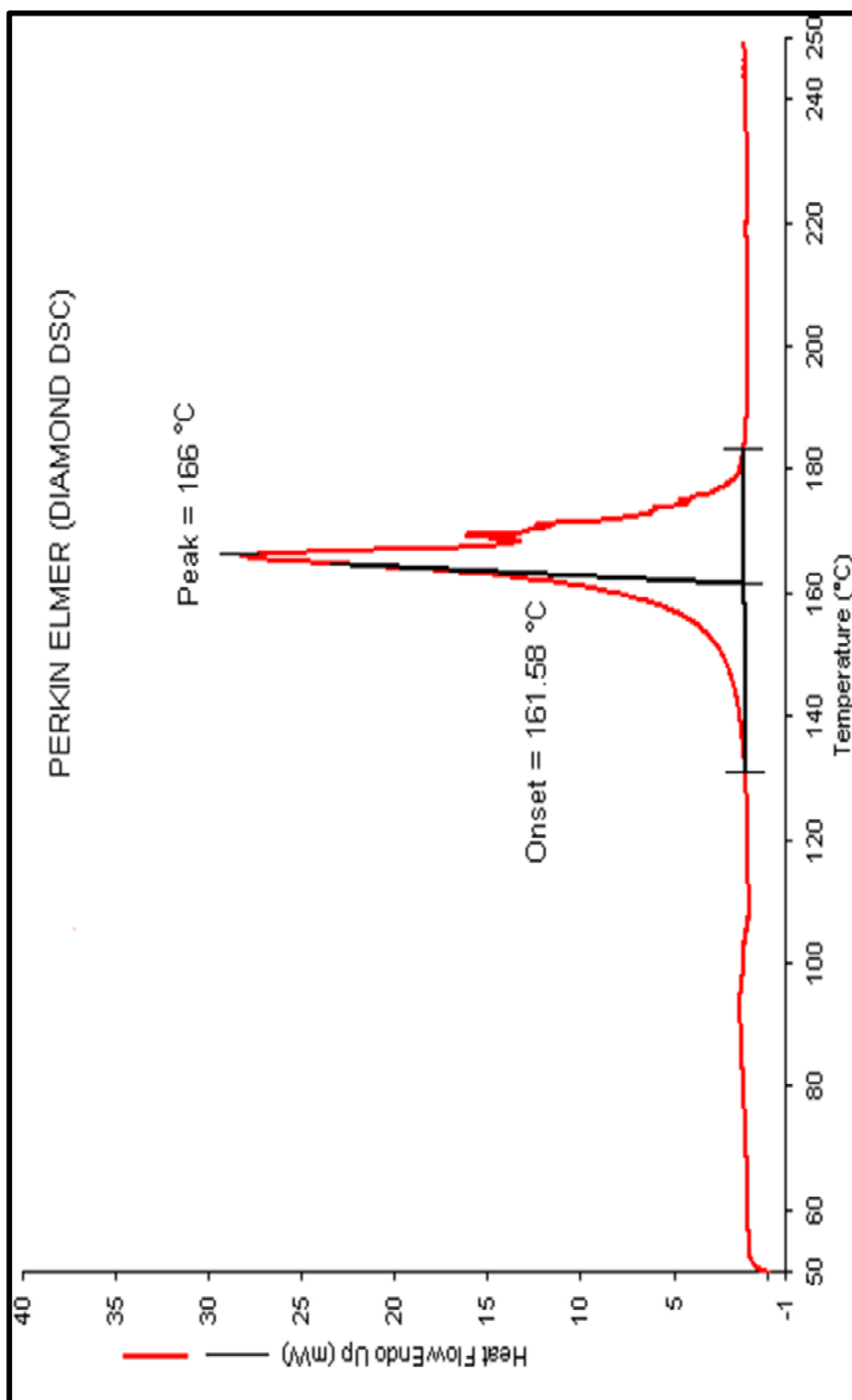


Fig. 3.15: DSC thermogram of ligand (TPTB)



REFERENCE

1. S. Hamad, and F. S. Abed, Synthesis of some new maleimide derivatives. *J. of Appli. chem.*, **3**(1), 56-63 (2014).
2. H. Hegde, V. Shetty and N. S. Shetty, Facile synthesis of some new maleamic acid and maleimide derivatives of 1,3-thiazoles. *J. of Chem. and Pharma. Res.*, **7**(8), 913-916 (2015).
3. F. W. Salman, S. W. Radhi and A. M odh, Preparation and study antibacterial activity of a new polymer *J. of Babylon Uni., Pure and applied sciences*, **2** (23), 759 (2015).
4. T. G. Tyurina et al., Amidation kinetics of succinic anhydride by amine-containing drugs. *J. Physc., Conf. Ser.*, doi.10.1088/1742-6596/1658/1/012063 (2020).
5. E. Vaclavova, P. Kelemen, Nonaqueous Potentiometric Titration of Copolymers Containing Itaconic Acid or its Monoesters. *Chem. Papers*, **48**(3), 203 (1994).



CHAPTER – IV

SYNTHESIS, CHARACTERIZATION AND ANTIMICROBIAL ACTIVITY OF METAL CHELATES

CONTENTS

- 4.1 EXPERIMENTAL**
- 4.2 METAL LIGAND (M:L) RATIO**
- 4.3 ELEMENTAL ANALYSIS**
- 4.4 INFRARED SPECTROSCOPY**
- 4.5 ELECTRONIC SPECTROSCOPY**
- 4.6 MAGNETIC PROPERTIES**
- 4.7 MEASUREMENT OF ELECTRICAL
CONDUCTIVITY**
- 4.8 MAGNETIC SUSCEPTIBILITY AND
REFLECTANCE SPECTRAL DATA CO-
RELATION**
- 4.9 THERMOGRAVIMETRIC ANALYSIS**
- 4.10 ANTIBACTERIAL ACTIVITY**
- 4.11 ANTIFUNGAL ACTIVITY**
- 4.12 CONCLUSION**

4.1 EXPERIMENTAL

The each ligands (TPAS-1 TO 5 and TPTB) was purified by dissolving in dilute alkali solution and reprecipitated by diluted HCL solution. All the ligands were processed up to dried amorphous powder state.

4.1.1 Preparation of Sodium Salt of Ligands

A purified and dried ligand sample (0.1 M) was mixed in 150 mL of acetone solvent and stirred. Aqueous molar NaOH solution (calculated amount) was added drop wise to the ligand solution. The thick solution was stirred for some hours till paste type precipitates appeared. A fixed quantity of water was added to make clear solution. The resulting solution was diluted to 250 mL water and this clear solution called as reagent solution. This aqueous solution was used for preparing metal chelates.

4.1.2 Synthesis of Metal Chelates of Ligands TPAS-1 to 5.

➤ Chelates with Cu^{2+} Meatal ions:

25 ml of Na^+ reagent solution of ligand (containing 10 mmol) was mixed dropwise to copper salt solution in 100 ml of deionized water, The pH of resultant mixture was adjusted by addition solid sodium acetate. A greenish – blue solid product was digested on boiling water bath for 2 hrs. It was filtered, washed by acetone and air -dried. The powder was dried in oven at 100°C for a one day. The yield was 75%.

➤ Chelates with Ni^{2+} Meatal ions:

25 ml of Na^+ reagent solution of ligand (containing 10 mmol) was mixed dropwise to nickle salt solution in 100 ml of deionized water, The pH of resultant mixture was adjusted by addition solid sodium acetate. A wet cake product was digested on boiling water bath for 2 hrs. It was filtered, washed by acetone and air -dried. The powder was dried in oven at 100°C for a one day. The yield was 72%.

➤ **Chelates with Co²⁺ Metal ions**

25 ml of Na⁺ reagent solution of ligand (containing 10 mmol) was mixed dropwise to cobalt salt solution in 100 ml of deionized water, The pH of resultant mixture was adjusted by addition solid sodium acetate. A solid floppy material was digested on boiling water bath for 2 hrs. It was filtered, washed by acetone and air -dried. The powder was dried in oven at 100°C for a one day. The yield was 66%.

➤ **Chelates with Mn²⁺ Metal ions:**

25 ml of Na⁺ reagent solution of ligand (containing 10 mmol) was mixed dropwise to manganese salt solution in 100 ml of deionized water, The pH of resultant mixture was adjusted by addition solid sodium acetate. A wet cake product was digested on boiling water bath for 2 hrs. It was filtered, washed by acetone and air -dried. The powder was dried in oven at 100°C for a one day. The yield was 75%.

➤ **Chelates with Zn²⁺ Metal Ions:**

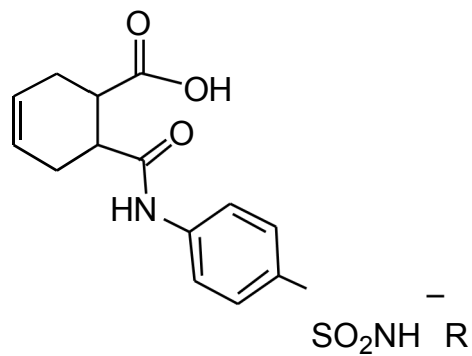
25 ml of Na⁺ reagent solution of ligand (containing 10 mmol) was mixed dropwise to zinc salt solution in 100 ml of deionized water, The pH of resultant mixture was adjusted by addition solid sodium acetate. A wet cake product was digested on boiling water bath for 2 hrs. It was filtered, washed by acetone and air -dried. The powder was dried in oven at 100°C for a one day. The yield was 67%. The dried chelate was pale yellowish powder.

4.1.3 Elemental analysis of metal chelates.

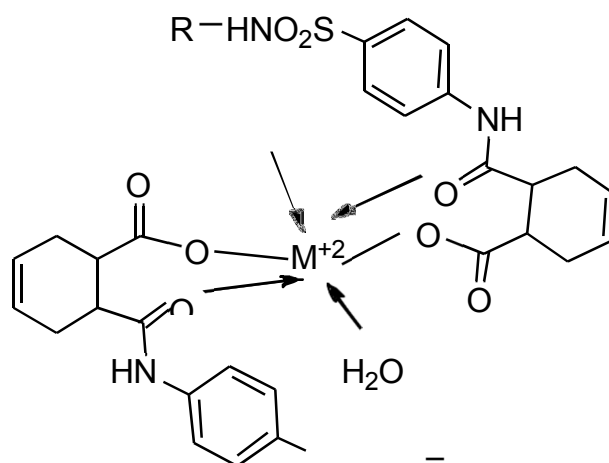
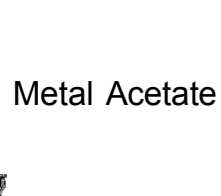
The elemental contents i.e. C, H, N and S elements of metal chelates were analyzing on elemental analyzer (Model: Thermofinigan Flash 1101 EA). The results of analysis are described in Tables 4.1 to 4.4. It indicate that the result are consistent with the structure shown in scheme 4.1.

4.2 METAL: LIGAND (M:L) RATIO

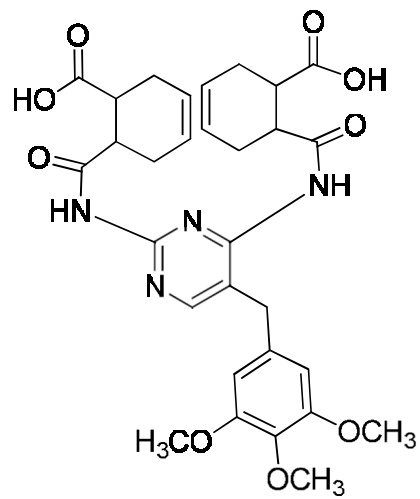
Metal % in chelate was estimated by literature procedure¹. In this process fix amount of ligand was taken in an evaporating dish and each one ml of Analar Concentrated HCL, H₂SO₄, and HCLO₄ were added. Then decompose the sample by evaporated to dryness. The residue was dissolved in distilled water and diluted to mark. The position of this solution was titrated against ethylenediamine tetra acetic acid (EDTA) solution and the metal % in chelate calculated. The results are mentioned in Table 4.1 to 4.6. The results indicate that Metal: Ligand (M:L) ration is 1:2 tor bivalent metals.



Ligands

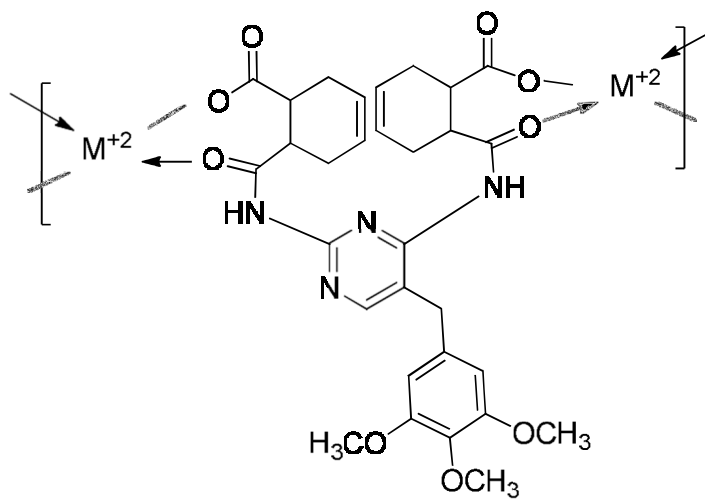


Metal chelates of TPAS-1 to TPAS-6



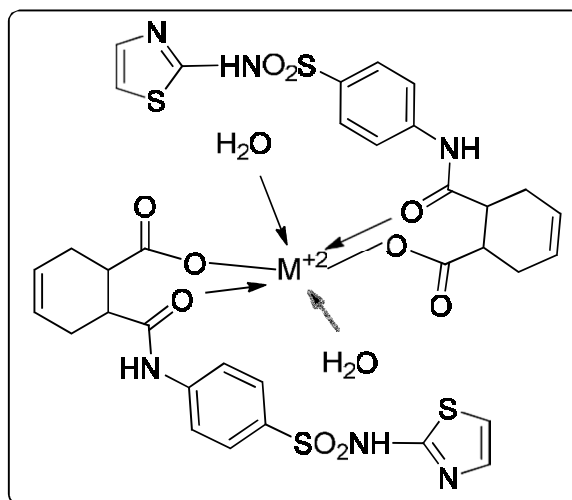
[Bis ligand - TPTB]

Metal acetate



Metal chelates of Bis ligand - TPTB

4.3 ELEMENTAL ANALYSIS

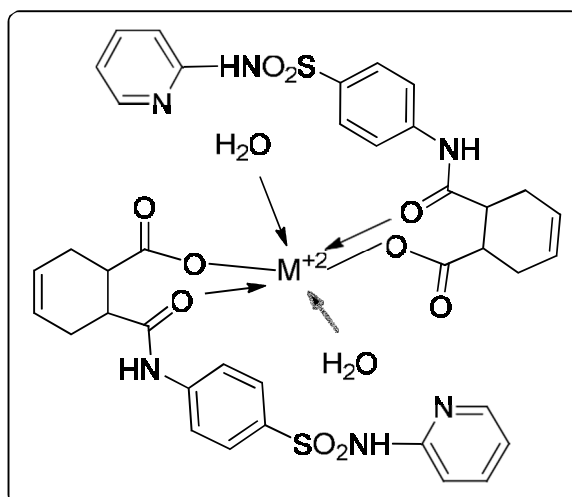


Metal chelates of ligand TPAS-1

Table 4.1: Properties of metal chelates of ligand TPAS-1

Metal Chelates	Molecular Formula	M.Wt.	Yield (%)
(TPAS-1) ₂ Cu ²⁺	C ₃₄ H ₃₂ N ₆ O ₁₀ S ₄ Cu ²⁺ .2H ₂ O	912.45	74
(TPAS-1) ₂ Ni ²⁺	C ₃₄ H ₃₂ N ₆ O ₁₀ S ₄ Ni ²⁺ .2H ₂ O	907.62	73
(TPAS-1) ₂ Mn ²⁺	C ₃₄ H ₃₂ N ₆ O ₁₀ S ₄ Mn ²⁺ .2H ₂ O	903.92	76
(TPAS-1) ₂ Co ²⁺	C ₃₄ H ₃₂ N ₆ O ₁₀ S ₄ Co ²⁺ .2H ₂ O	907.92	68
(TPAS-1) ₂ Zn ²⁺	C ₃₄ H ₃₂ N ₆ O ₁₀ S ₄ Zn ²⁺ .2H ₂ O	914.32	66

Metal Chelates	% Metal Analysis		Elemental Analysis							
			%C		%H		%N		%S	
	Cald.	Found	Cald.	Found	Cald.	Found	Cald.	Found	Cald.	Found
(TPAS-1) ₂ Cu ²⁺	6.96	7.00	44.71	44.70	3.94	3.90	9.21	9.20	14.02	14.00
(TPAS-1) ₂ Ni ²⁺	6.47	6.50	44.95	45.00	3.97	4.00	9.25	9.30	14.10	14.10
(TPAS-1) ₂ Mn ²⁺	6.08	6.10	45.13	45.10	3.98	4.00	9.30	9.30	14.16	14.20
(TPAS-1) ₂ Co ²⁺	6.50	6.50	44.83	44.80	3.96	4.00	9.25	9.30	14.09	14.10
(TPAS-1) ₂ Zn ²⁺	7.15	7.15	44.51	44.50	3.94	4.00	9.18	9.20	13.99	14.00

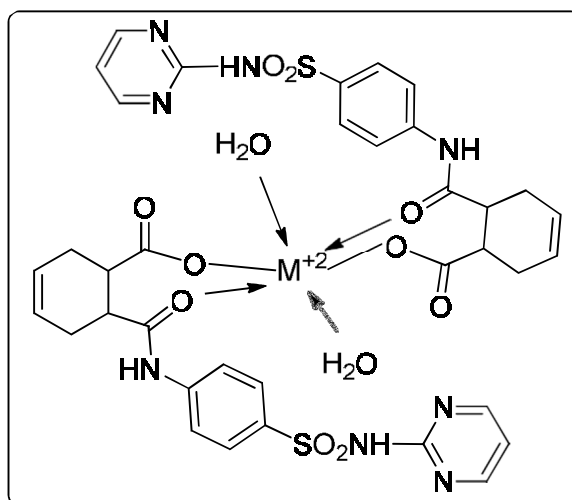


Metal chelates of ligand TPAS-2

Table 4.2: Properties of metal chelates of ligand TPAS-2

Metal Chelates	Molecular Formula	M.Wt.	Yield (%)
(TPAS-2) ₂ Cu ²⁺	C ₃₈ H ₃₆ N ₆ O ₁₀ S ₂ Cu ²⁺ .2H ₂ O	900.38	75
(TPAS-2) ₂ Ni ²⁺	C ₃₈ H ₃₆ N ₆ O ₁₀ S ₂ Ni ²⁺ .2H ₂ O	895.58	74
(TPAS-2) ₂ Mn ²⁺	C ₃₈ H ₃₆ N ₆ O ₁₀ S ₂ Mn ²⁺ .2H ₂ O	891.88	77
(TPAS-2) ₂ Co ²⁺	C ₃₈ H ₃₆ N ₆ O ₁₀ S ₂ Co ²⁺ .2H ₂ O	895.88	69
(TPAS-2) ₂ Zn ²⁺	C ₃₈ H ₃₆ N ₆ O ₁₀ S ₂ Zn ²⁺ .2H ₂ O	902.28	65

Metal Chelates	% Metal		Elemental Analysis											
	Analysis		%C			%H			%N			%S		
	Cald.	Found	Cald.	Found	Cald.	Found	Cald.	Found	Cald.	Found	Cald.	Found	Cald.	Found
(TPAS-2) ₂ Cu ²⁺	7.05	7.00	50.64	50.60	4.44	4.40	9.33	9.30	7.10	7.10	7.10	7.10	7.10	7.10
(TPAS-2) ₂ Ni ²⁺	6.55	6.50	50.91	50.90	4.47	4.50	9.38	9.40	7.15	7.15	7.20	7.20	7.20	7.20
(TPAS-2) ₂ Mn ²⁺	6.16	6.20	51.12	51.10	4.48	4.50	9.42	9.40	7.17	7.17	7.20	7.20	7.20	7.20
(TPAS-2) ₂ Co ²⁺	6.58	6.60	50.90	50.90	4.46	4.50	9.37	9.40	7.14	7.14	7.10	7.10	7.10	7.10
(TPAS-2) ₂ Zn ²⁺	7.20	7.20	50.53	50.50	4.43	4.40	9.31	9.30	7.09	7.09	7.10	7.10	7.10	7.10

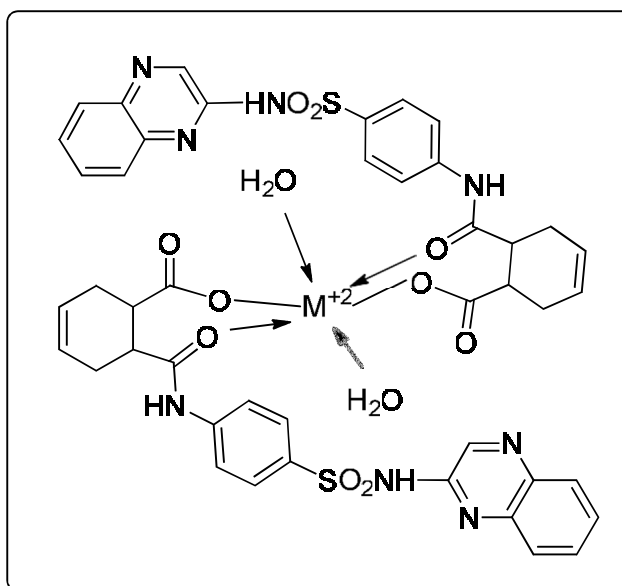


Metal chelates of ligand TPAS-3

Table 4.3: Properties of metal chelates of ligand TPAS-3

Metal Chelates	Molecular Formula	M.Wt.	Yield (%)
(TPAS-3) ₂ Cu ²⁺	C ₃₆ H ₃₄ N ₈ O ₁₀ S ₂ Cu ²⁺ .2H ₂ O	902.34	76
(TPAS-3) ₂ Ni ²⁺	C ₃₆ H ₃₄ N ₈ O ₁₀ S ₂ Ni ²⁺ .2H ₂ O	897.54	75
(TPAS-3) ₂ Mn ²⁺	C ₃₆ H ₃₄ N ₈ O ₁₀ S ₂ Mn ²⁺ .2H ₂ O	893.84	76
(TPAS-3) ₂ Co ²⁺	C ₃₆ H ₃₄ N ₈ O ₁₀ S ₂ Co ²⁺ .2H ₂ O	897.84	70
(TPAS-3) ₂ Zn ²⁺	C ₃₆ H ₃₄ N ₈ O ₁₀ S ₂ Zn ²⁺ .2H ₂ O	904.24	66

Metal Chelates	% Metal		Elemental Analysis							
	Analysis		%C		%H		%N		%S	
	Cald.	Found	Cald.	Found	Cald.	Found	Cald.	Found	Cald.	Found
(TPAS-3) ₂ Cu ²⁺	7.03	7.00	47.87	47.90	4.21	4.20	12.41	12.40	7.09	7.10
(TPAS-3) ₂ Ni ²⁺	6.54	6.50	48.13	48.10	4.23	4.20	12.48	12.50	7.13	7.10
(TPAS-3) ₂ Mn ²⁺	6.15	6.20	48.33	48.30	4.25	4.30	12.53	12.50	7.16	7.20
(TPAS-3) ₂ Co ²⁺	6.57	6.60	48.11	48.10	4.23	4.30	12.47	12.50	7.13	7.10
(TPAS-3) ₂ Zn ²⁺	7.23	7.20	47.77	47.80	4.20	4.20	12.38	12.40	7.08	7.10



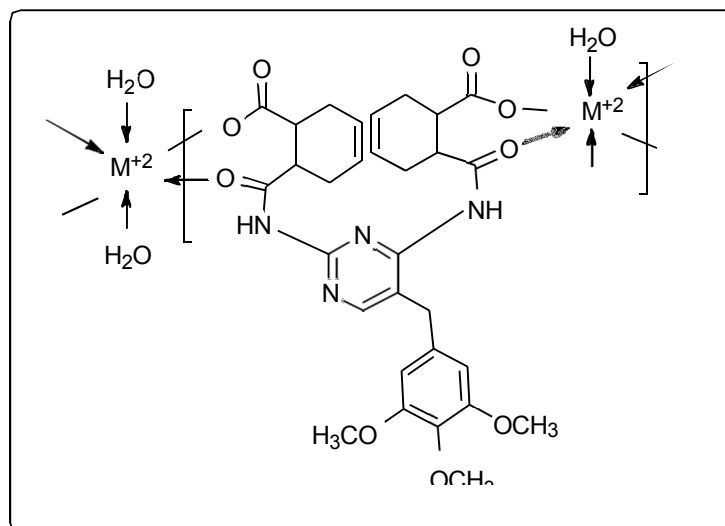
Metal chelates of ligand TPAS-4

Table 4.4: Properties of metal chelates of ligand TPAS-4

Metal Chelates	Molecular Formula	M.Wt.	Yield (%)
(TPAS-4) ₂ Cu ²⁺	C ₄₄ H ₃₈ N ₈ O ₁₀ S ₂ Cu ²⁺ .2H ₂ O	1002.46	75
(TPAS-4) ₂ Ni ²⁺	C ₄₄ H ₃₈ N ₈ O ₁₀ S ₂ Ni ²⁺ .2H ₂ O	997.66	77
(TPAS-4) ₂ Mn ²⁺	C ₄₄ H ₃₈ N ₈ O ₁₀ S ₂ Mn ²⁺ .2H ₂ O	993.96	75
(TPAS-4) ₂ Co ²⁺	C ₄₄ H ₃₈ N ₈ O ₁₀ S ₂ Co ²⁺ .2H ₂ O	997.96	72
(TPAS-4) ₂ Zn ²⁺	C ₄₄ H ₃₈ N ₈ O ₁₀ S ₂ Zn ²⁺ .2H ₂ O	1004.36	68

Sr. No.	Metal Chelates	% Metal Analysis		Elemental Analysis							
		Cald.	Found	%C		%H		%N		%S	
				Cald.	Found	Cald.	Found	Cald.	Found	Cald.	Found
1.	(TPAS-4) ₂ Cu ²⁺	6.33	6.30	52.67	52.70	4.19	4.20	11.17	11.20	6.38	6.40
2.	(TPAS-4) ₂ Ni ²⁺	5.88	5.90	52.72	52.70	4.21	4.20	11.23	11.20	6.41	6.40
3.	(TPAS-4) ₂ Mn ²⁺	5.53	5.50	53.12	53.10	4.23	4.20	11.27	11.30	6.44	6.40
4.	(TPAS-4) ₂ Co ²⁺	5.91	6.00	52.90	52.90	4.21	4.20	11.22	11.20	6.41	6.40
5.	(TPAS-4) ₂ Zn ²⁺	6.51	6.50	52.57	52.50	4.18	4.20	11.15	11.20	6.37	6.40

Metal Chelates	% Metal Analysis		Elemental Analysis							
			%C		%H		%N		%S	
	Cald.	Found	Cald.	Found	Cald.	Found	Cald.	Found	Cald.	Found
(TPAS-5) ₂ Cu ²⁺	6.54	6.50	44.48	44.50	3.70	3.70	11.53	11.50	6.59	6.60
(TPAS-5) ₂ Ni ²⁺	6.07	6.10	44.70	44.70	3.72	3.70	11.59	11.60	6.62	6.60
(TPAS-5) ₂ Mn ²⁺	5.71	5.70	44.87	44.90	3.74	3.70	11.63	11.60	6.65	6.60
(TPAS-5) ₂ Co ²⁺	6.10	6.10	44.68	44.70	3.72	3.70	11.58	11.60	6.62	6.60
(TPAS-5) ₂ Zn ²⁺	6.72	6.70	44.39	44.40	3.70	3.70	11.51	11.50	6.58	6.60



Metal chelates of Bis-ligand TPTB

Table 4.6: Properties of metal chelates of Bis-ligand TPTB

Metal Chelates	Molecular Formula	M.Wt.	Yield (%)
(TPTB) ₂ Cu ²⁺	C ₆₀ H ₆₄ N ₈ O ₁₈ Cu ²⁺ .2H ₂ O	1284.72	75
(TPTB) ₂ Ni ²⁺	C ₆₀ H ₆₄ N ₈ O ₁₈ Ni ²⁺ .2H ₂ O	1279.92	77
(TPTB) ₂ Mn ²⁺	C ₆₀ H ₆₄ N ₈ O ₁₈ Mn ²⁺ .2H ₂ O	1276.22	74
(TPTB) ₂ Co ²⁺	C ₆₀ H ₆₄ N ₈ O ₁₈ Co ²⁺ .2H ₂ O	1280.22	74
(TPTB) ₂ Zn ²⁺	C ₆₀ H ₆₄ N ₈ O ₁₈ Zn ²⁺ .2H ₂ O	1286.62	68

Metal Chelates	% Metal Analysis		Elemental Analysis					
			%C		%H		%N	
	Cald.	Found	Cald.	Found	Cald.	Found	Cald.	Found
(TPTB) ₂ Cu ²⁺	4.94	5.00	56.04	56.00	5.29	5.30	8.71	8.70
(TPTB) ₂ Ni ²⁺	4.59	4.60	56.25	56.30	5.31	5.30	8.75	8.70
(TPTB) ₂ Mn ²⁺	4.31	4.30	56.41	56.40	5.33	5.30	8.77	8.80
(TPTB) ₂ Co ²⁺	4.60	4.60	56.24	56.20	5.31	5.30	8.74	8.70
(TPTB) ₂ Zn ²⁺	5.08	5.10	55.96	56.00	5.28	5.30	8.70	8.70

4.4 INFRARED SPECTROSCOPY

The selected IR scans of metal chelates are presented in Figs. 4.1 to 4.8.

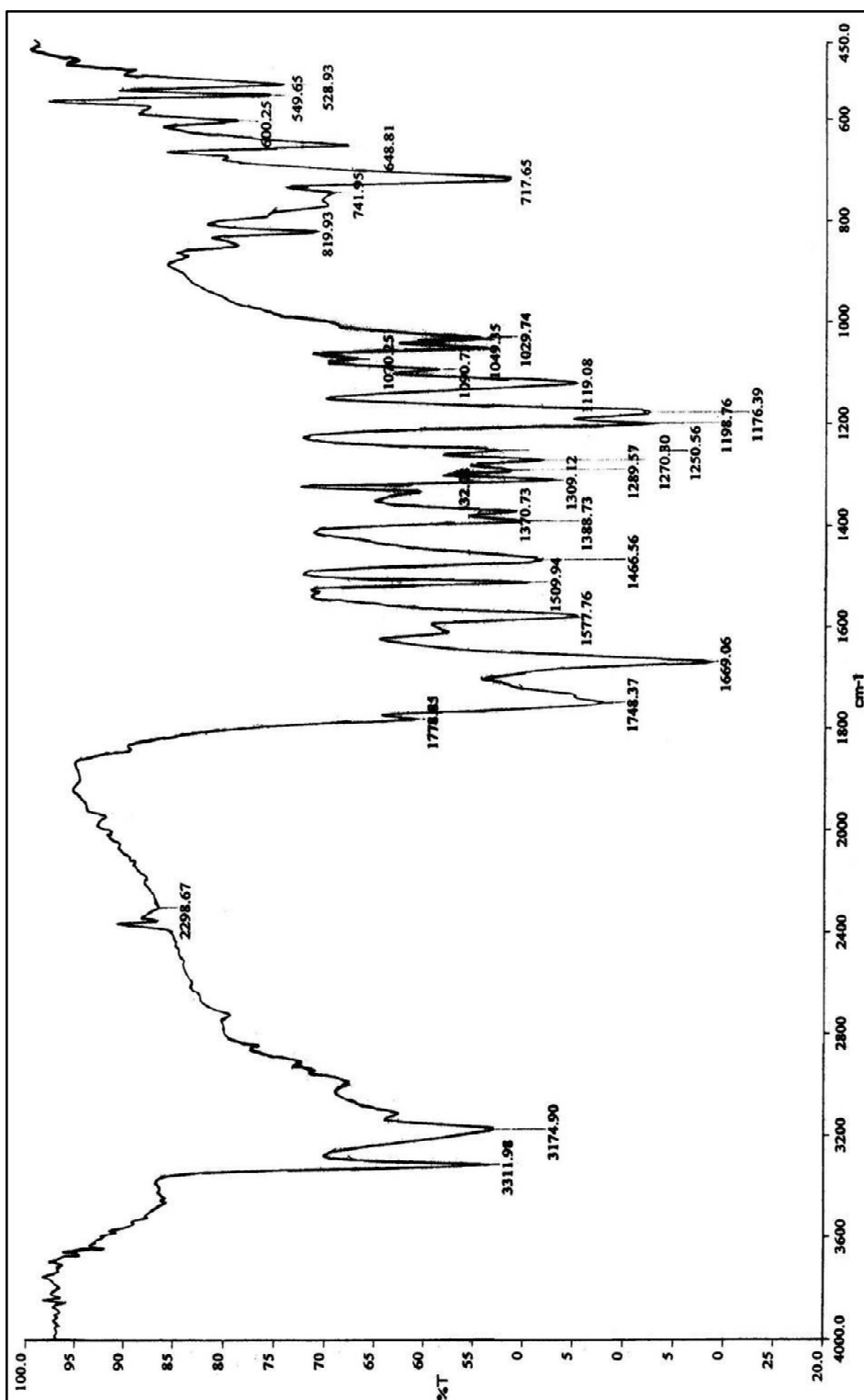


Fig. 4.1: IR spectrum of [TPAS-1]₂ Cu²⁺

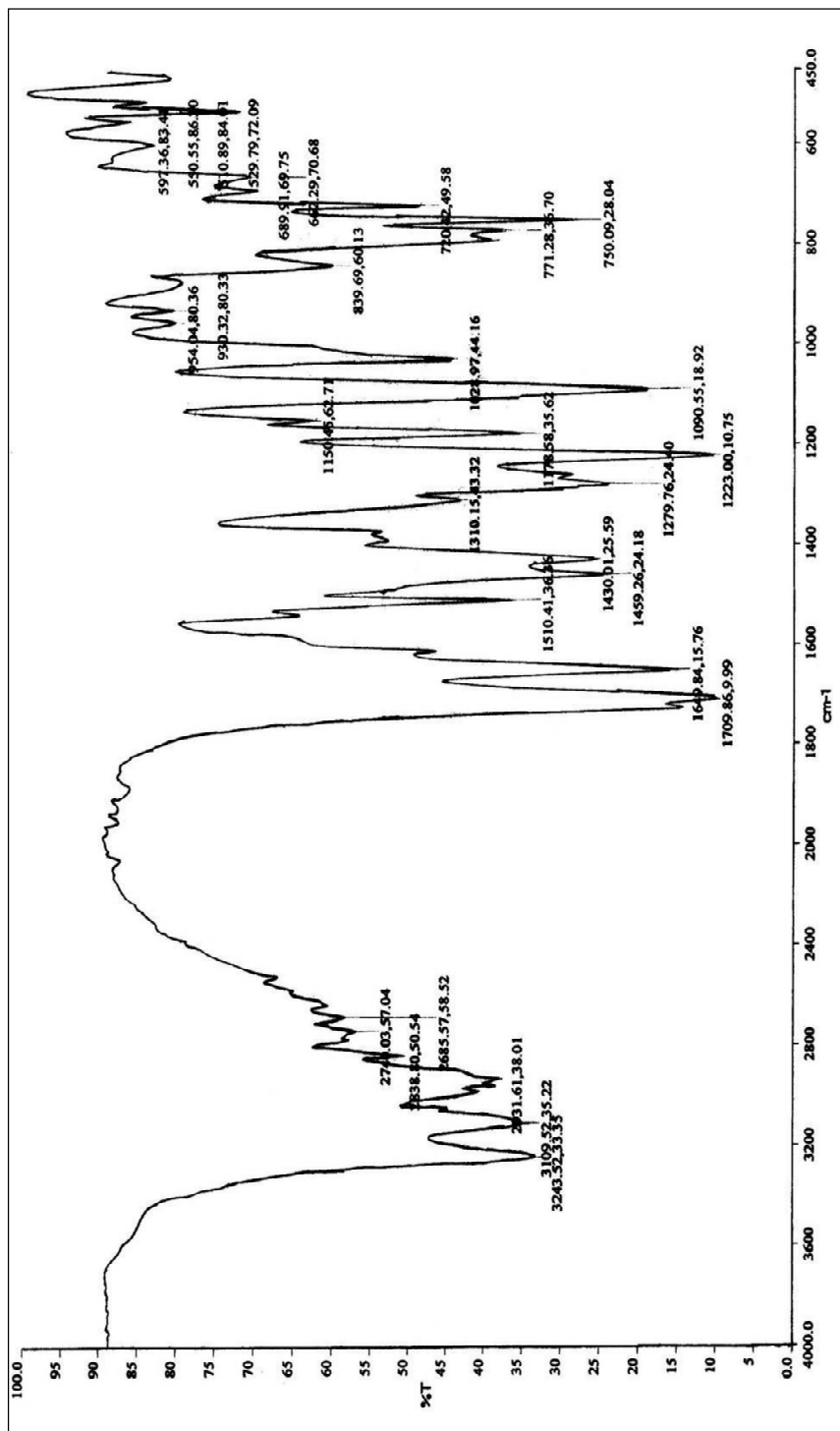


Fig. 4.2: IR spectrum of [TPAS-1]₂ Mn²⁺

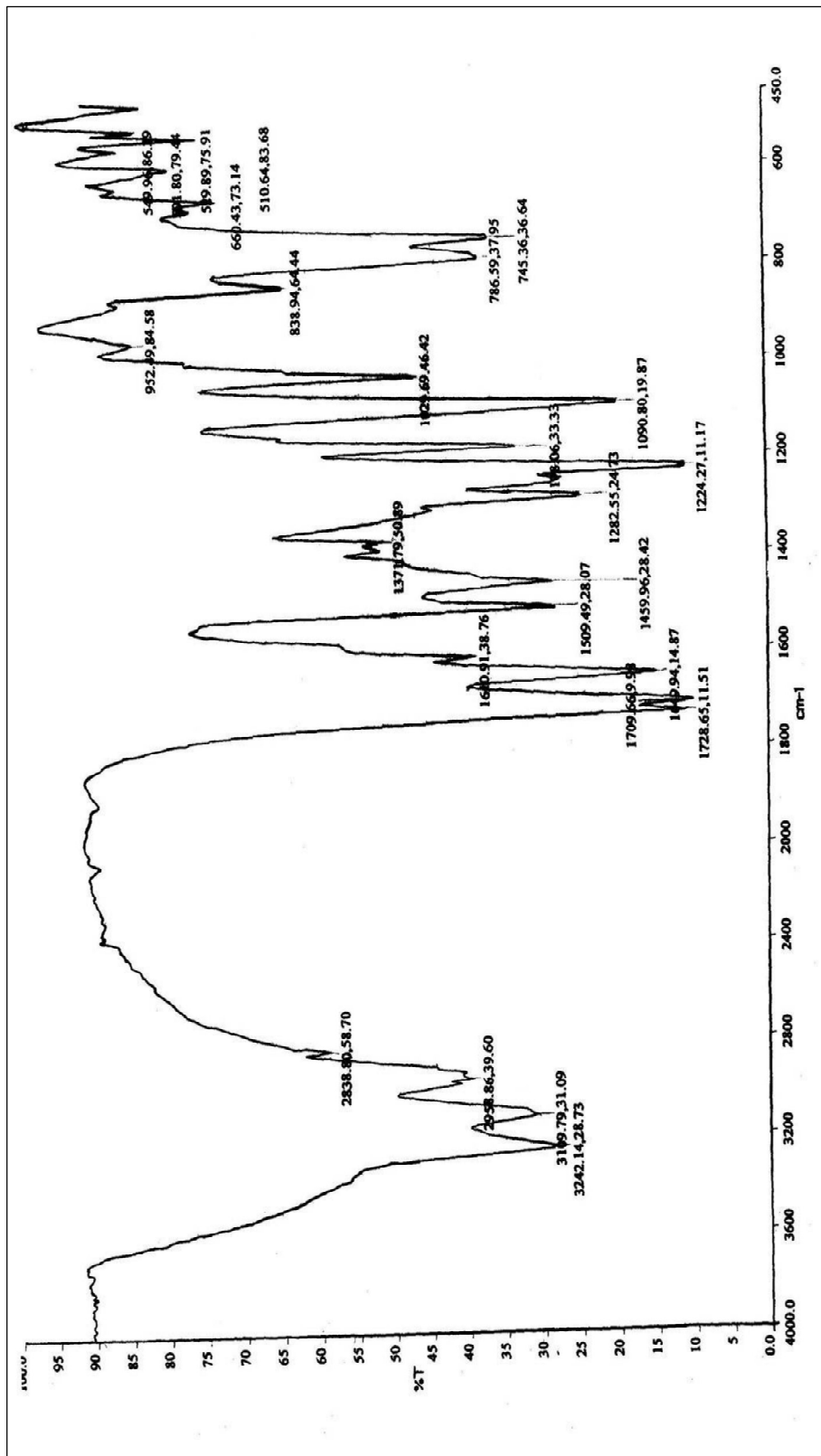


Fig. 4.3: IR spectrum of [TPAS-3]₂Co²⁺

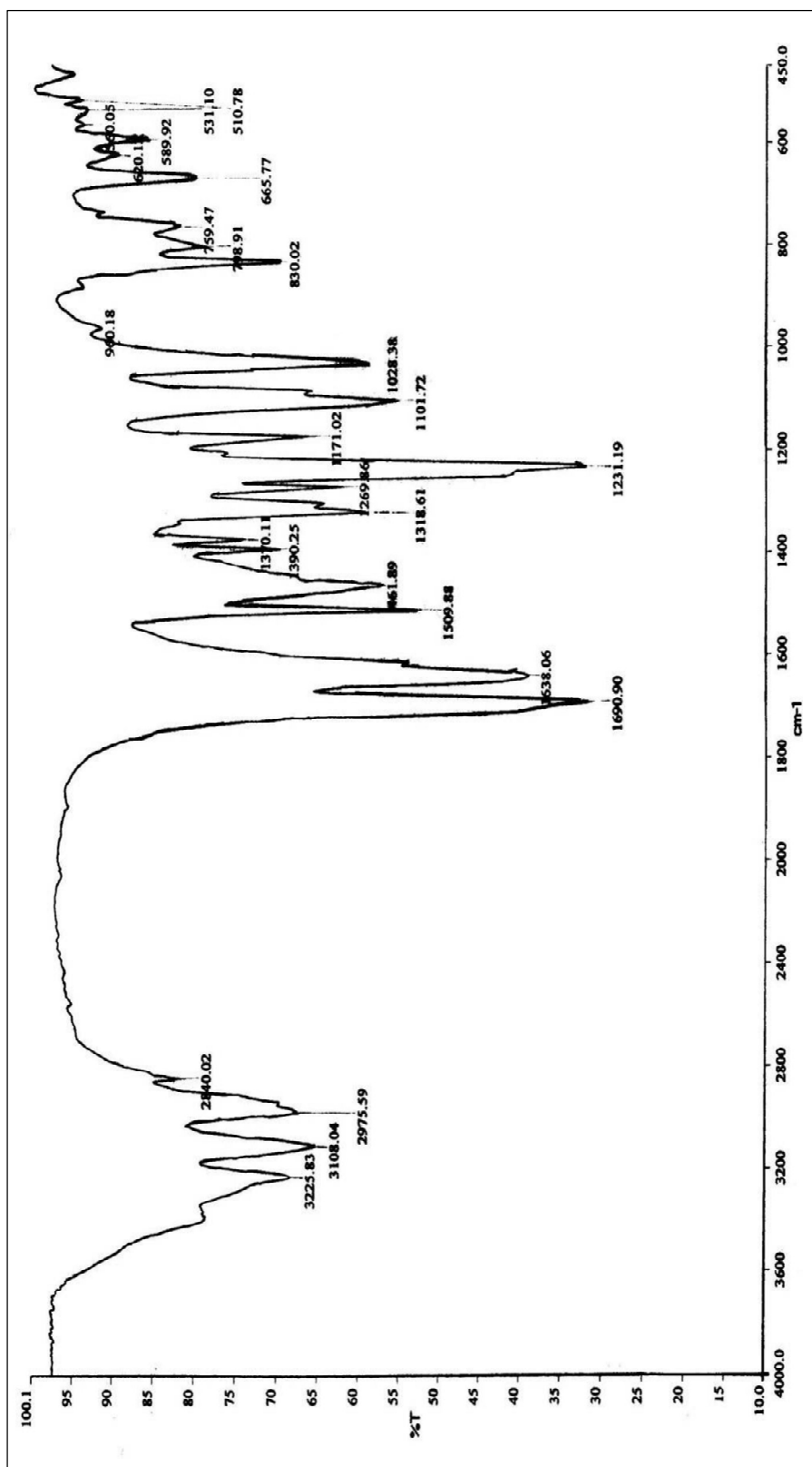


Fig. 4.4: IR spectrum of [TPAS-3]₂Mn²⁺

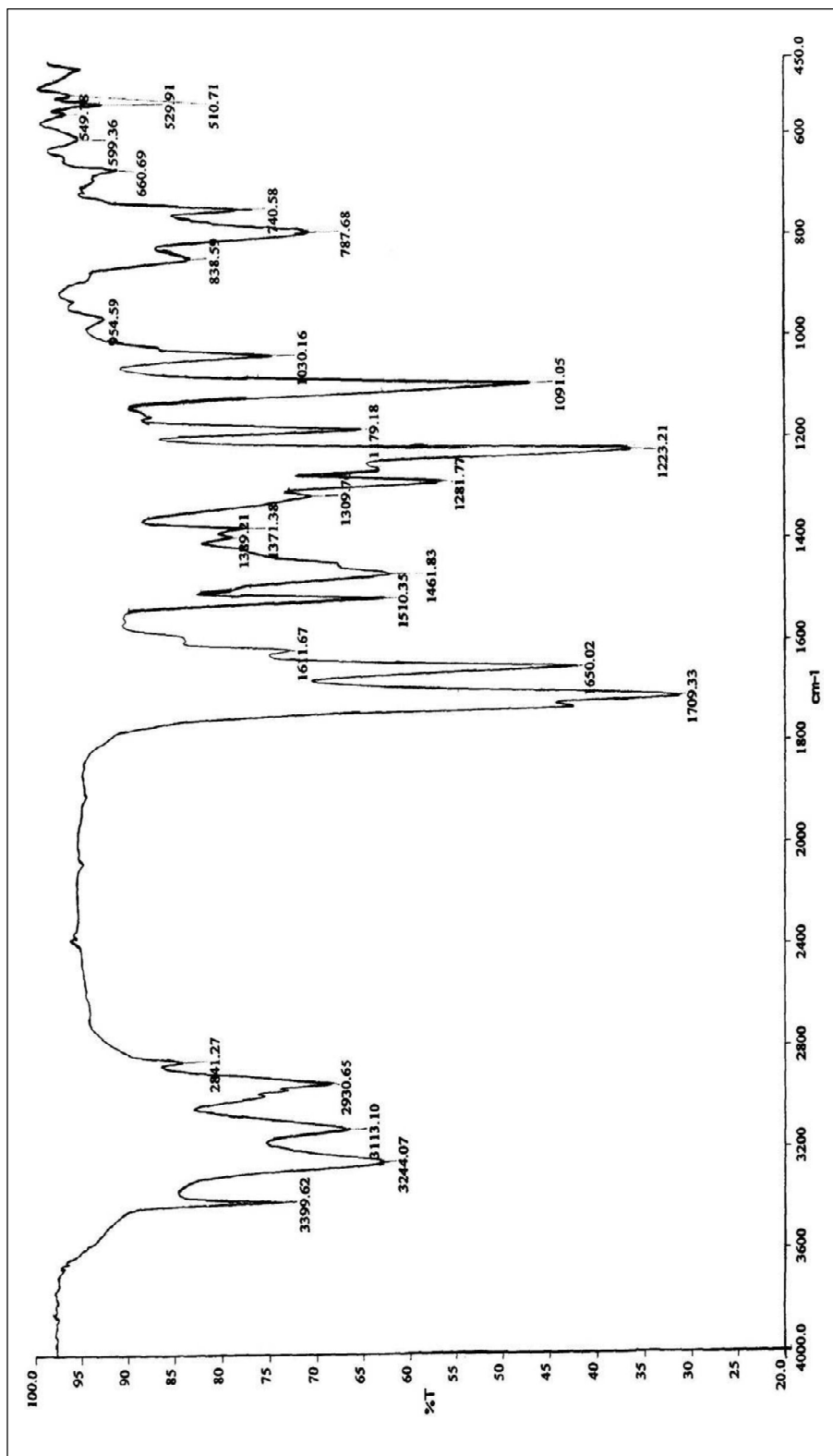


Fig. 4.5: IR spectrum of [TPAS-4]₂ Cu⁺²

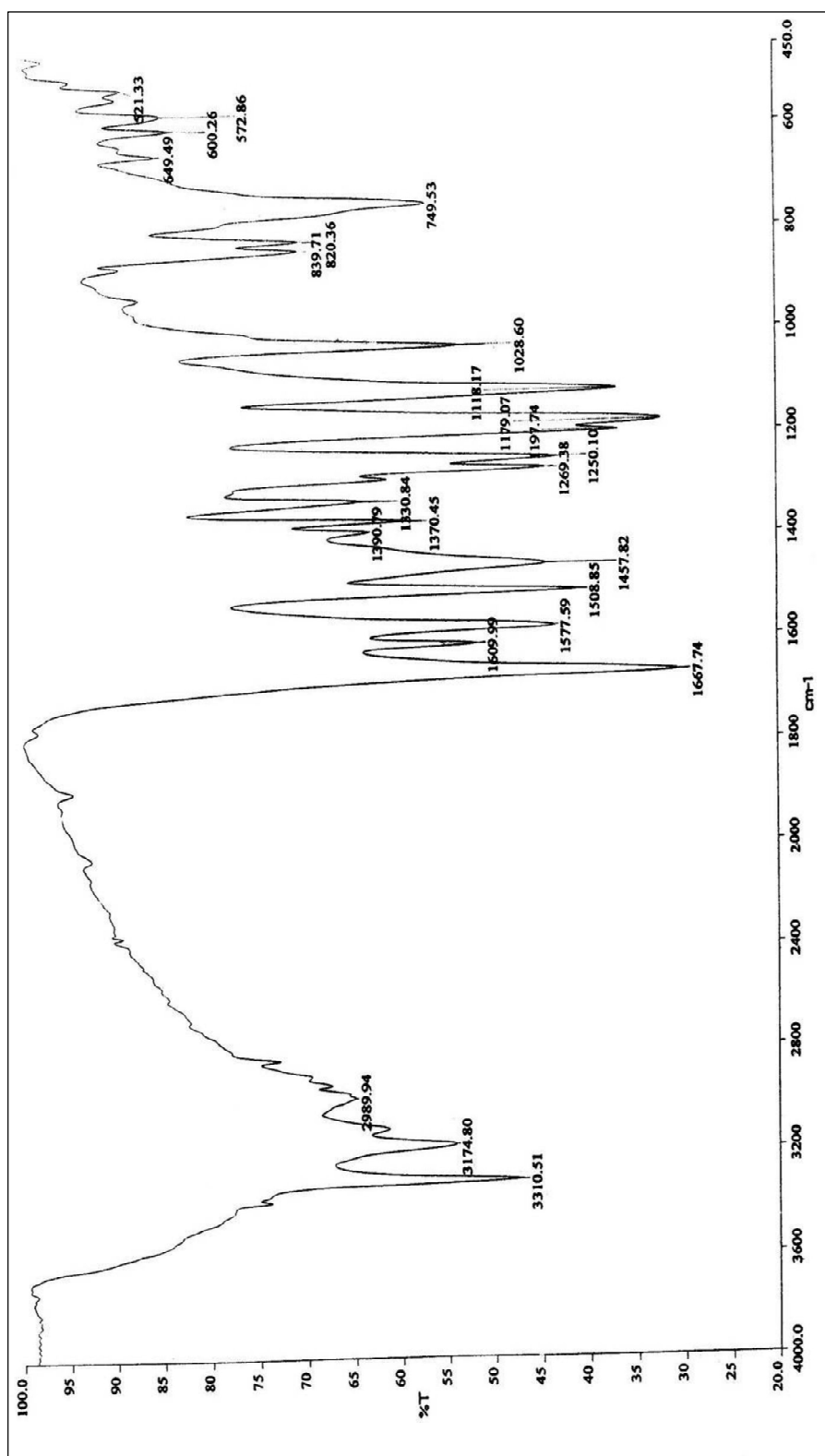


Fig. 4.6: IR spectrum of [TPAS-4]₂Co²⁺

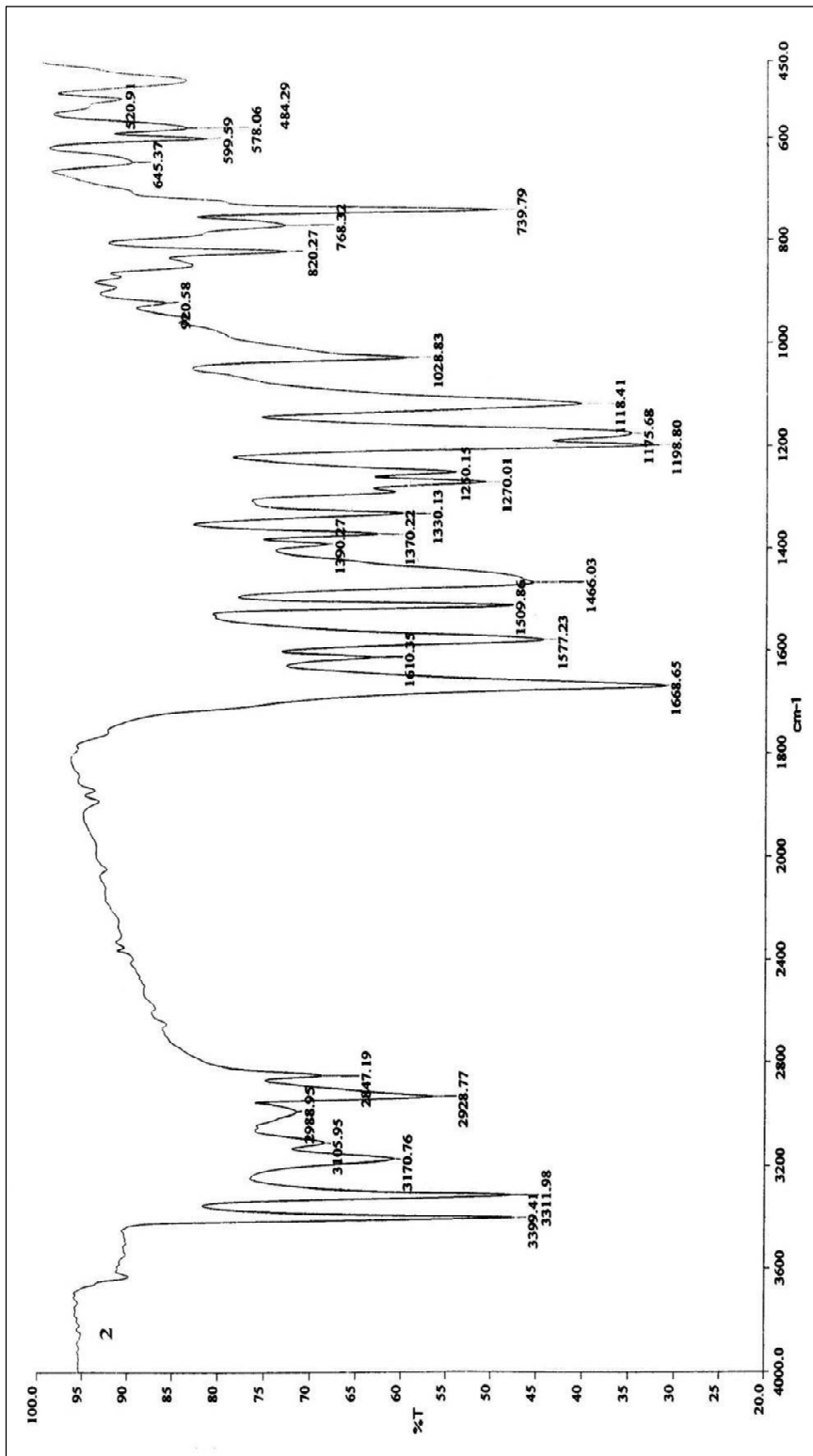


Fig. 4.7: IR spectrum of [TPAS-5]₂ Cu²⁺

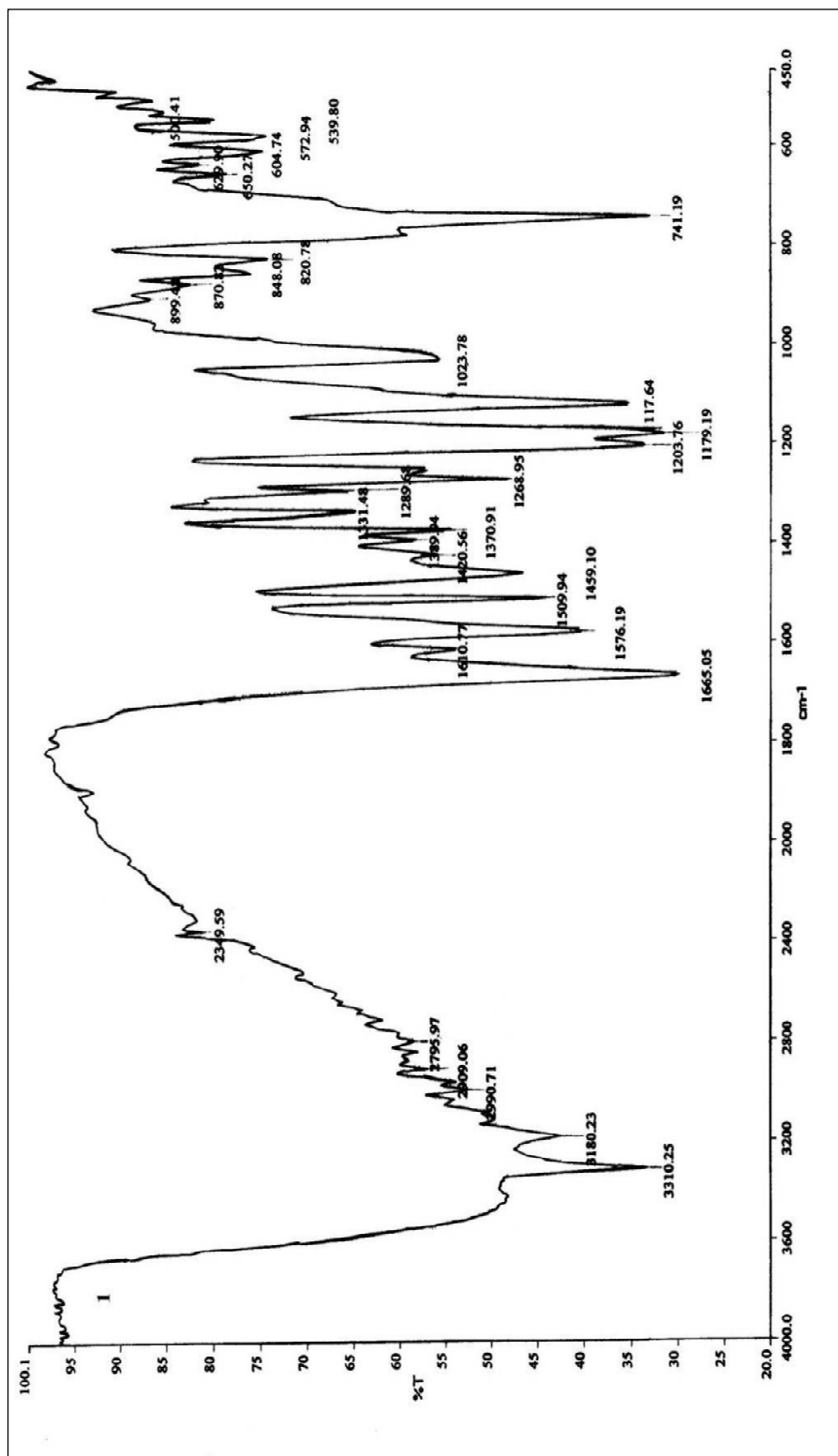


Fig. 4.8: IR spectrum of [TPTB]₂Cu²⁺

The IR spectra of selected metal chelates are shown in Fig. 4.1 to 4.8.

An inspection of IR spectra of ligands and their corresponding chelates revealed that:

- All the IR spectra have identical bands at their respective positions.
- Most of the bands appeared in the spectra of corresponding ligand are observed at the similar position in the IR spectra of their metal complexes.
- The band due to CO of COOH group appeared in the spectra of ligand is almost absent in the spectrum of complexes.
- The new strong band around 1600 cm^{-1} appeared and this might be responsible for COO^- anion. This is expected as the COOH group of ligand is participating in metal chelate formation.
- Only a new band at $1090\text{-}2000\text{ cm}^{-1}$ had appeared in the spectra of metal chelates.
- This may be assigned to $\nu_{\text{C-O}}$ of C-O-Metal bond formation.

As the produced chelates have complex structure, all the bands not appear properly.

4.5 ELECTRONIC SPECTROSCOPY

Electronic (i.e. UV – Visible) spectroscopy is important tool for structural property study of metal chelates. This is for involving.

- (i) Solid State properties,
- (ii) Stereochemistry,
- (iii) Spectral properties
- (iv) Photochemistry
- (v) Thermal reaction
- (vi) Analytical application

All the chelates are in powder forms, so the study has been carried in solid state. Magnesium oxides has been used as reference. Metal chelates may bear four types of transition in the solid spectral region 200 to 800 nm. Wave length.

The two most important types of absorption bands of transition metal chelates in uv-visible region mainly because of metal and ligand and d-d or f-f electron transitions. Kubelka-munk theory³ can direct the calculation of absorption co-efficient. Many studies have been done based on ligand – field theory⁴.

The electronic spectra of all metal produced metal chelates were run on Beckman-Dk-2A spectrophotometer. MgO was used as reference. Spectra of selected samples are presented in Fig. 4.9 to 4.12. Their assignments are included in Table 4.7 to 4.10.

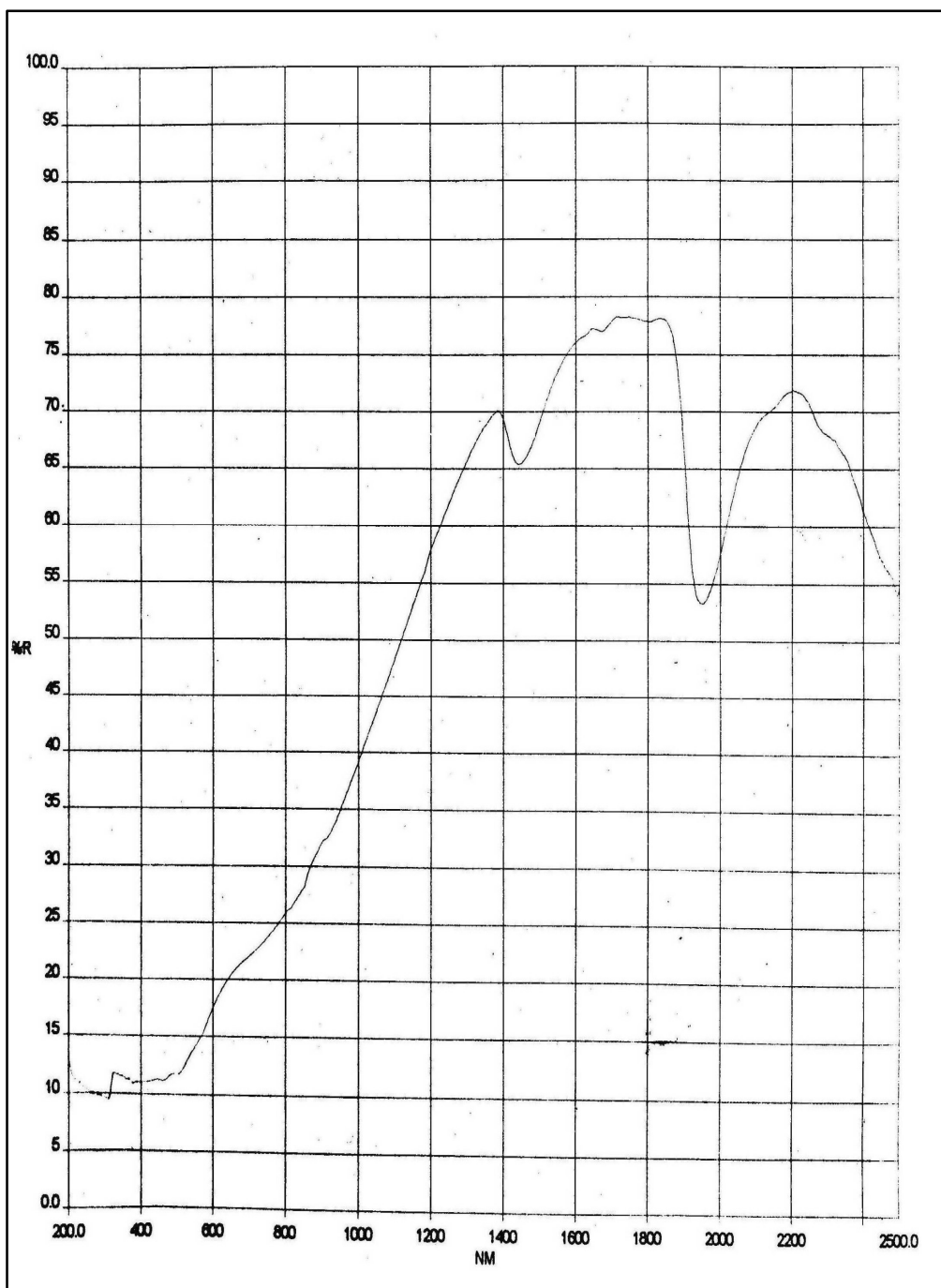


Fig. 4.9: Reflectance spectrum of (TPAS-1)₂-Cu²⁺

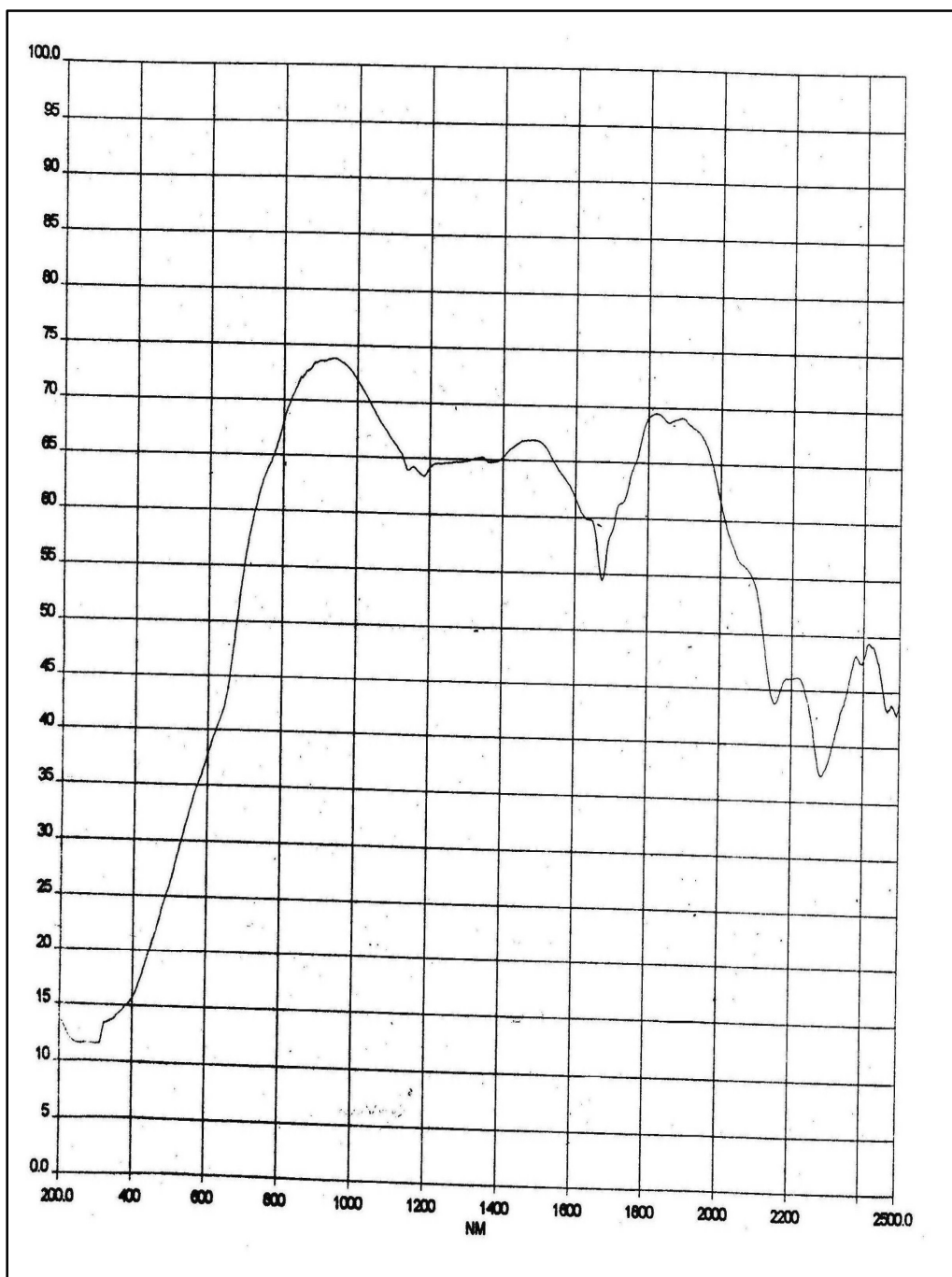


Fig. 4.10: Reflectance spectrum of (TPAS-3)₂-Co²⁺

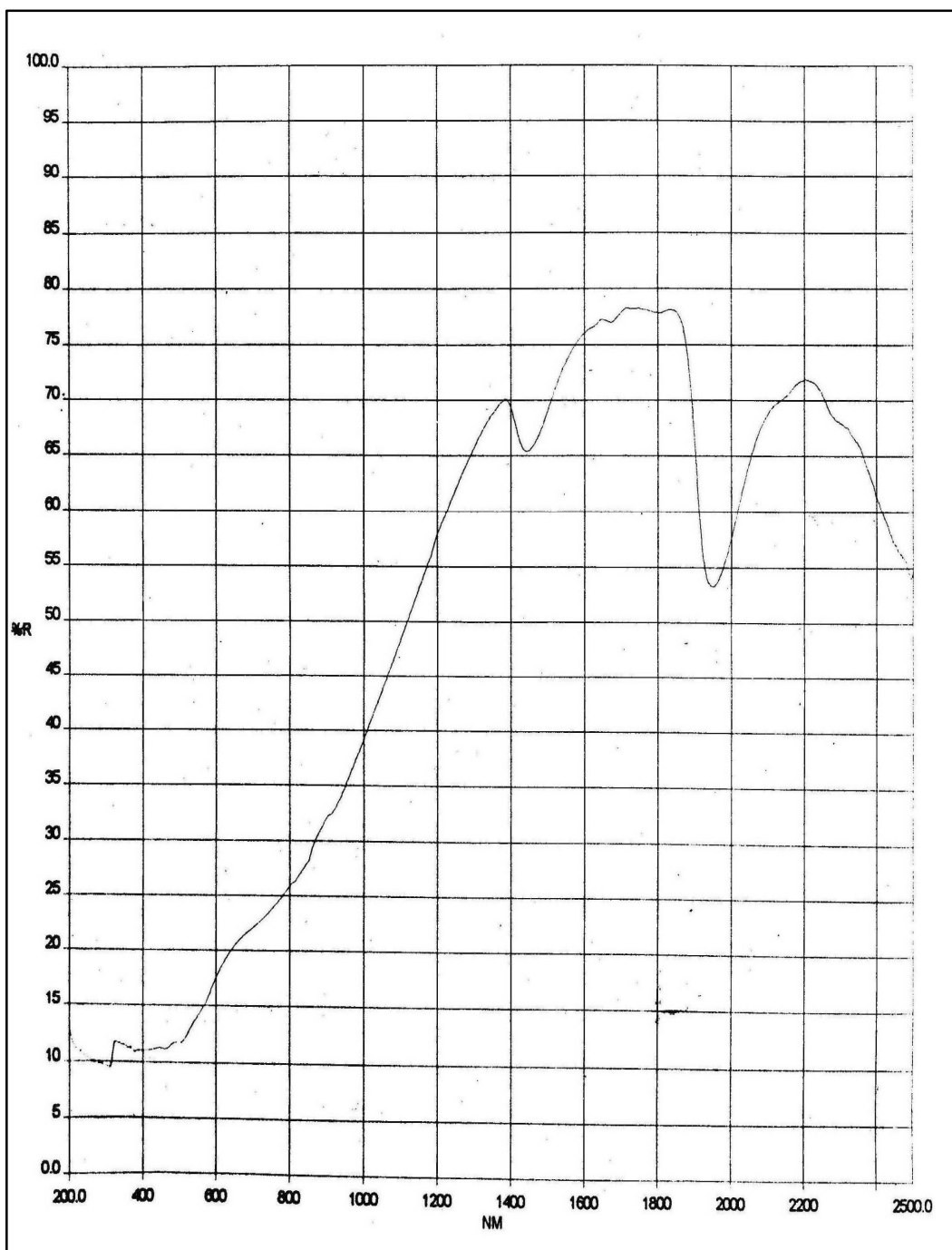


Fig. 4.11: Reflectance spectrum of (TPAS-5)₂Mn²⁺

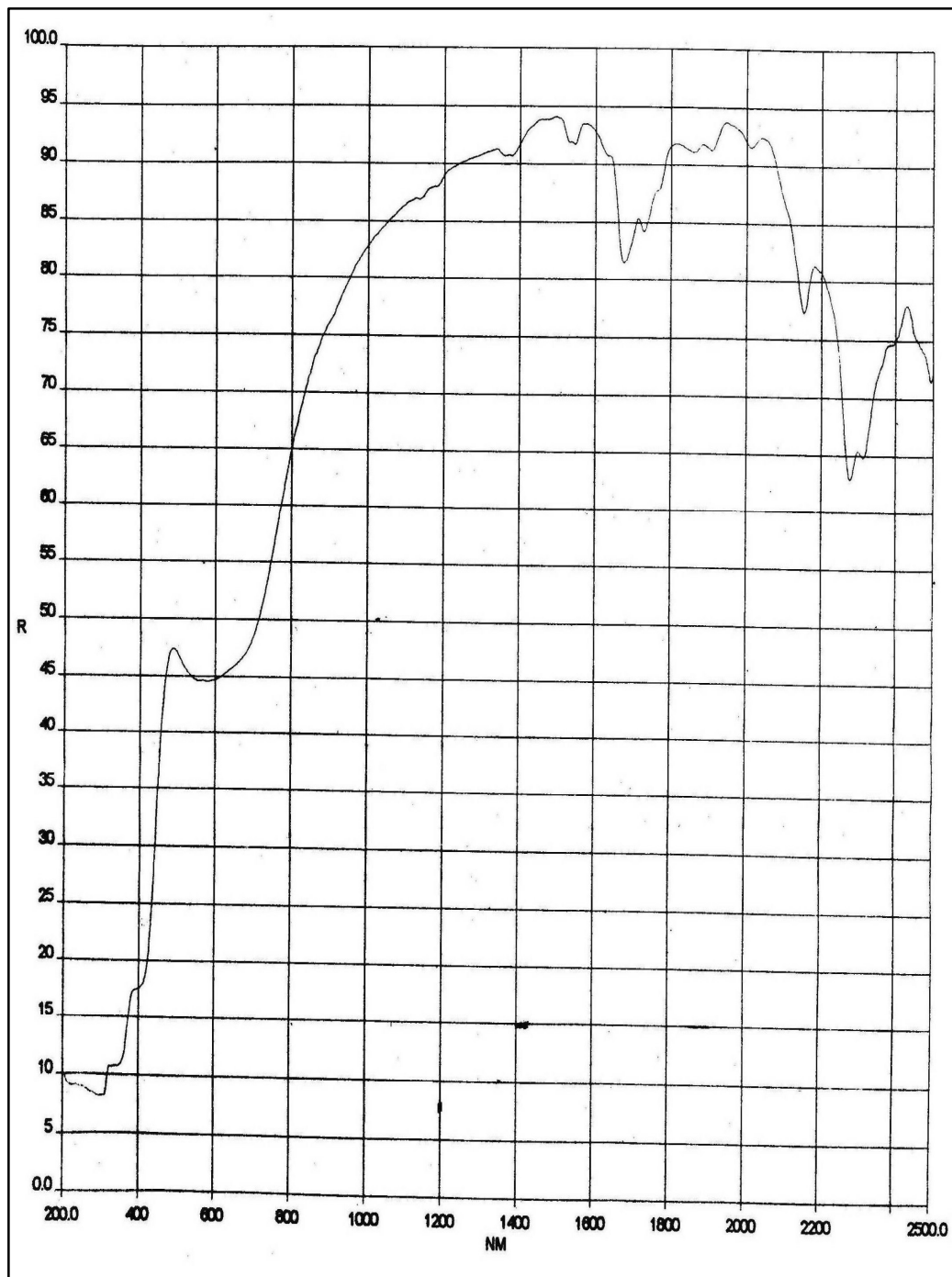


Fig.4.12: Reflectance spectrum of [TPTB]₂-Cu²⁺

Table 4.7: Reflectance spectrum data of Mn²⁺ chelates

Metal Chelates	Observed transition energies (cm ⁻¹)		
	⁶ A _{1g} →		
	⁴ A _{1g} (4E _g)	⁴ T _{2g} (4G)	⁴ T _{1g} (4G)
(TPAS-1) ₂ Mn ²⁺	24030	18650	16215
(TPAS-2) ₂ Mn ²⁺	23880	18340	16845
(TPAS-3) ₂ Mn ²⁺	23980	17643	15460
(TPAS-4) ₂ Mn ²⁺	23415	18592	16122
(TPAS-5) ₂ Mn ²⁺	23785	18411	16723
(TPTB) ₂ Mn ²⁺	22125	18535	16100

Table 4.8: Reflectance spectrum data of Co²⁺ Chelates

Metal Chelates	Observed transition energies (cm ⁻¹)		
	⁴ T _{1g} (F) →		
	⁴ T _{2g} (P)	⁴ A _{2g}	⁴ T _{2g} (F)
(TPAS-1) ₂ Co ²⁺	24653	19982	8784
(TPAS-2) ₂ Co ²⁺	23956	18116	8743
(TPAS-3) ₂ Co ²⁺	24114	19723	8667
(TPAS-4) ₂ Co ²⁺	22975	19035	8534
(TPAS-5) ₂ Co ²⁺	24933	19893	7421
(TPTB) ₂ Co ²⁺	24117	19887	9823

Table 4.9: Reflectance spectrum data of Ni²⁺ Chelates

Metal Chelates	Observed transition energies (cm ⁻¹)	
	³ A _{2g} → ³ T _{1g} (P)	³ A _{2g} → ³ T _{1g} (F)
(TPAS-1) ₂ Ni ²⁺	24122	15192
(TPAS-2) ₂ Ni ²⁺	22234	15793
(TPAS-3) ₂ Ni ²⁺	22197	14120
(TPAS-4) ₂ Ni ²⁺	22495	13124
(TPAS-5) ₂ Ni ²⁺	22313	15717
(TPTB) ₂ Ni ²⁺	24962	14147

Table.4.10: Reflectance spectrum data of Cu²⁺ Chelates

Metal Chelates	Observed transition energies (cm ⁻¹)	
	CT	² B _{1g} → ² A _{1g}
(TPAS-1) ₂ Cu ²⁺	23368	15654
(TPAS-2) ₂ Cu ²⁺	23990	15765
(TPAS-3) ₂ Cu ²⁺	24385	15623
(TPAS-4) ₂ Cu ²⁺	24505	15762
(TPAS-5) ₂ Cu ²⁺	24614	14971
(TPTB) ₂ Cu ²⁺	23993	15524

4.6 MAGNETIC PROPERTIES

Magnetic behavior of metal chelates is an important property. This can be anticipated based on metal and structural unit so for magnetic moment determinedly of metal chelates the two parameter i.e magnetic molar susceptibility (χ_m) and molecular weight of structural unit are required. The (χ_m) is defined as what extent the matter is susceptibility magnetic field. There are two types of magnetic field. Paramagnetic and diamagnetic.

Paramagnetic Field: Associated by electron spin and their angular momentum

Diamagnetic Field: Associated by orbital charge particle contribution. This is due to para electrons.

It occurs due to unpaired electron and free radicals. Paramagnetism is inversely proportional to temperature. The compounds having transition metal with unpaired electron are showing and having free radical showing paramagnetism.

Gauy method ⁵ is useful to determined magnetic susceptibility of metal chelates.

In this method to measure the force created by interactive of applied magnetic field and magnetic moment of the sample (i.e. metal chelates). This force D measured in terms of c (χ) value.

The cylindrical long sample tube with sample D susceptibility in a Gauy balance. The force is measured by applying the magnetic field. The tube constant were determined by using calibrant mercury tetrathiocyanatocobaltate(II) $\text{Hg}[\text{Co}(\text{CNS})_4]$.

The mesh powder of metal chelate sample was inserted with tapping till filling Fixed volume. However loose or tight packing of sample does not alter the susceptibility measurements. The tight packing is more desirable for minimizes the orientation changes of particles in the magnetic field⁶. This tight packing of powder in the tube can be obtained by inserting tiny equal portion of the powder in the tube with end part pounding of each addition. The empty tube was suspended in between two magnet pole then weighed. Its apparent weight (w) was noted in presence of magnetic field created by applying 4 and 6 amp electric current⁷. The difference in weight of tube (dw) at both current was noted.

According to Figgis⁸ reported that mercury tetrathiocyanatocobaltate (II) $\text{Hg}[\text{Co}(\text{CNS})_4]$ is best compound to be used as calibrant for magnetic susceptibility measurement. Scientist suggest that this compound is non-volatile, do not absorb moisture and its fine powder has good packing preparation. Its mass magnetic susceptibility (χ_g) is $16.44 \times 10^{-6} (\pm 0.5\%)$ at 20°C . So filling compound into tube the tube constant (shown in equation below) can be calculated. Thus the magnetic moment of unknown compound can be estimate of

$$\chi_g = \frac{\alpha + \beta dw_s}{W_s} \quad \dots(1)$$

Where

α = Air pocket correction Factor,

β = Tube constants,

W_s = Sample wt in g,

dw_s = Weight difference of the tube filled with sample with magnetic field off
and on.

The value of α is estimated using equation

$$\alpha = KV \quad \dots(2)$$

Where,

K = Volume of susceptibility of air (0.029×10^{-6} cgs unit), and

V = Volume of air.

The tube constant β is determined at different magnetic field strengths using mercury tetrathiocyanatocobaltate (II) as calibrant. The equation used to calculate this constant is:

$$\beta = \chi_r \frac{W_r - KV}{dW_r} \quad \dots(3)$$

Where,

χ_r = Magnetic susceptibility of calibrant (i.e. 16.44×10^{-6} cgs ± 0.5 % at 20°C)

W_r = Weight (g) of calibrant used in measurement

dW_r = Difference in weight (g) of calibrant with and without magnetic field.

K = Volume susceptibility of air (0.029×10^{-6} cgs unit), and

V = Volume of air.

The formula (1) is applied to calculate specific susceptibility of sample from the molecule magnetic susceptibility (χ_m) per gram of sample calculated by

$$\chi_m = \chi_g \times M_e \quad \dots(4)$$

Where,

M = Molecular weight of chelate.

The Diamagnetic corrections were made by using pascal's constant⁴⁻⁷.

$$\chi_{m(\text{corr})} = \chi_m - \text{Pascal's constant} \quad \dots(5)$$

Finally, the magnetic moment (μ_{eff}) was calculated by formula.

$$\mu_{\text{eff}} = \sqrt{(\chi_m')xT} \quad \dots(6)$$

The unit of μ_{eff} is in Bohr magneton. T is the absolute temperature.

The magnetic moment of all the metal chelates estimated and are presents in Table 4.11 to 4.16.

The Results indicate that the Cu^{+2} , Ni^{2+} , Mn^{2+} and Co^{2+} metal chelates have magnetic moment so these chelates are paramagnetic. However Zn^{2+} metal chelates are diamagnetic as expected. The result μ_{eff} value of each chelates are consistent with theoretical value^{8,10}.

4.7 MEASUREMENT OF ELECTRICAL CONDUCTIVITY

Conductivity Bridge 305 was used for measuring electrical conductivity of solutions metal complexes in DMF. The value of EC of all the metal chelates are presented in Table 4.11 to 4.16

The specific conductivity of metal chelates were calculated by,

Specific Conductivity = Cell constant x conductivity

$$\text{Molar conductivity} = \text{Sp. Conductivity} \times \frac{1000}{M}$$

M : molarity of the solution.

Table 4.11: Magnetic and conductivity data of metal chelates of ligand TPAS-1

Metal Chelates	$\chi_g \times 10^{-6}$ (cgs)	$\chi_m \times 10^{-6}$ (cgs)	Magnetic moment μ_{eff} (BM)	$\mu_{\text{eff}} = \sqrt{n(n+2)}$ BM	μ_{eff} (BM) Expected	\wedge_M^a
(TPAS-1) ₂ Mn ²⁺	17.55	14212	5.78	5.91	5.2-6.0	7.21
(TPAS-1) ₂ Co ²⁺	13.45	11125	5.25	3.87	4.4-5.2	19.20
(TPAS-1) ₂ Ni ²⁺	5.65	4760	3.45	2.82	2.9-3.4	9.10
(TPAS-1) ₂ Cu ²⁺	2.10	1815	2.15	1.73	1.7-2.2	7.10
(TPAS-1) ₂ Zn ²⁺	-	-	-	-	D(*)	8.14

Table. 4.12: Magnetic and conductivity data of metal chelates of ligand TPAS-2

Metal Chelates	$\chi_g \times 10^{-6}$ (cgs)	$\chi_m \times 10^{-6}$ (cgs)	Magnetic moment μ_{eff} (BM)	μ_{eff} = $\sqrt{n(n+2)}$ BM	μ_{eff} (BM) Expected	\wedge_M^a
(TPAS-2) ₂ Mn ²⁺	18.54	14676	5.98	5.91	5.2-6.0	7.09
(TPAS-2) ₂ Co ²⁺	14.10	11225	5.20	3.87	4.4-5.2	22.80
(TPAS-2) ₂ Ni ²⁺	5.80	4677	3.35	2.82	2.9-3.4	7.10
(TPAS-2) ₂ Cu ²⁺	2.42	1920	2.14	1.73	1.7-2.2	9.29
(TPAS-2) ₂ Zn ²⁺	-	-	-	-	D(*)	9.81

Table. 4.13: Magnetic and conductivity data of metal chelates of ligand TPAS-3

Metal Chelates	$\chi_g \times 10^{-6}$ (cgs)	$\chi_m \times 10^{-6}$ (cgs)	Magnetic moment μ_{eff} (BM)	μ_{eff} = $\sqrt{n(n+2)}$ BM	μ_{eff} (BM) Expected	\wedge_M^a
(TPAS-3) ₂ Mn ²⁺	17.94	14780	5.97	5.91	5.2-6.0	9.10
(TPAS-3) ₂ Co ²⁺	13.19	10925	5.16	3.87	4.4-5.2	29.10
(TPAS-3) ₂ Ni ²⁺	5.68	4705	3.39	2.82	2.9-3.4	8.20
(TPAS-3) ₂ Cu ²⁺	2.39	1974	2.20	1.73	1.7-2.2	7.98
(TPAS-3) ₂ Zn ²⁺	-	-	-	-	D(*)	10.02

Table 4.14: Magnetic and conductivity data of metal chelates of ligand TPAS-4

Metal Chelates	$\chi_g \times 10^{-6}$ (cgs)	$\chi_m \times 10^{-6}$ (cgs)	Magnetic moment μ_{eff} (BM)	μ_{eff} = $\sqrt{n(n+2)}$ BM	μ_{eff} (BM) Expected	\wedge_M^a
(TPAS-4) ₂ Mn ²⁺	18.55	14782	5.98	5.91	5.2-6.0	5.97
(TPAS-4) ₂ Co ²⁺	14.02	11219	5.20	3.87	4.4-5.2	23.68
(TPAS-4) ₂ Ni ²⁺	5.84	4682	3.38	2.82	2.9-3.4	9.20
(TPAS-4) ₂ Cu ²⁺	2.42	1956	2.19	1.73	1.7-2.2	7.10
(TPAS-4) ₂ Zn ²⁺	-	-	-	-	D(*)	9.62

Table 4.15: Magnetic and conductivity data of metal chelates of ligand TPAS-5

Metal Chelates	$\chi_g \times 10^{-6}$ (cgs)	$\chi_m \times 10^{-6}$ (cgs)	Magnetic moment μ_{eff} (BM)	μ_{eff} = $\sqrt{n(n+2)}$ BM	μ_{eff} (BM) Expected	\wedge_M^a
(TPAS-5) ₂ Mn ²⁺	17.83	14585	5.94	5.91	5.2-6.0	6.72
(TPAS-5) ₂ Co ²⁺	12.90	10635	5.10	3.87	4.4-5.2	28.10
(TPAS-5) ₂ Ni ²⁺	5.40	4435	3.27	2.82	2.9-3.4	9.10
(TPAS-5) ₂ Cu ²⁺	2.32	1888	2.15	1.73	1.7-2.2	4.12
(TPAS-5) ₂ Zn ²⁺	-	-	-	-	D(*)	9.12

Table 4.16: Magnetic and conductivity data of metal chelates of ligand TPTB

Metal Chelates	$\chi_g \times 10^{-6}$ (cgs)	$\chi_m \times 10^{-6}$ (cgs)	Magnetic moment μ_{eff} (BM)	$\mu_{\text{eff}} = \sqrt{n(n+2)}$ BM	μ_{eff} (BM) Expected	\wedge_M^a
(TPTB) ₂ Mn ²⁺	17.54	14733	5.97	5.91	5.2-6.0	7.92
(TPTB) ₂ Co ²⁺	13.14	11102	5.21	3.87	4.4-5.2	27.20
(TPTB) ₂ Ni ²⁺	5.45	4598	3.36	2.82	2.9-3.4	9.65
(TPTB) ₂ Cu ²⁺	2.25	1905	2.16	1.73	1.7-2.2	7.10
(TPTB) ₂ Zn ²⁺	-	-	-	-	D(*)	9.12

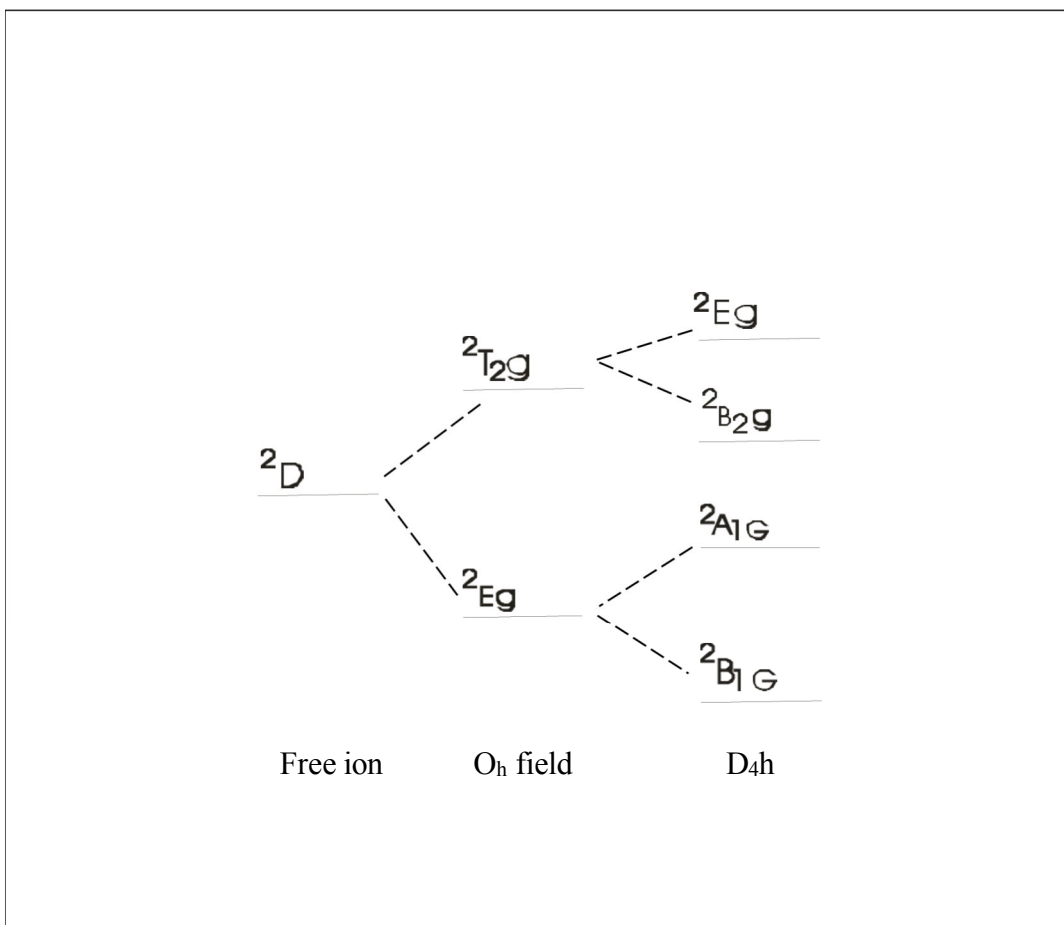
The data show that metal chelates are less polar in DMF low value i.e $< 10 \Omega^{-1} \text{ cm}^2 \text{ mol}^{-1}$ of metal chelates indicate that they are non- electrolyte¹¹.

4.8 MAGNETIC SUSCEPTIBILITY AND REFLECTANCE SPECTRAL DATA CO- RELATION

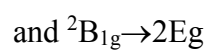
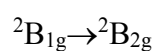
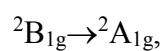
Cu²⁺ chelates

As electronic configuration Cu²⁺ is 3d⁹ the copper ion containing compounds bear magnetic moment with 1.73 BM value. Theoretical magnetic of copper compounds is in the range of 1.7 to 3.0 BM While the measured μ_{eff} mainly in the range of 1.7 to 2.2 BM. The major Cu²⁺ complexes have tetragonally distorted structure. There are four short co-planer and two longer axial bands, so complexes to be square planer.

Geometrically broad band near 15,000 cm⁻¹ is observed so Cu²⁺chelate have little value for assignment of molecules structure. It was observed that tetragonal distortion is common for Cu²⁺ complex. Two main bands found^{12,13}. The energy levels are.



The Cu²⁺ ion in ground state is distorted octahedral field of D_{4h} Symmetry. Its is dx²-y² (b_{1g}) electron orbital. The transition



assigned tetragonal state. All these exists at

12,000-17,000 cm⁻¹

15,000-18,000 cm⁻¹

and 17,000-20,000 cm⁻¹ respectively.

The six co-ordinated Cu²⁺ chelates are distorted octahedral structure (i.e. Jahn – Teller distortion).

In present case (μ_{eff}) of all Cu^{2+} chelates are in the range of 19-20 B.M. This assigned that all Cu^{2+} chelates have distorted octahedral geometry, This also agreed with earlier researchers^{14,15}.

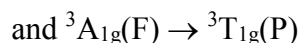
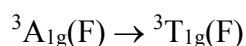
The bands around $15625\text{--}16000\text{ cm}^{-1}$ and $23625\text{--}24000\text{ cm}^{-1}$ observed in the reflectance of all Cu^{2+} chelates may attributed to ${}^2\text{B}_{1g} \rightarrow {}^2\text{A}_{1g}$ and charge transfer respectively. This also may assigned distorted octahedral geometry for Cu^{2+} chelates.

Ni^{2+} Chelates

There are two unpaired electrons in 3d orbital of Ni^{2+} i.e. Ni^{2+} ($3d^8$). Thus, Ni^{2+} chelates magnetic moment near to spin value for octahedral geometry. Its value of μ_{eff} is high which indicate distorted octahedral chelates. Six co-ordinated Ni^{2+} bears following absorption bands with their transition assignment.

Absorption band cm^{-1}	Transition assignment
7000-13000	${}^3\text{A}_{2g} \rightarrow {}^3\text{T}_{2g}(\text{F})$
11000-20000	${}^3\text{A}_{2g} \rightarrow {}^3\text{T}_{1g}(\text{F})$
19000-27000	${}^3\text{A}_{2g} \rightarrow {}^3\text{T}_{1g}(\text{P})$

In present case the all Ni^{2+} chelates of their μ_{eff} is in the range of 2.9 to 3.4 B.M. Which shoe distorted octahedral geometry. High value of μ_{eff} might be attributed to orbital contribution¹⁶. The electronic spectra of Ni^{2+} chelates give two bands at 15625 and 22471 Cm^{-1} . May arised from transitions:



Respectively. This indicated octahedral geometry for all Ni^{2+} chelates.

Table 4.9 show the assignment. The calculations given below

$${}^3A_{2g} \rightarrow {}^3T_{1g} (F) \quad \nu_2 \quad E \approx 18Dq$$

$${}^3A_{2g} \rightarrow {}^3T_{1g} (P) \quad \nu_3 \quad E \approx 12Dq + 15B$$

It is possible to assign $\nu_2 \approx 15,000$ and

$$\nu_3 \approx 22,000 \text{ cm}^{-1}.$$

$$2\nu_2 = 36Dq = 2 \times 15,000$$

$$= 30,000 \text{ cm}^{-1}$$

$$3\nu_3 = 36Dq + 45B$$

$$= 3 \times 22,000$$

$$= 66,000 \text{ cm}^{-1}$$

$$3\nu_3 - 2\nu_2 = 66,000 - 30,000$$

$$45B = 36,000 \text{ cm}^{-1}$$

$$15B = 12,000 \text{ cm}^{-1}$$

$$B = 800 \text{ cm}^{-1}$$

$$12Dq + 15B = 22,000 \text{ cm}^{-1}$$

$$12Dq = 22,000 - 12,000$$

$$= 10,000 \text{ cm}^{-1}$$

$$10Dq = 12,000 \times 10 / 12$$

$$= 10,000 \text{ cm}^{-1}$$

So, these ${}^3A_{2g} \rightarrow {}^3T_{2g}$ will be $9,166 \text{ cm}^{-1}$ in agreement with the reported value in literature for the octahedral Ni^{2+} complexes.

Co²⁺ chelates

Co²⁺ ions have has 3d⁷ electronic configuration. So Co²⁺ chelates have magnetic moment equal to spin only (3.87 B.M). The non generate ground state increases the spin- only value contributed from higher orbitally degeneration which exists μ_{eff} 4.5 to 5.5 B.M.

The spectra of Co²⁺ due to d-d transition of octahedral species with ⁴T_{1g} or ²E_g depends on spin value. The Cu²⁺chelates in octahedral structure show bands given below^{17,18}.

	Spectral Range Cm⁻¹	Transitions
Near	8000-10000	⁴ T _{1g} (F) → ⁴ T _{2g} (F)
Far	15000-17000	⁴ T _{1g} (F) → ⁴ T _{2g} (P)

It is observed that magnitude of magnetic moments lie in the range of 4.4-4.8 BM. These values indicate the possibility of octahedral complexes. Examination of the electronic spectral data reported in table: 4.8 indicate that transitions observed in the range are assigned to transition and another band in the region and may be attributed to and transitions respectively.

Range	Transition
8000–9000 cm ⁻¹	⁴ T _{2g} (F) → ⁴ T _{1g} (P)
15625–16650 cm ⁻¹	⁴ T _{2g} (F) → ⁴ T _{1g} (P)
23000 cm ⁻¹	⁴ T _{2g} (F) → ⁴ T _{2g} (F)

So based on magnetic moment and spectral Co^{2+} chelates have octahedral geometry as repeated^{19,20}.

The high spin Co^{2+} chelates are with transition of octahedral structure which are:

$${}^4T_{1g} (F) \rightarrow {}^4T_{2g} (v_1) \quad E \approx 8Dq \text{ at } \sim 8,000 \text{ cm}^{-1}$$

$${}^4T_{1g} (F) \rightarrow {}^4A_{2g} (v_2) \quad E \approx 18Dq \text{ at } \sim 16,000 \text{ cm}^{-1}$$

$$\text{and } {}^4T_{1g} (F) \rightarrow {}^4T_{1g} (P) v_3 \quad E \approx 6Dq + 15B \text{ at } \sim 20,000 \text{ cm}^{-1}$$

In the present study all the Co^{2+} complexes give three bands in the range at

$$8000 - 9000 \text{ cm}^{-1}$$

$$19,000 \text{ and } - 20,000$$

$$22,000-25,000 \text{ cm}^{-1}$$

Which can be attributed to Above transition. There are shown in Table 4.8

$$3v_3 - v_2 = 3 \times 24,660 - 18,867$$

$$= 18Dq + 45B - 18Dq$$

$$= 45B$$

$$\therefore 15B = 18,371 \text{ cm}^{-1}$$

$$v_3 = 24,660 = 6Dq + 18,371$$

$$\therefore Dq = 1048 \text{ cm}^{-1}$$

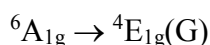
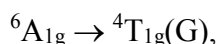
$$v_1 = 8Dq = 8385 \text{ cm}^{-1}$$

This agrees well with the observed v_1 value of 8928 cm^{-1} .

Chelates Mn²⁺

Mn²⁺ chelates are expected to μ_{eff} near to spin only value i.e 5.92 B.M. for unpaired electron in 3d orbital due to oxidation state of Mn²⁺ ion there are two value of μ_{eff} for Mn²⁺ chelates²¹.

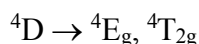
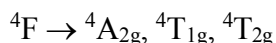
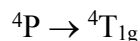
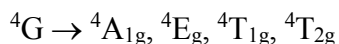
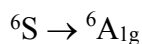
Mn²⁺ chelates give the band in 18000–20000 cm⁻¹ region and weak band in 23600–24350 cm⁻¹ region for octahedral geometry¹⁹.



and ${}^6A_{1g} \rightarrow {}^4A_{1g}(G)$ transitions.

In the produced study the magnetic moment (μ_{eff}) of all Mn⁺² chelates is in the range of 5.5 to 5.9 B.M. The low μ_{eff} value of produced chelates mainly responsible from oxidation of Mn⁺² \rightarrow Mn⁺³, due to spin exchange. The band exist at 16225 cm⁻¹ arised from ${}^6A_{1g} \rightarrow {}^4T_{1g}(G)$ and second at 24050 cm⁻¹ attributed to ${}^6A_{1g} \rightarrow {}^4T_{2g}(G)$ transition¹⁷.

All these features indicate octahedral geometry. Mn⁺² has a d⁵ orbital so in ground state Mn⁺² is ${}^6A_{1g}$. This gives 4G , 4D , 4P , 4F and 6S . These terms attributed to field.



Metal chelates of Zn²⁺

Zn²⁺ metal complexes are predicted to show diamagnetic nature as there is no unpaired electron (3d¹⁰). They have generally tetrahedral geometry²².

4.9 THERMOGRAVIMETRIC ANALYSIS

Thermogravimetric analysis of all the metal chelate of all ligands (i.e. of TPAS-1 to TPAS-5 and TPTB) was carried out on Perkin- Elmer Pyris,1 TGA. The TGA data of all the metal chelates are presented in Table- 4.17 to 4.22. Typical TG thermograms are given in Figure 4.13 to 4.15. It was revealed that each complex degrades in two steps. The first stage of decomposition of chelates is in range temperature of 250-500⁰ C with a mass loss of about 10%, which indicated the presence of associated water molecules.

Examination of the TG curves of all the chelates and TG data shown revealed that:

- Each chelate degrades in two steps.
- The degradation of all the chelates start in the temperature range of 200 to 350⁰C depending upon the natures of chelate.
- The weight loss amount in this first stage is in between 5 to 7 % This may be due to water molecules attached in to the chelates.
- The second stage of decomposition of all chelates is rapid with the loss of mass about 50%. This is due to “in situ” formation of metal oxide during degradation, which accelerated the degradation of chelate.
- The last stage of digestion cause a mass loss of about 80%. This is due to loss of molecular fragments of ligand.

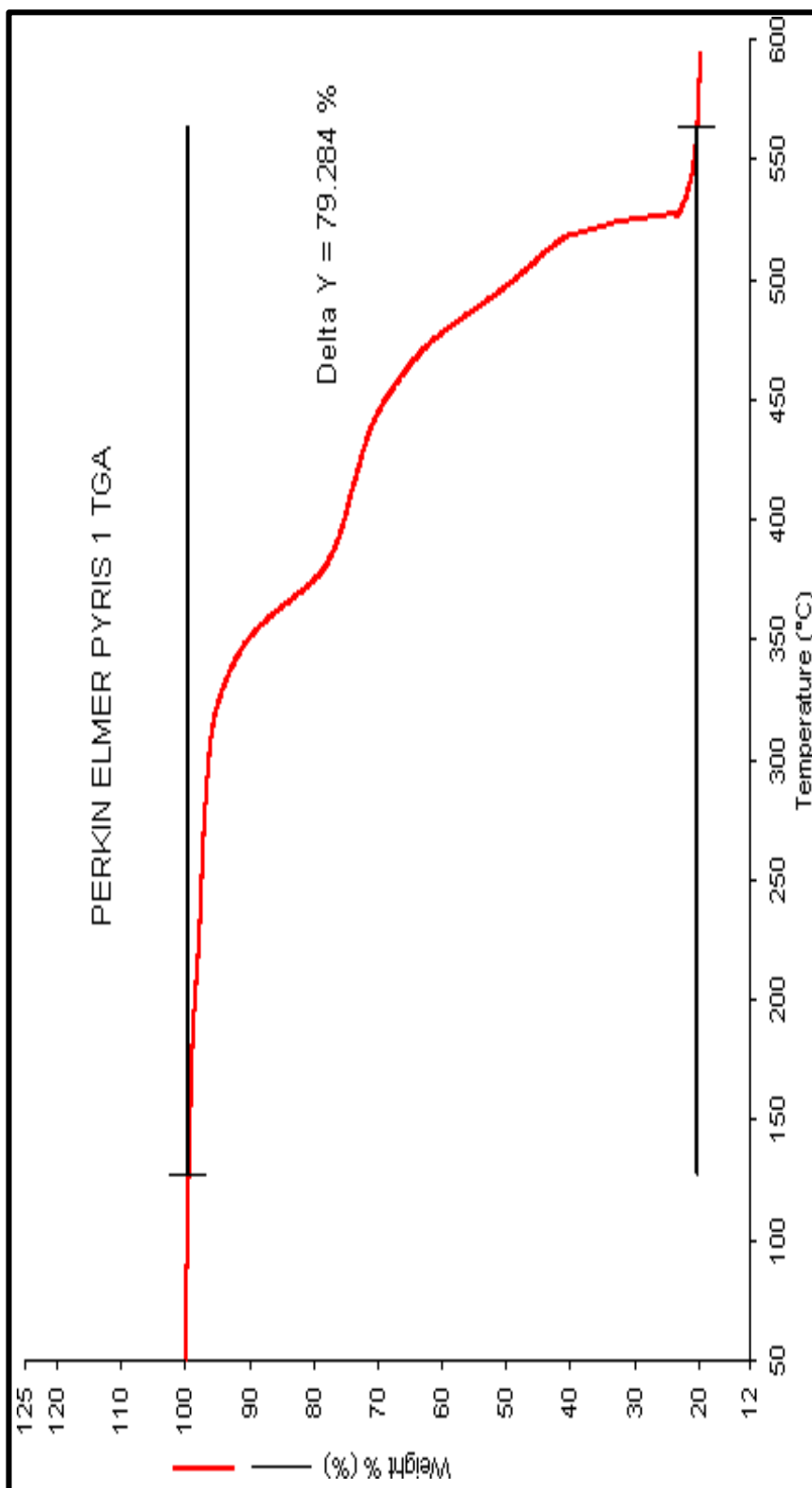


Fig.4.13: TGA thermogram of [TPAS-2] Mn²⁺

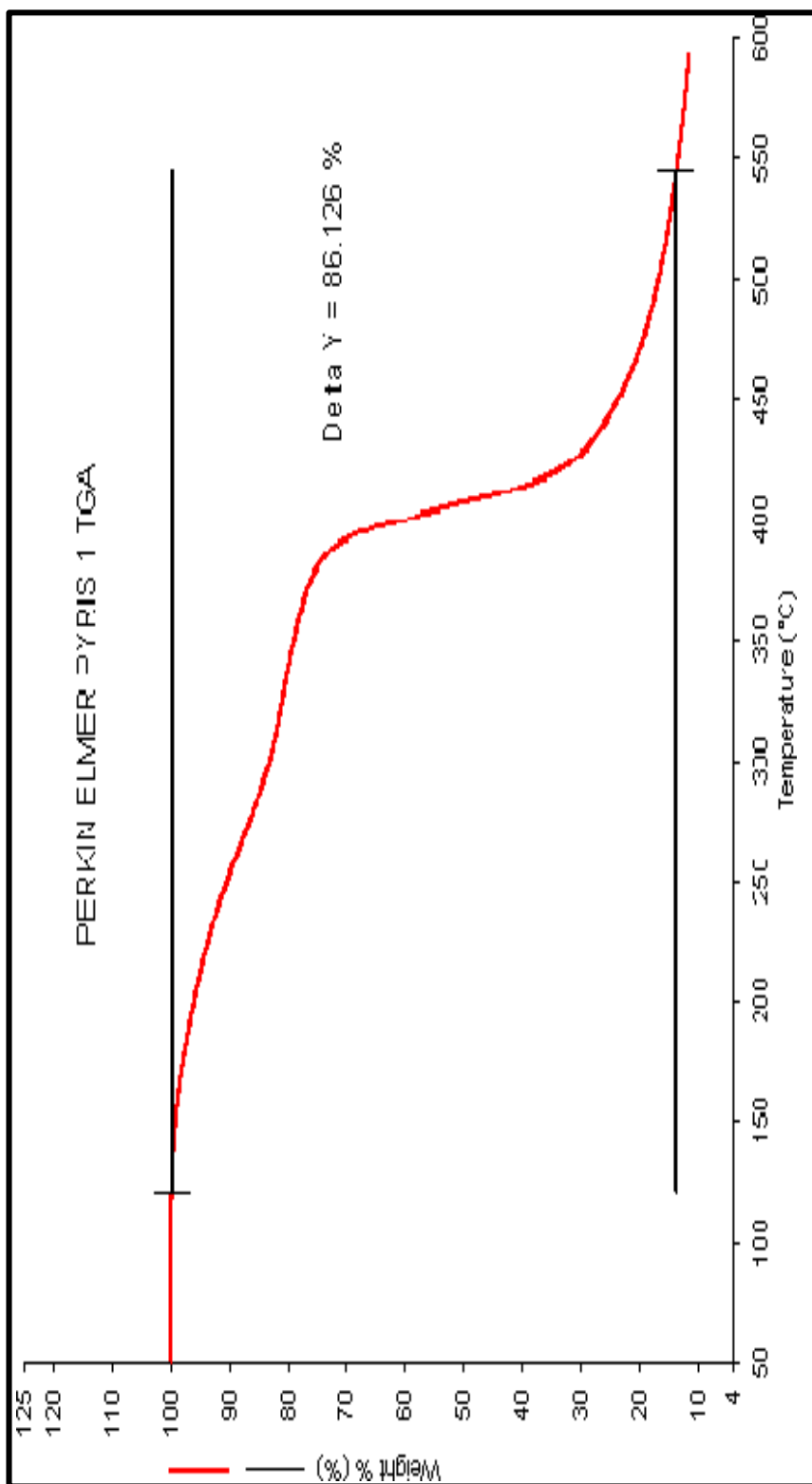


Fig.4.14: TGA thermogram of [TPAS-4] Ni²⁺

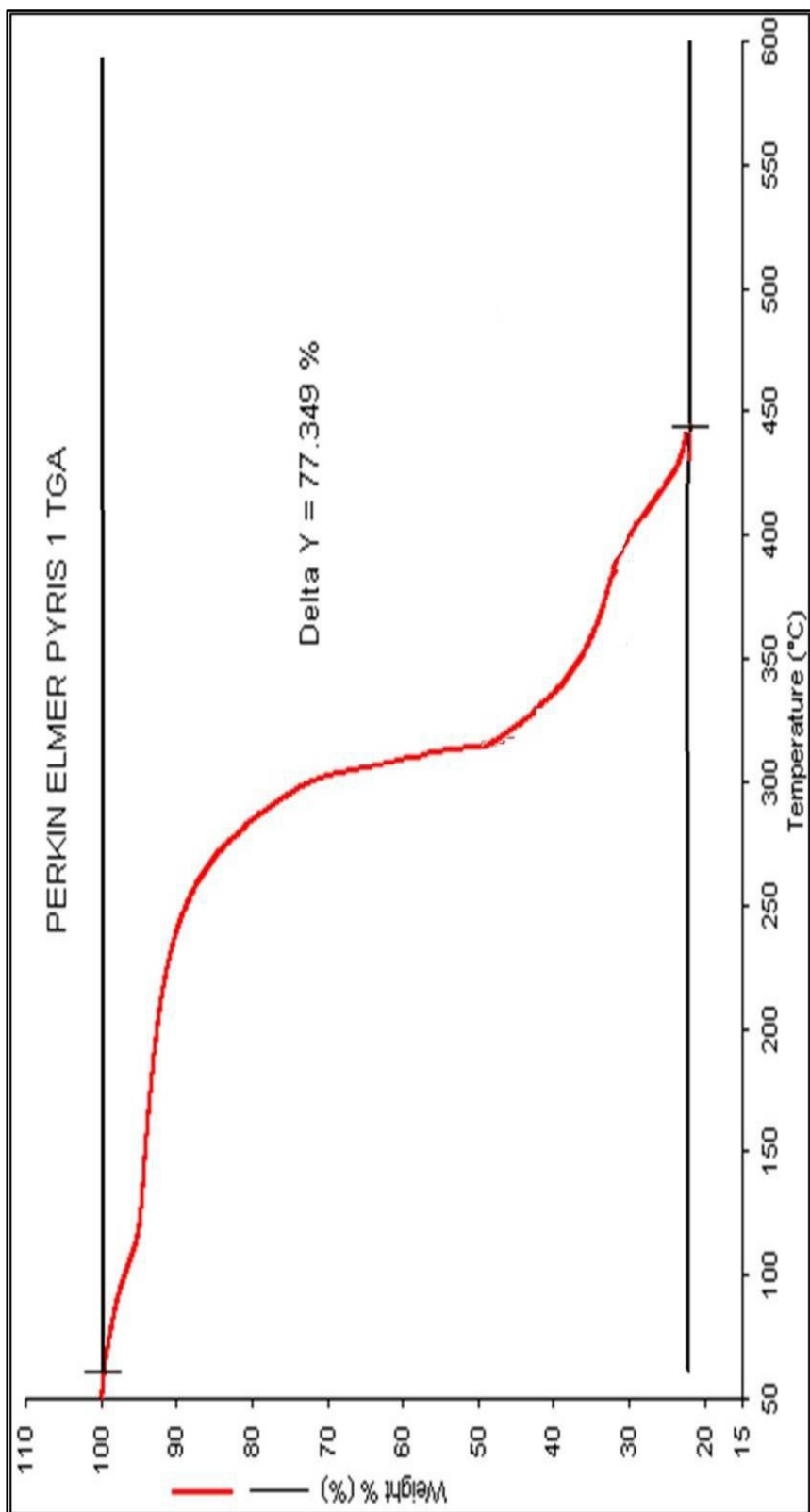


Fig 4.15: TGA thermogram of [TPAS-5] Cu²⁺

Table 4.17: Thermogravimetric analysis of metal chelates of TPAS-1

Chelate	% Weight loss at temperature (⁰ C)			
	250	300	350	400
[TPAS-1] Cu ²⁺	6.5	7.7	15	29
[TPAS-1] Zn ²⁺	3.2	5.5	25	34
[TPAS-1] Co ²⁺	6.9	14.7	26	36
[TPAS-1] Ni ²⁺	7.6	21	29	42
[TPAS-1] Mn ²⁺	7.9	25.3	32	46

Table 4.18: Thermogravimetric analysis of metal chelates of TPAS-2

Chelate	% Weight loss at temperature (⁰ C)			
	250	300	350	400
[TPAS-2] Cu ²⁺	12.2	17	46	75
[TPAS-2] Zn ²⁺	13	18	50	72
[TPAS-2] Co ²⁺	14	19	55	71
[TPAS-2] Ni ²⁺	15.5	20.5	63	78
[TPAS-2] Mn ²⁺	16.5	22	43	82

Table 4.19: Thermogravimetric analysis of metal chelates of TPAS-3

Chelate	% Weight loss at temperature ($^{\circ}\text{C}$)			
	250	300	350	400
[TPAS-3] Cu^{2+}	6.7	9.7	62	73
[TPAS-3] Zn^{2+}	5.6	10.4	61	76
[TPAS-3] Co^{2+}	7.7	11	65	73
[TPAS-3] Ni^{2+}	6.6	8	67	72
[TPAS-3] Mn^{2+}	7.8	10.4	66.5	82

Table 4.20: Thermogravimetric analysis of metal chelates of TPAS-4

Chelate	% Weight loss at temperature ($^{\circ}\text{C}$)			
	250	300	350	400
[TPAS-4] Cu^{2+}	6.4	18.4	22	45
[TPAS-4] Zn^{2+}	11	19.6	24	44
[TPAS-4] Co^{2+}	7.8	18.7	24	51
[TPAS-4] Ni^{2+}	6.7	20.3	25	50
[TPAS-4] Mn^{2+}	8.4	24	28	52

Table 4.21: Thermogravimetric analysis of metal chelates of TPAS-5

Chelate	% Weight loss at temperature (⁰ C)			
	250	300	350	400
[TPAS-5] Cu ²⁺	6.6	9.4	56	68
[TPAS-5] Zn ²⁺	5.6	10.4	61	72
[TPAS-5] Co ²⁺	7.4	11	64	75
[TPAS-5] Ni ²⁺	6.6	10	65	72
[TPAS-5] Mn ²⁺	7.6	10.3	66	77

Table 4.22: Thermogravimetric analysis of metal chelates of TPTB

Chelate	% Weight loss at temperature (⁰ C)			
	250	300	350	400
[TPTB] Cu ²⁺	68	74	78	83
[TPTB] Zn ²⁺	73	75	80	82
[TPTB] Co ²⁺	71	81	84	87
[TPTB] Ni ²⁺	72	75	78	85
[TPTB] Mn ²⁺	76	80	85	91

4.10 ANTIBACTERIAL ACTIVITY

4.10.1 Materials and Methods

- (i) All the ligand TPAS-1 to 5 and TPTB and their method chelates have been monitored for antibacterial and antifungal activity.
- (ii) Antibacterial activity evaluation:

This was confirmed out by Agra- dise diffusion method. First the culture medium was prepared by talking following investigations.

Peptone: 1.0 g

Sodium Chloride: 0.5 g

Meat Extract (i.e. Beef): 0.3 g

Distilled Water: 100 ml

pH :7.6

Agar: 20 g

The components were dissolved in distilled water and pH was maintained to 7.6 then Agar powder was mixed with it. The syrup was taken in different glass tubes which were plugged by cotton and sterilised at 121°C under 15 lbs /inch pressure for quarter hour. This is called Nutrient Agar Broth (NAB)

(iii) Testing method

This study has been adopted as per method reported. NAB was melted in hot water bath and cooled at 50°C with stirring. It was inoculated by 0.5 – 0.6 ml of fresh bacteria culture (listed below) and mixed well. Then Poured (25ml) in to sterlied each petri dish. The poured material was allowed to set (2 hrs) and then ‘wells’ were made by punching in to NAB surface by steriled glass rod. Into these wells 0.1 ml of test sample in one solution of test sample in DMF was added by micro pipette. The plates were closed by lids. They kept aside for 7 days, Standard drugs were taken as reference.

Following bacteria have been taken for the study.

<i>Staphylococcus aureus</i>	Gram positive
<i>Streptococcus Pyogenes</i>	Gram positive
<i>Escherrchia</i>	Gram negative
<i>Pseudomonas areuginosa</i>	Gram negative

After seven days the zone of inhibition of growth of bacteria by the test sample was measured in mm. The data are given in Table 4.23 to 4.26.

Chloramphenicol and Ciprofloxacin drugs have been taken as standard (Table 4.23).

Table 4.23: Antibacterial activity of standard drugs

Standard	Zone of Inhibition* (mm) (activity index) ^{std}			
	Gram positive		Gram Negative	
	<i>S. aureus</i>	<i>S. Pyogenes</i>	<i>E. Coli</i>	<i>P. aeruginosa</i>
Chloramphenicol	22	23	29	21
Ciprofloxacin	19	21	23	24

Antifungal activity of standard drugs

Standard	Zone of Inhibition* (mm) (activity index) ^{std}	
	<i>C. albicans</i>	<i>A. Niger</i>
Nystatin	20	23
Greseofulvin	27	27

* = average zone of inhibition in mm,

Activity index = Inhibition zone of the sample / Inhibition zone of the standard

Table 4.24: Antibacterial activity of ligands TPAS-1, TPAS-2 and their metal chelates.

Sample	Zone of inhibition* (mm) (Activity index) ^{std}			
	Gram Positive		Gram Negative	
	<i>S. aureus</i>	<i>S. Pyogenus</i>	<i>E. Coli</i>	<i>P. aeruginosa</i>
TPAS-1	08	09	11	11
(TPAS-1) ₂ Cu ²⁺	14	15	15	17
(TPAS-1) ₂ Mn ²⁺	14	12	15	11
(TPAS-1) ₂ Co ²⁺	13	12	15	13
(TPAS-1) ₂ Zn ²⁺	18	17	14	16
(TPAS-1) ₂ Ni ²⁺	21	16	13	18
TPAS-2	11	10	08	09
(TPAS-2) ₂ Cu ²⁺	10	13	12	17
(TPAS-2) ₂ Mn ²⁺	14	09	13	17
(TPAS-2) ₂ Co ²⁺	16	17	11	16
(TPAS-2) ₂ Zn ²⁺	18	21	11	16
(TPAS-2) ₂ Ni ²⁺	11	16	18	19

Table 4.25: Antibacterial activity of ligands TPAS-3, TPAS-4 and their metal chelates.

Sample	Zone of inhibition* (mm) (Activity index) ^{std}			
	Gram Positive		Gram Negative	
	<i>S. aureus</i>	<i>S. Pyogenus</i>	<i>E. Coli</i>	<i>P. aeruginosa</i>
TPAS-3	11	10	08	11
(TPAS-3) ₂ Cu ²⁺	16	19	17	18
(TPAS-3) ₂ Mn ²⁺	13	14	15	13
(TPAS-3) ₂ Co ²⁺	17	14	16	17
(TPAS-3) ₂ Zn ²⁺	14	15	16	18
(TPAS-3) ₂ Ni ²⁺	14	17	14	15
TPAS-4	17	18	18	20
(TPAS-4) ₂ Cu ²⁺	21	20	21	22
(TPAS-4) ₂ Mn ²⁺	18	20	19	21
(TPAS-4) ₂ Co ²⁺	22	21	21	18
(TPAS-4) ₂ Zn ²⁺	20	20	23	20
(TPAS-4) ₂ Ni ²⁺	21	18	18	19

Table 4.26: Antibacterial activity of ligands TPAS-5 and TPTB and their metal chelates.

Sample	Zone of inhibition* (mm) (Activity index) ^{std}			
	Gram Positive		Gram Negative	
	<i>S. aureus</i>	<i>S. Pyogenus</i>	<i>E. Coli</i>	<i>P. aeruginosa</i>
TPAS-5	12	11	10	11
(TPAS-5) ₂ Cu ²⁺	11	10	12	13
(TPAS-5) ₂ Mn ²⁺	15	15	11	09
(TPAS-5) ₂ Co ²⁺	17	18	16	14
(TPAS-5) ₂ Zn ²⁺	21	18	16	15
(TPAS-5) ₂ Ni ²⁺	20	20	20	20
TPTB-5	08	10	11	09
(TPTB) ₂ Cu ²⁺	11	16	12	16
(TPTB) ₂ Mn ²⁺	18	09	15	14
(TPTB) ₂ Co ²⁺	10	10	08	08
(TPTB) ₂ Zn ²⁺	12	13	12	11
(TPTB) ₂ Ni ²⁺	10	07	14	16

4.11 ANTIFUNGAL ACTIVITY

For monitoring the antifungal activity of all the produced samples was carried out by using plant pathogens. These are:

- (a) *C. albicans*
- (b) *A. Nigar*

The antifungal activity of all the ligand and their metal chelates was evaluated

at 1000 ppm concentration of wave plant pathogens. Each of these fungus inoculated on sterilized potato dextrose. Agar (PDA) medium in a pre-sterilized petri dish (PDA prepared from 200 g Potato, 20 g Dextrose and 20 g of Agar and water 1 lit). Thus test sample was added in petri dish and then auto cooked 120°C for 15 min under 15 lb/inch pressure. The petri dish were closed and kept for seven days. After the zone of inhibition were measure in percentage by formula,

$$\text{Zone of inhibition \%} = \left(\frac{A - B}{A} \right) \times 100$$

Where A : Area of colony control play

B : Area of colony in test play

The result are shown in Table 4.27 to 4.29.

Table 4.27: Antifungal activity of ligand TPAS-1, TPAS-2 and their metal chelates

Sample	Zone of inhibition (mm) (activity index) ^{std}	
	<i>C. albicans</i>	<i>A. Niger</i>
TPAS-1	07	10
(TPAS-1) ₂ Cu ²⁺	19	21
(TPAS-1) ₂ Mn ²⁺	18	20
(TPAS-1) ₂ Co ²⁺	17	19
(TPAS-1) ₂ Zn ²⁺	18	21
(TPAS-1) ₂ Ni ²⁺	17	18
TPAS-2	10	11
(TPAS-2) ₂ Cu ²⁺	16	17
(TPAS-2) ₂ Mn ²⁺	18	18
(TPAS-2) ₂ Co ²⁺	11	13
(TPAS-2) ₂ Zn ²⁺	13	16
(TPAS-2) ₂ Ni ²⁺	17	18

Table 4.28: Antifungal activity of ligand TPAS-3, TPAS-4 and their metal chelates

Sample	Zone of inhibition (mm) (activity index) ^{std}	
	<i>C. albicans</i>	<i>A. Niger</i>
TPAS-3	08	11
(TPAS-3) ₂ Cu ²⁺	18	19
(TPAS-3) ₂ Mn ²⁺	17	21
(TPAS-3) ₂ Co ²⁺	16	18
(TPAS-3) ₂ Zn ²⁺	20	18
(TPAS-3) ₂ Ni ²⁺	18	18
TPAS-4	08	12
(TPAS-4) ₂ Cu ²⁺	17	17
(TPAS-4) ₂ Mn ²⁺	16	18
(TPAS-4) ₂ Co ²⁺	13	15
(TPAS-4) ₂ Zn ²⁺	16	14
(TPAS-4) ₂ Ni ²⁺	16	13

Table 4.29: Antifungal activity of ligand TPAS-5, TPTB and their Metal chelates.

Sample	Zone of inhibition (mm) (activity index) ^{std}	
	<i>C. albicans</i>	<i>A. Niger</i>
TPAS-5	10	11
(TPAS-5) ₂ Cu ²⁺	18	17
(TPAS-5) ₂ Mn ²⁺	19	20
(TPAS-5) ₂ Co ²⁺	18	18
(TPAS-5) ₂ Zn ²⁺	20	19
(TPAS-5) ₂ Ni ²⁺	18	19
TPTB	09	12
(TPTB) ₂ Cu ²⁺	15	18
(TPTB) ₂ Mn ²⁺	17	19
(TPTB) ₂ Co ²⁺	13	14
(TPTB) ₂ Zn ²⁺	15	13
(TPTB) ₂ Ni ²⁺	18	11

4.12 CONCLUSION

In the present study, sulfa drug containing ligands were prepared. The ligands were proposed by simple condensation of tetrahydrophthalic anhydride and various sulfa drugs. Five simple ligands and one bis ligands were prepared and characterised on the basis of elemental analysis, spectral studies. thermogravimetric analysis and C, H, N, S-content. IR/NMR spectral features of all the ligands are almost identical with slight variation of group frequency and type of proton. The LC-MS data give the molecular mass peak for ligands. All these facts confirmed the structure of ligands. The thermogravimetric analysis of all the ligand support carboxylic group, which on thermal degradation eliminates CO₂ gas. Such degradation of ligand was shown in thermogram, which agree with theoretical value.

Metal complexes of Cu²⁺, Ni²⁺, Co²⁺, Mn²⁺ and Zn²⁺ metal ions with each ligand were synthesized. All the metal complexes are insoluble in water and common organic solvents. All the metal complexes suggest that M:L ratio is 1:2 while that of metal complexes of bis ligand suggest M:L ratio is 1:1.

IR spectra of all the metal complexes of each series are almost identical in terms of all aspects, only discernible difference is observed in IR spectra of metal complexes. The broad band due to OH of COOH in the region 4000-2500 cm⁻¹ was narrowing due to coordination bond formation of COOH with metal ion. However, the narrowing band may be due to coordinated water molecule. The new band due to M-O was observed. The band due to C=O group of COOH in the ligand is almost vanished and the new band due to COO⁻ anion appeared. These IR spectral features confirm the metal complexation.

Thermal degradation of all the metal complexes suggest that each complex degrade initially due to associated water. Then rapid degradation due to *in situ* acceleration by metal oxide formation during thermal degradation.

The magnetic moment and reflectance spectra of all the metal complexes suggest geometry of each type of ligand. The results suggested that Cu²⁺ and Ni²⁺ metal complexes have tetrahedral geometry and paramagnetic. The Co²⁺ and Mn²⁺ complexes have octahedral geometry and paramagnetic. As expected, Zn²⁺ metal complexes are diamagnetic.

The results of antimicrobial activity of all the ligands and their metal complexes indicated that all these compounds are more or less toxic against bacteria and fungi. The results show that the Cu^{2+} metal complexes are more toxic.

□□□

REFERENCES

- [1] A. I. Vogel, A Textbook of Quantitative Chemical Analysis Revised by J. Bessett, R. C. Denny, J. H. Feffery and J. Mondhaus. ELBS, 5th Edition, Pearsons, Indian edition (2004).
- [2] R. A. Ahmadi and S. Amani, Synthesis, Spectroscopy, Thermal Analysis, Magnetic Properties and Biological Activity Studies of Cu(II) and Co(II) Complexes with Schiff Base Dye Ligands Molecules, **17**(6), 6434-6448 (2012).
- [3] H. A. Bayoumi, A. Alaghaz, and M. Aljahdali, Cu(II), Ni(II), Co(II) and Cr(III) Complexes with N₂O₂- Chelating Schiff's Base Ligand Incorporating Azo and Sulfonamide Moieties: Spectroscopic, Electrochemical Behavior and Thermal Decomposition Studies. *Int. J. Electrochem. Sci.*, **8**, 9399-9413 (2013).
- [4] S. L. Simmons, The application of diffuse reflectance spectroscopy to the chemistry of transition metal coordination compounds. *Co-ord. Chem. Rev.*, **14**(2), 181-196 (1974).
- [5] L. N. Mulay, Magnetic Susceptibility, John Willey and Sons, Interscience Publishers, New York (1972).
- [6] G. Kortum and H. Schöter, The acquisition of quantitative absorption spectra of solid substances in reflection. *Z. Naturforsch.*, **2a**, 652-657 (1947).
- [7] G. Kortum and H. Schöter, *Z. Electrochem.*, **57**, 353 (1953).
- [8] B. N. Figgis, The magnetochemistry of complexes in modern Coordination chemistry. Interscience, New York, 403-406 (1960).
- [9] H. A. Bayoumi and A. N. Alaghaz, Cu(II), Ni(II), Co(II) and Cr(III) Complexes with N₂O₂- Chelating Schiff's Base Ligand Incorporating Azo and Sulfonamide Moieties: Spectroscopic, Electrochemical Behavior and Thermal Decomposition Studies. *Int. J. Electrochem. Sci.*, **8**, 9399-9413 (2013).
- [10] E. L. Simmons, The application of diffuse reflectance spectroscopy to the chemistry of transition metal coordination compounds. *Co-ord. Chem. Rev.*, **14**(2), 181-196 (1974).
- [11] R. A. Ahmadi, And S. Amani, Synthesis, Spectroscopy, Thermal Analysis, Magnetic Properties and Biological Activity Studies of Cu(II) and Co(II)

- Complexes with Schiff Base Dye Ligands. *Molecules*, **17**(6), 6434- 6448 (2012).
- [12] P. S. N. Reddy and B. V. Agarwala, Synthesis and Characterization of New Schiff Base Complexes of 2-Pyridinecarboxaldehyde and Thiosemicarbazides. *Syn. React. Inrg. Chem.*, **17**, doi.10.1080/00945718708059456 (1987).
- [13] A. K. Patel, V. M. Patel, R. M. Patel, S. Singh and J. D. Joshi, Synthesis, Characterization and Antimicrobial Activities of Ni(II), Cu(II), Zn(II) and Cd(II) Ternary Complexes Involving 8-Quinolinol as Primary Ligand and Bidentate Glycine or Tridentate Aspartic Acid as Secondary Ligand. *Synth. React. Inorg. Met. Org. Chem.*, **29**(2), doi.10.1080/00945719909349443 (1999).
- [14] C. K. Jorgenson, Comparative Crystal Field Studies of some Ligands and the Lowest Singlet State of Paramagnetic Nickel(II) Complexes. *Acta. Chem. Scand.*, **9**, 1362-1377 (1955).
- [15] D. C. Patel and P. K. Bhattacharya, Studies in some Ni(II) and Cu(II) complexes. *J. Ind. Chem. Soc.*, **49**, 1041-1043 (1972).
- [16] J. Lewis and R. S. Wilkins, *Modern Coordination chemistry*, New york, 290 (1960).
- [17] B. Sing and R. Sing, Transition metal complexes of 3-(4-pyridyl)-triazoline-5-thione *J. Inorg. Nucl. Chem.*, **34**(11), 3449-3454. (1972).
- [18] B. Sing and U. Agarwal, Transition metal complexes of 1-substituted tetrazoline-5-thiones. *J. Inorg. Nucl. Chem.*, **8**, 2515-2525 (1969).
- [19] S. Satpathi, H. C. Rai and B. S. Sahoo, Antiferromagnetic spincoupling in low spin cobalt(II) and medium spin manganese (II) dimers. *J. Ind. Chem. Soc.*, **52**, 701 (1975).
- [20] P. K. Patel and P. D. Patel, Synthesis, Characterization, Metal Complexation Studies and Biological screening of some Newly Synthesized Metal Complexes of 1-(4-carboxy-3-hydroxy-N-isopropyl phenyl amino methyl)

benzotriazole with Some Transition Metals. *Int. J. of Chem Tech. research*, **2**(2), 1147-1152 (2010).

- [21] P. R. Reddy, M. Radhika, and P Manjula, Synthesis and characterization of mixed ligand complexes of Zn(II) and Co(II) with amino acids: Relevance to zinc binding sites in zinc fingers. *J. Chem. Sci.*, **117** (3), 239-246 (2005).
- [22] A. V. Nikolav, V. A. Logvineko and L. T. Mychina, *Thermal Analysis*, Academic Press, New York, **2**, 779 (1969).



PUBLICATIONS

**SYNTHESIS, CHARACTERIZATION AND ANTIMICROBIAL ACTIVITY OF
COORDINATION POLYMERS DERIVED FROM BISTETRAHYDRO
PHTHALAMIC ACID OF TRIMETHOPREM DRUG**

Chintankumar P.1*, Piyush V.2, Jayesh B.3

1,3Department of Chemistry, PAHER University, Udaipur, Rajasthan, INDIA*

2Principal, Sheth M.N. Science College, Patan, Gujrat, INDIA **Email-**

Email: - cp627846@gmail.com

Abstract

The trimethoprem drug was condensed with tetrahydrothalic anhydride. The resultant Bis tetrahydrophalamic acid of trimetroprem namely; 2, 4-Bis (5-carboxycyclone hex -1-en-6carbomyl)-(3, 4, 5-trimethoxyphenyl) methyl pyrimidine, characterised duly. The coordination polymers of this bis ligand were BTPT prepared by using metal ions viz; Cu⁺², CO⁺², Ni⁺², Mn⁺², and Zn⁺². The coordination polymers and parent ligand BTPT were analysed by metal: ligand ratio, spectral features, magnetic moment, large molecular weight and thermogravimetry. The antimicrobial activity of all the Mn- ligands and polymers were evaluated by Agar-cup-method

Keywords: *Coordination polymers, Spectral study, metallsalts ligand, magnetic moment, Spectral study, thermogravimetry, Number average molecular weight Mn-*

Published in: Eur. Chem. Bull. 12 (10), 1721-1727(2022) ISSN 2063-5346

**Synthesis, Metal Complexing Properties and Antifungal Activity Of Sulpha Drug
Containing Ligand**

Chintankumar P.1*, Piyush V.2, Jayesh B.3

1,3Department of Chemistry, PAHER University, Udaipur, Rajasthan, INDIA*

2Principal, Sheth M.N. Science College, Patan, Gujrat, INDIA **Email-**

Email: - cp627846@gmail.com

Abstract

Sulphathiazole (ST), a drug on condensation with tetrahydrophthalic anhydride (THPA) yield a ligand, 6-((4-(N-(thiazol-2-yl) sulfamoyl) phenyl) carbamoyl) cyclohex-3-enecarboxylic acid (THPAST). Metal complexes of THPAST were synthesised with transition metal ions i.e. Cu^{2+} , Co^{2+} , Ni^{2+} , Mn^{2+} , and Zn^{2+} . The synthesised ligands (THPAST) and its metal complexes were analysed by various parameters like elemental analysis, Spectral analysis and magnetic moments. All the samples were monitored against common fungi for their antifungal activity.

Keywords: *Tetrahydrophthalic anhydride, Metal complexes, elemental analysis, Spectral analysis, magnetic moment and antifungal activity.*

Published in: Jour. Pharm. Neg. Res. 42 (1): 65-70 (2023) ISSN: 0976-9234